ABSTRACT

LIU, JIA. Transmitter-based Multiple Access Interference Rejection and Diversity Techniques for Code-division Multiple Access Systems. (Under the direction of Dr. Alexandra Duel-Hallen)

For the downlink of direct sequence code-division multiple access (DS-CDMA) systems, transmitter (Tx)-based multiple access interference (MAI) cancellation techniques, termed multiuser precoding, and Tx-based diversity techniques can significantly increase system capacity while remaining low complexity at mobile stations (MS). We have proposed novel linear and nonlinear decorrelating precoding algorithms. Hybrid transmitter designs were developed to combine MAI cancellation and diversity techniques. We have also analyzed the important duality between Tx-based multiuser precoding and receiver (Rx)-based multiuser detection.

The class of decorrelating precoding techniques is simple, efficient and satisfies the minimum mean square error (MMSE) criterion. The nonlinear decorrelating Tomlinson-Harashima precoding (THP) inherently outperforms linear MAI cancellation methods. For frequency-selective fading channels, we developed the THP with Pre-RAKE combiner (PreRAKETHP) and Multipath Decorrelating THP (MDTHP) designs. While the PreRAKETHP is the optimal THP design by both ZF and MMSE criteria, it is computationally complex because the MAI cancellation filters depend on the instantaneous channel gain coefficients and therefore need to be updated frequently. In the MDTHP, the precoding filter is independent of the channel state information (CSI). The MDTHP is simpler than PreRAKETHP at the expense of moderate performance loss.

1. REPORT DATE **2005**	2. REPORT TYPE	3. DATES COVERED **00-00-2005 to 00-00-2005**

4. TITLE AND SUBTITLE		5a. CONTRACT NUMBER
Transmitter-Based Multiple Access Interference Rejection and Diversity Techniques for Code-Division Multiple Access Systems		5b. GRANT NUMBER
		5c. PROGRAM ELEMENT NUMBER
6. AUTHOR(S)		5d. PROJECT NUMBER
		5e. TASK NUMBER
		5f. WORK UNIT NUMBER
7. PERFORMING ORGANIZATION NAME(S) AND ADDRESS(ES) **North Carolina State University,Department of Electrical Engineering,Raleigh,NC,27695**		8. PERFORMING ORGANIZATION REPORT NUMBER
9. SPONSORING/MONITORING AGENCY NAME(S) AND ADDRESS(ES)		10. SPONSOR/MONITOR'S ACRONYM(S)
		11. SPONSOR/MONITOR'S REPORT NUMBER(S)

12. DISTRIBUTION/AVAILABILITY STATEMENT **Approved for public release; distribution unlimited**

13. SUPPLEMENTARY NOTES

14. ABSTRACT

15. SUBJECT TERMS

16. SECURITY CLASSIFICATION OF:			17. LIMITATION OF ABSTRACT	18. NUMBER OF PAGES **120**	19a. NAME OF RESPONSIBLE PERSON
a. REPORT **unclassified**	b. ABSTRACT **unclassified**	c. THIS PAGE **unclassified**			

For Pulse Amplitude Modulated (PAM) and Quadrature Amplitude Modulated (QAM) systems with small constellation index, the practical performance of THP is degraded due to the side effects of modulo operation. In contrast, linear precoding is not influenced by modulation and is simpler to implement. We have developed several linear precoding techniques. The PreRAKE Linear Decorrelating Precoding (PreRAKELDP) is the optimal ZF and MMSE precoding method. The Multipath Decorrelating Precoding (MDP) provides a simpler but suboptimal scheme. It is shown that the PreRAKELDP and MDP outperform the existing linear precoding techniques with similar complexity. The system performance is further improved by employing multiple antennas in transmitter design.

Both multiuser precoding and transmit diversity techniques require the knowledge of CSI at transmitter. For rapidly varying channels, the long range channel prediction (LRP) provides the accurate CSI in time. We have demonstrated that the LRP method enables the proposed Tx-based techniques for practical systems.

TRANSMITTER-BASED MULTIPLE ACCESS INTERFERENCE

REJECTION AND DIVERSITY TECHNIQUES FOR CODE-DIVISION

MULTIPLE ACCESS SYSTEMS

by

JIA LIU

A dissertation submitted to the Graduate Faculty of
North Carolina State University
in partial fulfillment of the
requirements for the degree of
Doctor of Philosophy

ELECTRICAL ENGINEERING

Raleigh

2005

APPROVED BY:

_____	_____
Hamid Krim	Kailash C. Misra
_____	_____
Keith Townsend	Alexandra Duel-Hallen
	Chair of Advisory Committee

*To my husband Yun, my parents and sister
for their endless love*

BIOGRAPHY

Jia Liu received her B.S. degree in Electrical Engineering from Nankai University, Tianjin, China, in 1997. She worked as a design engineer of firmware development for Navigation Guiding Instruments Corp., Tianjin, China, from 1997 to 1999. In August 1999, she started her graduate studies at North Carolina State University in the Department of Electrical and Computer Engineering. She received her M.S. degree and was enrolled in the Ph.D. program in December 2000. She has been working as a research assistant at the Center for Advanced Computing and Communication since Fall 2001. Her research interests are in signal processing for digital communications.

ACKNOWLEDGMENTS

TABLE OF CONTENTS

TABLE OF FIGURES

Chapter 1

INTRODUCTION

1.1 Background

Wireless communication is dramatically changing our lives. The ability to communicate anytime and anywhere increases our quality of lives and improves our business productivity. In cellular wireless systems, the network consists of numerous mobile users communicating with one or multiple base stations (BS) that are interconnected with a mobile telephony switching office. Originated from the spread-spectrum techniques, the code-division multiple access (CDMA) systems can support simultaneous digital communication among a large community of relatively uncoordinated users. CDMA exhibits potential capacity increase over the conventional time-division multiple access (TDMA) and frequency-division multiple access (FDMA), because CDMA capacity is only interference limited, while TDMA and FDMA are primarily bandwidth limited [GJP91]. The inherent frequency diversity of wideband signals enables CDMA to efficiently suppress the narrow-band interference in radio link. Direct sequence (DS) CDMA has been widely applied in the second and third generations cellular standards (IS-95, WCDMA and CDMA2000). It is also a very promising option for the next generation wireless communications.

In practical wireless channels, the multiple access interference (MAI) is a major limitation to the performance of DS-CDMA systems. Due to multiple reflections in multipath fading channels and asynchronous transmission, the received signal contains delayed, distorted replicas of the original transmitted signal. For each user, the MAI includes the interference from other users and self-interference. Over the past decade, various MAI

1

rejection techniques have been developed. This research has primarily focused on receiver (Rx)-based multiuser detection (MUD) [Ver98] that results in a complex receiver while the transmitter remains simple. Thus, MUD techniques are mostly suitable for the uplink. For the downlink CDMA channel, the requirements of small-size low-power mobile station (MS) have motivated the development of Tx-based MAI pre-rejection techniques in BS, termed multiuser precoding. In addition to Tx-based MAI cancellation, Tx-based diversity techniques also efficiently improve system capacity. For frequency-selective fading channels, to simplify the mobile user receivers, the transmitter (Tx)-based PreRAKE combining is more suitable for the downlink than the conventional RAKE receiver [EN95]. This technique can utilize multipath diversity as efficiently as RAKE receiver. The Tx-based antenna array is another efficient diversity technique to increase the received signal to noise ratio [BZP04, GD05]. In the practical design of multiuser precoding techniques, the problems of MAI rejection, transmit power control and diversity strategies need to be considered comprehensively.

The class of decorrelating zero-forcing (ZF)-based precoding techniques is simple, efficient and satisfies the minimum mean square error (MMSE) criterion [VJ98, BD00], thus is most promising in practical applications. Inspired by Tomlinson-Harashima equalization [LM94], the nonlinear method of Tomlinson Harashima Precoding (THP) proposed in [WFVH04] utilizes a feedback (FB) loop and a feed-forward (FF) filter to jointly cancel MAI. An independent work on THP [LD03] presented the significant duality between THP and the Decision-Feedback (DF) MUD [Due93]. Both [WFVH04, LD03] assume that the non-orthogonal effective spreading codes on the downlink arise due to multipath fading. However, the channel models employed in these papers do not reflect the frequency-selective

fading channel environment, and can only be viewed as flat fading non-orthogonal CDMA channels. The THP designs for frequency-selective fading channels are presented in [LD04, LDg04, LDj04]. In this thesis, we first illustrate the principle of THP for the simple case of single-path channels with additive white Gaussian noise (AWGN) and flat Rayleigh fading channels. Then we develop two specific THP designs for frequency-selective fading channels, THP with PreRAKE combiner (PreRAKETHP) and Multipath Decorrelating THP (MDTHP). The PreRAKETHP and MDTHP incorporate Tx-based diversity combining techniques in different ways. In PreRAKETHP, the MAI cancellation is followed by the pre-RAKE combining [EN95]. While this precoder is the optimal THP design for multipath channels, it requires high computational complexity, since its MAI cancellation filters depend on the rapidly time variant mobile radio channel coefficients and need to be updated frequently. In MDTHP, the diversity combining is incorporated into the MAI cancellation, and the precoding filter is independent of the channel. Thus, MDTHP is simpler than PreRAKETHP, and results in moderate bit error rate (BER) loss.

Several MAI cancellation techniques used in transmitter for the downlink of CDMA systems have analogous structure and similar performance to those employed in the receiver for the uplink. We address this duality and show that THP outperforms previously proposed Tx- and Rx-based linear and nonlinear decorrelating methods in [VJ98, BD00, TC94, Gun03, GDv03, GDc03, HS94, SK97, ZB96, Due93]. In addition to CDMA systems, THP is also an efficient interference rejection approach for various multi-input/multi-output (MIMO) systems, such as orthogonal frequency division multiplexing (OFDM) and multiple-antenna channels [WFVH04]. THP is especially beneficial as an alternative to decision-feedback receivers in coded systems [LM94, Pro01].

3

In addition to nonlinear decorrelating precoding techniques, several linear decorrelating precoding techniques are presented in this thesis. Compared to nonlinear THP precoding, the linear methods have lower complexity and higher error rate, but their performance is not influenced by modulation method. In the previously proposed linear deocrrelating precoders [VJ98, BD00, Gun03, GDv03], the global power scaling is commonly used to normalize the transmit power. It is shown that the precoding performance is degraded by the power scaling. In [VJ98], the MMSE-based linear precoding with transmit power constraint is also investigated. We propose two novel linear precoding methods, PreRAKE Linear Decorrelating Precoding (PreRAKELDP) and Multipath Decorrelating Precoding (MDP) [LDm05]. In the PreRAKELDP transmitter, the preRAKE combiner is preceded by a linear precoding filter. Based on different transmit power control strategies, we propose two solutions for the precoding filter. One is the ZF-based filter with individual user power scaling, in which each user's average transmit power is normalized by a power scaling factor. The other is the MMSE-based filter under the total transmit power constraint. (Note that if the individual-user transmit power constraint rather than the total transmit power constraint is enforced, the MMSE solution is identical to the ZF solution [VJ98, BD00].) When these two PreRAKELDP solutions are compared, the ZF precoder is much simpler while the MMSE precoder has obviously better performance. It should be noted that to achieve a simple and practical transmitter design for a system with large user number, the allocation of individual user transmit powers is not taken into account in the PreRAKELDP designs. Since the pre-RAKE combiner is equivalent to a matched filter which is matched to the multipath fading channels, the PreRAKELDP with individual user power scaling and that with total transmit power constraint are the optimum linear ZF and MMSE precoders,

respectively, under the condition that the transmit power of individual user is not specified. In the MDP transmitter, the multipath diversity combining is incorporated into the MAI cancellation process, and the decorrelating filter is independent of the channel fading coefficients and only determined by users' signature sequences. As a result, the computational complexity of the MDP is lower than that of the PreRAKELDP, Pre-RDD and the precoders in [VJ98, BD00].

Compared to the existing Tx-based and Rx-based linear decorrelating methods, the PreRAKELDP with total power constraint has the best performance and highest complexity; the PreRAKELDP with individual power scaling has similar performance to the Pre-RDD and RDD; the MDP has identical error rate to the Rx-based Multipath Decorrelating Detector (MDD) [LD03]. The two proposed precoders outperform those in [VJ98, BD00, GDv03, Gun03].

A crucial assumption for Tx-based interference cancellation methods is that the transmitter has the knowledge of channel conditions. The channel state information (CSI) can be estimated at the receiver and sent to the transmitter via a feedback channel. Thus, feedback delay and overhead, processing delay and practical constraints on modulation, coding and antenna switching rates have to be taken into account in the performance analysis of adaptive transmission methods. For very slow fading channels, outdated CSI is sufficient for reliable adaptive transmission. However, for faster fading that corresponds to realistic mobile speeds, the channel profile is quite different at the time of transmission when compared to the outdated CSI. As a result, even small delay will cause significant performance degradation due to the channel variation. To enable Tx-based signal processing techniques, the CSI at the instant of transmission should be reliably predicted, based on the

outdated CSI feedback from the mobile. Most existing channel prediction methods require large computational complexity or are only suitable for very short range prediction [LPL95, HM89, ZS96, WD95]. The long-range channel prediction (LRP) is a linear adaptive prediction technique proposed in [EDH98, DHH00]. In this thesis, we investigate transmitter precoding aided by the LRP. The LRP algorithm characterizes the fading channel using the autoregressive (AR) model and computes the MMSE estimate of a future fading coefficient sample based on a number of past observations. The superior performance of this algorithm relative to conventional methods is due to its low sampling rate. Given a fixed model order, lower sampling rate results in longer memory span, permitting prediction further in the future. We employ the LRP algorithm to enable the proposed Tx diversity and precoding methods in practical WCDMA systems.

1.2 Outline of the Thesis

The goal of this thesis is to investigate and compare the Tx-based and Rx-based decorrelating MAI cancellation methods, with the application of transmit diversity and long-range channel prediction. The thesis is outlined as follows:

Chapter 2 first describes the frequency-selective channel model of uplink CDMA, the linear and nonlinear (DF) decorrelating multiuser detection methods are then presented and their complexity and performance are compared.

From Chapter 3 to Chapter 5, we concentrate on the downlink CDMA channels. In Chapter 3, we first describe the centralized and decentralized channel model with single-path additive white Gaussian noise (AWGN) and flat Rayleigh fading. The THP designs for these centralized and decentralized channels are presented, respectively.

Based on the THP principle introduced for single-path channels, we develop the THP techniques for multipath channels in Chapter 4. By combining the THP algorithm with multipath diversity in different ways, we present the PreRAKETHP and MDTHP designs in detail. The duality between these THP methods and Rx-based DF methods is analyzed. We also briefly review the principle of LRP. The performance of THP aided by LRP is observed in simulation experiments.

In Chapter 5, we focus on the linear decorrelating precoding methods. The previously proposed decorrelating methods are first presented for the purpose of comparison. Then we describe the novel PreRAKELDP and MDP. In these derivations, multiple transmit antennas are considered. These two proposed methods are compared with the nonlinear THP, linear decorrelating precoders and linear decorrelating multiuser detectors. Finally, the significant conclusions of this thesis are summarized in Chapter 6.

Chapter 2

DECORRELATING MULTIUSER DETECTION FOR UPLINK CDMA

2.1 Frequency-selective Fading Uplink CDMA Channel Model

For the uplink of CDMA systems, MS transmit signals towards BS. Consider the uplink of a K-user DS/CDMA system with a set of pre-assigned normalized signature sequences $s_i(t)$, $i = 1, 2, \ldots, K$, where each sequence is restricted to a symbol interval of duration T. The data symbol for the ith user in the nth symbol interval is denoted by $b_i(n)$. In practical wireless environment, the transmit signals are corrupted by fading and additive noise. If the data symbol duration is much smaller than the channel coherence, the channel is slowly fading, implying that the channel characteristics can be estimated accurately. If signal bandwidth is greater than the channel coherence bandwidth, the signal is subject to different gains and phase shifts across the band, thus the fading is said to be frequency-selective [Pro01]. The practical CDMA channels are usually frequency selective, due to the large bandwidth of spread-spectrum signals. In this case, the received signal includes multiple versions of the transmitted waveform which are attenuated and delayed in time. The frequency-selective slow fading channel can be modeled by a tapped-delay line [Pro01]. Suppose there are N resolvable paths from each MS to the BS. In the nth transmit symbol interval, $c_{i,l}(n) = \alpha_{i,l}(n)e^{j\varphi_{i,l}(n)}$ represents the gain of the lth path component over the channel between the ith user transmitter and the receiver, $\forall\ i = 1,2,\ldots,K$ and $l = 0,1,\ldots, N$-1. In the special case of Rayleigh fading, $c_{i,l}(n)$ is a complex Gaussian random process; equivalently, the magnitudes $\alpha_{i,l}(n)$ are Rayleigh-distributed and the phases $\varphi_{i,l}(n)$ are uniformly

distributed. Due to uncorrelated scattering assumption, the channel gains corresponding to different paths are statistically independent.

Suppose K users transmit a stream of $2M+1$ data bits simultaneously, and their signals are received synchronously at the BS, then the equivalent low-pass received signal is

$$r(t) = \sum_{n=-M}^{M} \sum_{i=1}^{K} \sum_{l=0}^{N-1} c_{i,l}(n)b_i(n)s_i(t-nT-lT_c)) + n(t), \qquad (2.1)$$

where T_c is the chip duration and $n(t)$ is a white Gaussian noise process with zero mean and power spectrum density N_0. From equation (2.1), it is seen that even if the spreading codes are orthogonal, due to multipath fading, in the received signal there is multiple access interference (MAI), including inter-user interference, inter-symbol interference (ISI) and inter-chip interference (ICI). When the chip interval T_c is much smaller than the symbol interval T and the multipath delay spread T_m is on the order of a few chip intervals, the ISI due to channel dispersion may be neglected [ZB96]. For synchronous channels with this assumption, (2.1) can be simplified by only considering a single symbol interval $[0, T)$,

$$r(t) = \sum_{i=1}^{K} \sum_{l=0}^{N-1} c_{i,l}b_is_i(t-lT_c) + n(t), \qquad (2.2)$$

Where $c_{i,l} = c_{i,l}(0)$ and $b_i = b_i(0)$.

The data symbols of all users can be expressed as a vector $\mathbf{b} = [b_1, b_2,..., b_K]^T$. Suppose the data symbols are M-ary PAM modulated with the minimum Euclidean distance $2A_i$, i.e., $b_i \in \{-(M-1)A_i, -(M-3)A_i,...,(M-3)A_i, (M-1)A_i\}$, $i = 1, 2,..., K$. Define the signature sequence vectors $\mathbf{s}_i(t) = [s_i(t)\ s_i(t-T_c)\ ...\ s_i(t-(N-1)T_c)]^T$, $i = 1, 2,..., K$. For all the K users,

define the vector of delayed signature sequences, $\mathbf{s}(t) = [\mathbf{s}_1(t)^T \; \mathbf{s}_2(t)^T \; \dots \; \mathbf{s}_K(t)^T]^T$, and the correlation matrix of delayed signature sequences

$$\mathbf{R} \equiv \int_0^T \mathbf{s}(t)\mathbf{s}^T(t)dt, \tag{2.3}$$

The channel gain vector for the ith user is defined as $\mathbf{c}_i = [c_{i,0} \; c_{i,1} \; \dots \; c_{i,N-1}]^T$; and for K users, define KN-row, K-column matrix $\mathbf{C}$ as

$$\mathbf{C} = diag\{\mathbf{c}_i\} = \begin{bmatrix} \mathbf{c}_1 & \mathbf{0} & \mathbf{0} & \dots & \mathbf{0} \\ \mathbf{0} & \mathbf{c}_2 & \mathbf{0} & \dots & \mathbf{0} \\ \dots & \dots & \dots & \dots & \dots \\ \mathbf{0} & \mathbf{0} & \dots & \dots & \mathbf{c}_K \end{bmatrix}, \tag{2.4}$$

in which $\mathbf{0} = \{0\}_{N \times 1}$. The conjugate transpose of $\mathbf{c}_i$ is $\mathbf{c}_i^H = [c_{i,0}{}^*, c_{i,1}{}^*, \dots, c_{i,N-1}{}^*]$. Hence, the conjugate transposed matrix of $\mathbf{C}$ is $\mathbf{C}^H = diag\{\mathbf{c}_i^H\}$, which has K rows and KN columns.

By employing the D-transform and spectral factorization as in [Due95], the above synchronous system model can be extended to the asynchronous case. Since the mathematical model for asynchronous channels is in the form similar to that for synchronous channels, the MAI cancellation approaches for asynchronous channels can be easily derived from those for synchronous case. Therefore, without loss of generality, we only demonstrate MAI cancellation methods for synchronous channels.

2.2 Linear Decorrelating Multiuser Detection Techniques

2.2.1 RAKE Decorrelating Detector (RDD)
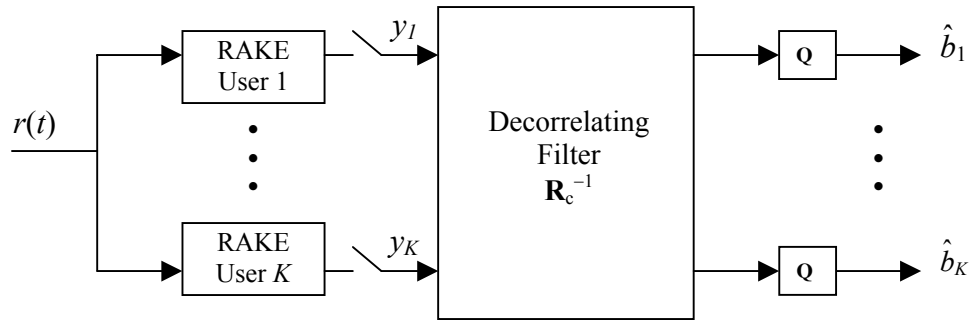
Figure 2.1 Decorrelating Detector (RDD) for a *K*-user *N*-channel paths/user system

The conventional RAKE receiver is optimal in the absence of MAI; therefore it can be employed for single-user systems. However, the RAKE receiver suffers from near-far effects in the presence of interfering signals received over independent fading channels [KS93]. Even with perfect channel tracking, the near-far problem imposes a fundamental limit on the performance of conventional RAKE receiver.

In order to exploit the multipath diversity offered by the multipath propagation, but avoid the prohibitive complexity of optimal MLSE detection, the method of RAKE decorrelating detector (RDD) applies a bank of conventional RAKE combiners, which is followed by a linear decorrelating filter [HS94]. The receiver structure for a *K*-user and *N*-channel paths/user system is shown in Fig. 2.1.

Assuming the BS can perfectly estimate the channel coefficients, the front-end of the RDD receiver consists of K RAKE combiners. The outputs are incorporated into a vector, $\mathbf{y} = [y_1, y_2,\ldots, y_K]^T$. The outputs of the RAKE MF bank are sampled at the end of each symbol interval, and the resulting output vector $\mathbf{y}$ is composed of K elements, $y_1, y_2,\ldots, y_K$, which are given by

$$y_k = \int_0^T r(t)\mathbf{c}_k{}^H\mathbf{s}_k(t)dt, \quad k = 1, 2,\ldots, K, \tag{2.5}$$

where $\mathbf{c}_k$ and $\mathbf{s}_k(t)$ follow the same definitions as those in section 2.1. For all the K users, the RAKE combining output vector can be expressed by

$$\mathbf{y} = \mathbf{R}_c\mathbf{b} + \mathbf{n}, \tag{2.6}$$

where $\mathbf{R}_c \equiv \mathbf{C}^H\mathbf{R}\mathbf{C}$ is a $K{\times}K$ matrix. The element on the ith row jth column of $\mathbf{R}_c$ is

$R_{cij} = \int_0^T \mathbf{s}_i(t)\mathbf{c}_i\mathbf{c}_j{}^H\mathbf{s}_j(t)dt, \ \forall \ i,j = 1, 2,\ldots, K$. The noise vector $\mathbf{n}$ is zero-mean Gaussian with autocorrelation matrix $N_0\mathbf{R}_c$. If $\mathbf{y}$ is filtered by $\mathbf{R}_c^{-1}$, the MAI can be cancelled,

$$\mathbf{R}_c^{-1}\mathbf{y} = \mathbf{b} + \mathbf{R}_c^{-1}\mathbf{n}. \tag{2.7}$$

For BPSK systems, the average transmit SNR per bit for the kth user is given by [Pro01]

$\gamma_{bk} \equiv \dfrac{E_{bk}}{N_0} = \dfrac{A_k{}^2}{2N_0}$, $k = 1, 2,\ldots, K$. Therefore, the theoretical SER can be expressed in terms of γ_{bk},

$$Pe_k = Q\left(\sqrt{\frac{2\gamma_{bk}}{[\mathbf{R}_c^{-1}]_{k,k}}}\right), \tag{2.8}$$

where $[\mathbf{R}_c^{-1}]_{kk}$ is the kth diagonal element of matrix $\mathbf{R}_c^{-1}$.

It is illustrated in [LV89] that the conventional decorrelating detector for single path signals provides optimum linear multiuser detector performance in the maximum-likelihood sense when the users' energies are unknown. The RDD is a linear detector which do not require knowledge of the user energies. If $\hat{s}_i(t) \equiv \sum_{l=0}^{N-1} c_{i,l} s_i(t - lT_c)$ is regarded as the ith user's signature waveform, the RDD has the structure similar to the conventional decorrelating detector; hence, the RDD should provide the optimum performance over all linear multiuser detectors for multipath signals of unknown energy.

2.2.2 Multipath Decorrelating Detector (MDD)
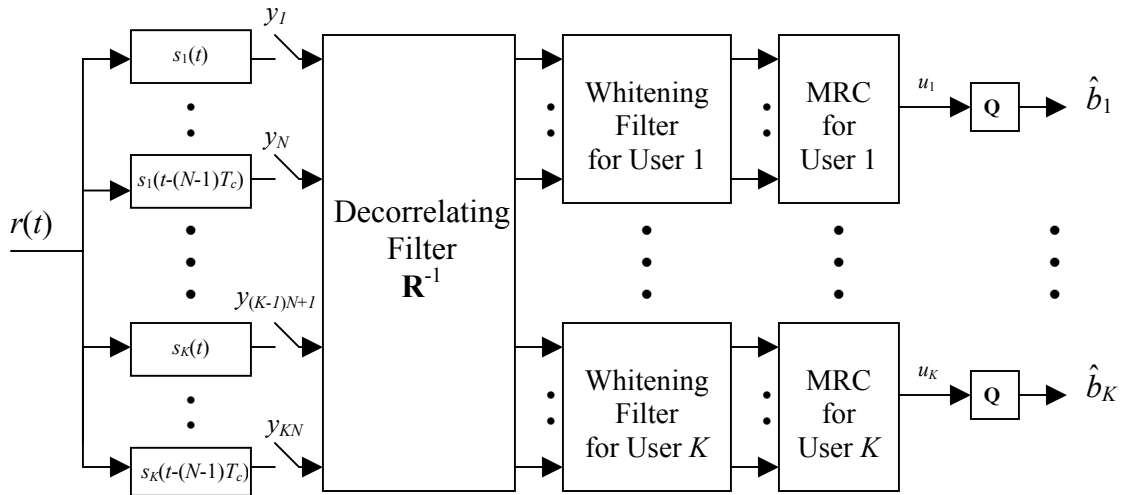
Figure 2.2 Multipath Decorrelating Detector (MDD) for a *K*-user *N*-channel paths/user system

13

Compared to RDD, MDD is a simpler but suboptimal linear multiuser detector. As shown in Fig. 2.2, the front end of the MDD detector consists of KN correlators. Represent the KN outputs of the correlators by a vector, $\mathbf{y} = [y_1, y_2,\ldots, y_{KN}]^T$. Then $\mathbf{y}$ is given by

$$\mathbf{y} = \int_0^T r(t)\mathbf{s}(t)dt = \mathbf{RCb} + \mathbf{n}. \tag{2.9}$$

$\mathbf{n}$ is the Gaussian noise vector with zero mean and autocorrelation matrix $N_0\mathbf{R}$. To eliminate MAI, the decorrelating filter is defined as $\mathbf{R}^{-1}$. The decorrelated result is

$$\mathbf{v} = \mathbf{R}^{-1}\mathbf{y} = \mathbf{Cb} + \mathbf{n}_v \tag{2.10}$$

We know in the vector $\mathbf{v} = [v_1, v_2, \ldots, v_{KN}]^T$, every N elements correspond to one user, thus it is convenient to define $\mathbf{v}_k = [v_{(k-1)N+1}, v_{(k-1)N+2}, \ldots, v_{kN}]^T$, $\forall\, k = 1, 2,\ldots, K$, then $\mathbf{v} = [\mathbf{v}_1^T, \mathbf{v}_2^T,\ldots, \mathbf{v}_K^T]^T$. From equation (2.10), we have

$$\mathbf{v}_k = \mathbf{c}_k b_k + \mathbf{n}_k, \quad k = 1, 2,\ldots, K, \tag{2.11}$$

in which $\mathbf{n}_k = [n_{(k-1)N+1}, n_{(k-1)N+2}, \ldots, n_{kN}]^T$. The autocorrelation matrix of $\mathbf{n}_k$ is $N_0[\mathbf{R}^{-1}]_{k,k}$, ($[\mathbf{R}^{-1}]_{i,j}$ is the i,jth $N \times N$ block of $\mathbf{R}^{-1}$). Due to noise correlation among the N branches for the kth user at the output of the decorrelating filter, the whitening operation is introduced prior to combining. The whitening filter for the kth user $\mathbf{D}_k^{-T}$ is obtained from Cholesky factorization [GV96], $[\mathbf{R}^{-1}]_{k,k} = \mathbf{D}_k^T\mathbf{D}_k$, $\forall k = 1,2,\ldots,K$. The whitened result, denoted by $\mathbf{v}_{wk}$, is given by

$$\mathbf{v}_{wk} = \mathbf{D}_k^{-T}\mathbf{v}_k = \mathbf{D}_k^{-T}\mathbf{c}_k b_k + \mathbf{n}_{wk}, \quad k = 1, 2,\ldots, K. \tag{2.12}$$

The whitened noise $\mathbf{n}_{wk} = \mathbf{D}_k^{-T}\mathbf{n}_k$ is zero-mean and Gaussian with the autocorrelation matrix $N_0\mathbf{I}_{N \times N}$.

In the scenario of whitened noise, maximal ratio combining (MRC) is the optimal combiner in the sense of achieving the highest SNR at the input of detection device [Pro01].

Although MRC is the optimal combiner, the noise-whitening process in MDD re-introduces the self-interference for every user, since the N branches of signal for each user becomes correlated when the noise components are whitened. This self-interference degrades system performance. Each element of the combined result, $\mathbf{u} = [u_1, u_2,\ldots, u_K]$, which is also the decision variable for each user, equals

$$u_k = (\mathbf{D}_k^{-T}\mathbf{c}_k)^H\mathbf{v}_{\mathrm{w}k} = \mathbf{c}_k^H([\mathbf{R}^{-1}]_{k,k})^{-1}\mathbf{c}_k b_k + \mathbf{c}_k^H\mathbf{D}_k^{-1}\mathbf{n}_{\mathrm{w}k},\quad k = 1, 2,\ldots, K. \quad (2.13)$$

We can calculate that the noise component for user k is white Gaussian with power $N_0\mathbf{c}_k([\mathbf{R}^{-1}]_{k,k})^{-1}\mathbf{c}_k^H$. Hence, the instantaneous BER for user k can be expressed in terms of γ_{bk},

$$Pe_k = Q\left(\sqrt{2\mathbf{c}_k^H([\mathbf{R}^{-1}]_{k,k})^{-1}\mathbf{c}_k\gamma_{bk}}\right),\quad k = 1, 2,\ldots, K. \quad (2.14)$$

It has been mathematically proved that the performance of RDD is better than MDD (see Appendix of [HS94]). On the other hand, MDD has lower complexity, since the $KN{\times}KN$ matrix inversion for MDD is not dependent on the channel coefficients and only need to be done when the set of active signature waveforms changes; while RDD require the inversion of the $K{\times}K$ matrix $\mathbf{R}_\mathrm{c}$ during almost each symbol interval because the matrix is dependent on the channel conditions.

2.3 Decision-Feedback Decorrelating Multiuser Detection Techniques

For single-path channels, the nonlinear DF decorrelator achieves better performance than linear decorrelator [Due93]. Similarly, we will see that in the case of multipath channels, the DF approaches outperform the linear decorrelators discussed above. In section 2.3, we will discuss the two DF MUDs which employ the same MF structure as RDD and MDD, respectively.

2.3.1 RAKE Decorrelating Decision-Feedback Receiver (RDDFR)
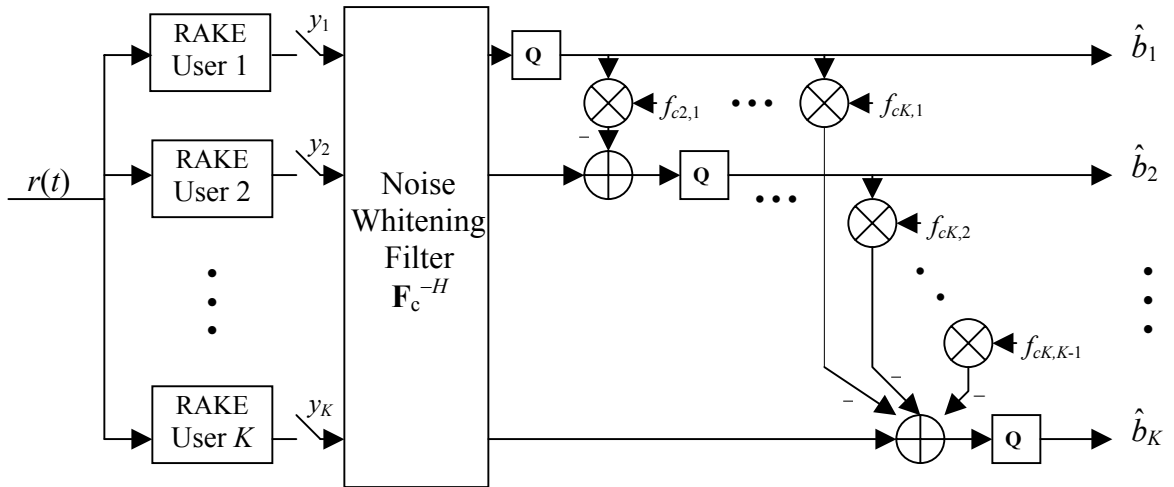
Figure 2.3 RAKE Decorrelating Decision Feedback Multiuser Receiver (RDDFR) for a *K*-user *N*-channel paths/user system

As we have discussed for the method of RDD, if we use RAKE matched filters at the front end of the receiver, the resulting output is given by equation (2.6), in which the correlation matrix $\mathbf{R}_c = \mathbf{C}^H \mathbf{R} \mathbf{C}$ is symmetric and positive definite. Therefore, by Cholesky

16

factorization, we obtain $\mathbf{R}_c = \mathbf{F}_c^H \mathbf{F}_c$, in which $\mathbf{F}_c = \{f_{ci,j}\}_{K \times K}$ is an upper triangular matrix. In the proposed RDDFR detector, following the RAKE MF bank is a noise-whitening feed-forward filter, as shown in Fig. 2.3. The output vector of the filter $\mathbf{F}_c^{-H}$ is equal to

$$\widetilde{\mathbf{y}} = \mathbf{F}_c^{-H}\mathbf{y} = \mathbf{F}_c\mathbf{b} + \mathbf{z}, \tag{2.15}$$

where vector $\mathbf{z} = [z_1, z_2,..., z_K]^T = \mathbf{F}_c^{-H}\mathbf{n}$. As shown in section 2.2.1, the autocorrelation matrix of $\mathbf{n}$ is $N_0\mathbf{R}_c$. Consequently, the autocorrelation matrix of $\mathbf{z}$ is $N_0\mathbf{I}$, that is, the noise is whitened by the feed-forward filter.

Similar to the DF MUD for single-path channels, in order to reduce the error propagation effect, we assume the K users are ordered according to their transmit signal power, i.e., user 1 is the strongest and user K is the weakest. Define the feedback filter as

$$\mathbf{B} = \mathbf{F}_c - diag(\mathbf{F}_c), \tag{2.16}$$

which is a lower triangular matrix with all-zero diagonal. As shown in Fig. 2.3, first the symbol of user 1 is estimated. From equation (2.15), we know the feed-forward filter output for user 1 is $\widetilde{y}_1 = f_{c1,1}b_1 + z_1$. Hence, the decision variable for user 1 should be $f_{c1,1}^{-1}\widetilde{y}_1$. Suppose the estimated symbol corresponding to b_1 is denoted by $\hat{b}_1$. For user i, $i = 2, 3,..., K$, the decision variable is $f_{ci,i}^{-1}(\widetilde{y}_i - \sum_{j=1}^{i-1} f_{ci,j}\hat{b}_j + z_i)$. If define a vector $\hat{\mathbf{b}} = [\hat{b}_1, \hat{b}_2 ,..., \hat{b}_K]^T$, the decision device inputs for all K users can be expressed by

$$diag(\mathbf{F}_c)^{-1}(\widetilde{\mathbf{y}} - \mathbf{B}\hat{\mathbf{b}}) = \hat{\mathbf{b}} + diag(\mathbf{F}_c)^{-1}\mathbf{F}_c(\mathbf{b}-\hat{\mathbf{b}}) + diag(\mathbf{F}_c)^{-1}\mathbf{z} \tag{2.17}$$

It is seen that the system performance is degraded by error propagation, which is reflected by the second term in equation (2.17). The ideal SER can be obtained by assuming there is no decision error, i.e., $\hat{\mathbf{b}} = \mathbf{b}$. For the kth user, $k = 1, 2,…, K$, the ideal BER is

$$Pe_k = Q\left(\sqrt{2f_{ck,k}{}^2 \gamma_{bk}}\right). \tag{2.18}$$

Now we compare the theoretical performance of the nonlinear RDDFR and that of the linear RDD given by equation (2.8). Note that $\mathbf{R}_c{}^{-H}=\mathbf{F}_c{}^{-H}\mathbf{F}_c{}^{-1}$ and therefore $(\mathbf{R}_c{}^{-1})_{kk} \geq [(\mathbf{F}_c{}^{-1})_{kk}]^2 = f_{ckk}{}^{-2}$ ($(\mathbf{R}_c{}^{-1})_{kk} = [(\mathbf{F}_c{}^{-1})_{kk}]^2$ is satisfied only when $k = 1$). Thus the ideal RDDFR outperforms the RDD (the optimal decorrelating linear MUD) for all users $k > 1$; for the first user, these two methods have the same theoretical performance. Since it has been proved in [HS94] that the RDD outperforms the MDD, the RDDFR also outperforms MDD theoretically. With the analysis similar to that for the optimality of the RDD, it is easy to conclude that the *ideal* RDDFR is the optimal decorrelating decision-feedback MUD. However, the practical performance of RDDFR is degraded by the error propagation effect. Similar to the DF MUD for AWGN channels [Due93], the error propagation effect can be mitigated by ordering the users from the strongest to the weakest.

2.3.2 Multipath Decorrelating Decision-Feedback Receiver (MDDFR)

The MDDFR was proposed in [SK97]. In this method, the KN correlators are employed at the front end of the receiver in the same way as for MDD in Fig. 2.4, the output of the correlators is given by equation (2.9). From the definition of $\mathbf{R}$ in equation (2.3), it can be observed that $\mathbf{R}$ is symmetric and positive definite. Thus by Cholesky factorization, $\mathbf{R} = \mathbf{F}^T\mathbf{F}$, in which $\mathbf{F} = \{f_{ij}\}_{KN \times KN}$ is a real lower triangular matrix. As shown in Fig. 2.4, following the MF bank is a linear filter $\mathbf{F}^{-T}$, the resulting output is

$$\mathbf{F}^{-T}\mathbf{y} = \mathbf{F}\mathbf{C}\mathbf{b} + \mathbf{n}_w, \tag{2.19}$$

where $\mathbf{n}_w = (\mathbf{F}^T)^{-1}\mathbf{n}$ is a zero-mean white Gaussian noise vector.

Divide the $NK \times NK$ matrix $\mathbf{F}$ into K^2 square blocks, each block is an $N \times N$ matrix; and represent the block on the ith row jth column by $[\mathbf{F}]_{i,j}$. The maximal-ratio combining (MRC) is performed for user 1 first. The first N branches of the whitening filter outputs are filtered by $\mathbf{c}_1^H[\mathbf{F}]_{1,1}^T$, thus the input to the decision device for user 1 is

$$v_1 = \mathbf{c}_1^H[\mathbf{F}]_{1,1}^T [\mathbf{F}]_{1,1}\mathbf{c}_1 b_1 + z_1, \tag{2.20}$$

where z_1 is the noise component. The symbol decision for user 1, denoted by $\hat{b}_1$, is fed back to the remaining users to help to cancel the MAI due to user 1. In this way, using the channel coefficients (which are assumed to be perfectly known at the base station) and the decisions of the previous $k-1$ users, the MAI cancellation and MRC for user k, $k = 2, 3,..., K$, is performed as

$$v_k = \mathbf{c}_k^H([\mathbf{F}]_{k,k})^T \sum_{i=1}^{k-1}[\mathbf{F}]_{k,i}\mathbf{c}_i(b_i - \hat{b}_i) + \mathbf{c}_k^H([\mathbf{F}]_{k,k})^T[\mathbf{F}]_{k,k}\mathbf{c}_k b_k + z_k, \tag{2.21}$$

where $\hat{b}_i$ is the symbol decision corresponding to b_i. Similar to the decorrelating DF MUD for single-path channels [Due93], to minimize error propagation, the K users should be sorted from the strongest to the weakest, i.e., the first user should be the one whose signal has the strongest power, and the last user is the weakest one. By assuming no error propagation, we can obtain the ideal SER

$$Pe_k = Q\left(\sqrt{\mathbf{c}_k^H[\mathbf{F}]_{k,k}^T[\mathbf{F}]_{k,k}\mathbf{c}_k\gamma_{bk}}\right). \tag{2.22}$$

19

The MDDFR is a suboptimal MUD even if the error propagation effect is ignored. An intuitive explanation is that the *KN* correlators at the front end of receiver are not the matched filters perfectly matched to the multipath fading channels. The theoretical performance comparison between the MDDFR and the optimal RDDFR follows the same derivation as in the comparison between the PreRAKETHP and MDTHP, which is provided in section 4.3.2.

Although the error rate of the MDDFR is higher than that of RDDFR, it should be noted that MDDFR has the advantage of low computational complexity, since the operation of matrix factorization is made on **R**, which is independent of channel state information.

The nonlinear MDDFR is closely related to the linear MDD, noticing that they have the identical front-end correlator bank. Compare the decision statistic of MDTHP, $\mathbf{c}_k^H[\mathbf{F}]_{kk}^T[\mathbf{F}]_{kk}\mathbf{c}_k$, with that of MDD, $\mathbf{c}_k^H([\mathbf{R}^{-1}]_{kk})^{-1}\mathbf{c}_k$. Based on the theorem for the inverse of a partitioned symmetric matrix [HJ85], it is easy to prove that $\mathbf{c}_k^H[\mathbf{F}]_{kk}^T[\mathbf{F}]_{kk}\mathbf{c}_k \geq \mathbf{c}_k^H([\mathbf{R}^{-1}]_{kk})^{-1}\mathbf{c}_k$ (the equality is satisfied for $i = 1$). Therefore, for user 1 MDDFR and MDD have the same performance, and for other users MDDFR outperforms MDD, if the error propagation effect is not considered.
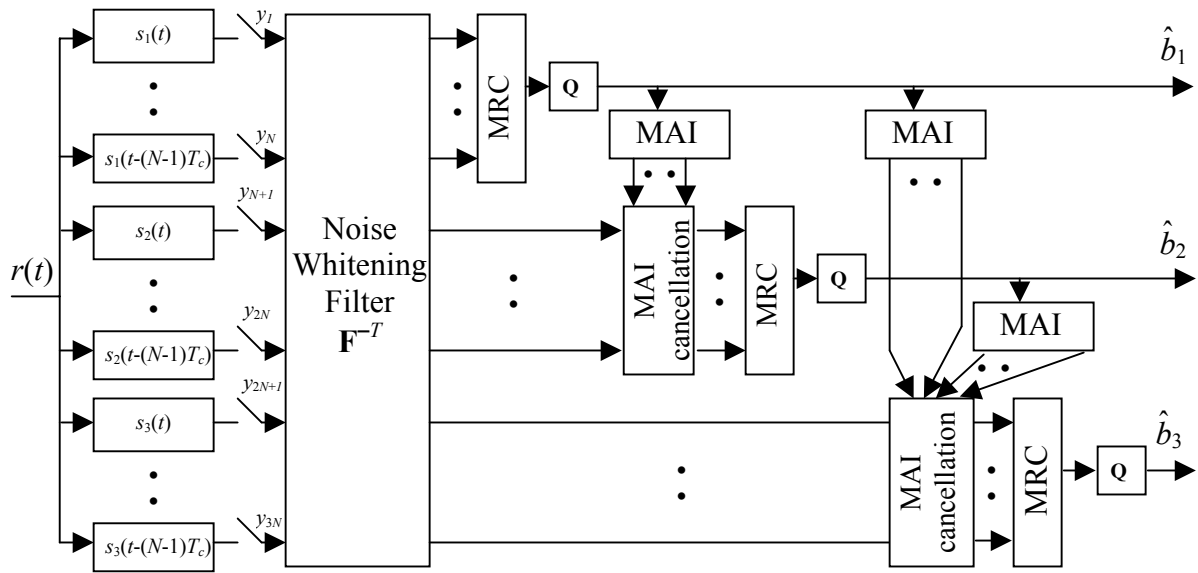
Figure 2.4 Multipath Decorrelating Decision Feedback Multiuser Receiver (MDDFR) for a 3-user *N*-channel paths/user system

2.4 Numerical Analysis

We consider the uplink of an 8-user, 4 channel paths/user BPSK system. Suppose the transmit power for all users are equal and the signature sequences for all users are orthogonal Hadamard sequences with 32-chip length. The user ordering for nonlinear DF MUD is not considered in this example. In Fig. 2.5, the performance of the dissussed linear decorrelating methods RDD and MDD and nonlinear decorrelating RDDFR and MDDFR are observed. The BER is averaged over all users. The single user bound (SUB) and conventional RAKE receiver are also simulated as references. It is obvious that the conventional RAKE receiver has poor performance in multiuser channels. Although theorectical analysis shows the nonlinear RDDFR and MDDFR have better performance than RDD and MDD, respectively, the practical performance of the nonlinear methods is degraded by the error propagation. It can be observed that the performance advantage of the nonlinear methods relative to the linear methods diminishes as transmit power increases. It is confirmed by this example that the optimal decorrelating linear MUD (RDD) and nonlinear MUD (RDDFR) respectively outperform the suboptimal linear MUD (MDD) and nonlinear MUD (MDDFR).
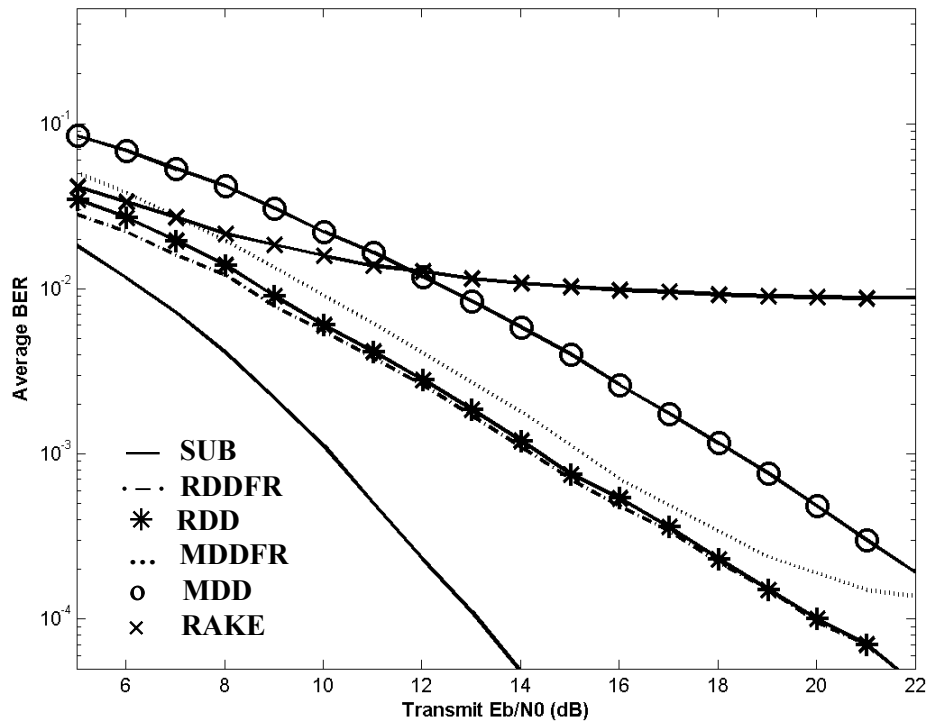
Figure 2.5 **Performance comparison of different MUD approaches, 8 users, 4 channel paths/user, BPSK, equal transmit power for all users.**

Chapter 3

TOMLINSON-HARASHIMA MULTIUSER PRECODING (THP) FOR

SINGLE-PATH CHANNELS

3.1 THP for Single-path AWGN Channels

3.1.1 Single-path Centralized Channels (CC)
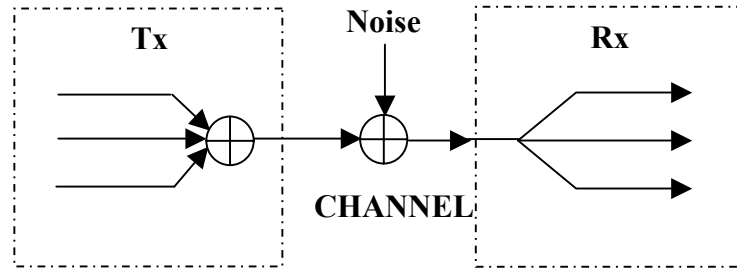
Figure 3.1 Centralized Channel Model

The system diagram of CC model is shown in Fig. 3.1. In the CC model, both the transmitter and the receiver are centralized for all users (or all sub-channels in multi-channel systems), which make it possible to perform the Tx-Rx joint optimization with balanced complexity for the transmitter and receiver. The CC model with MIMO DF detector has been applied in multicarrier [VCLM98], space-time [LP02, ANC01] and other MIMO systems [Due92].

For a K-user system, denote the transmit data symbols during the symbol interval of interest $[0, T)$ by a vector $\mathbf{b} = (b_1, b_2, \ldots, b_K)^T$. For high-speed downlink CDMA channels, the higher-order modulation is favorable because the data transmission efficiency can be

24

improved without increasing MAI [TSG01, BBG00]. In this chapter, we use pulse amplitude modulation (PAM) as an example in derivation, while quadrature amplitude modulation (QAM) is also considered in numerical experiments. Suppose the symbols are M-ary PAM modulated with the equivalent baseband minimum Euclidean distance $2A_i$, i.e., $b_i \in \{-(M-1)A_i, -(M-3)A_i, \ldots, (M-3)A_i, (M-1)A_i\}$, $\forall i = 1, 2, \ldots, K$. Let the vector of normalized signature waveforms for K users be $\mathbf{s}(t) = [s_1(t), s_2(t), \ldots, s_K(t)]^T$. For the CC systems, the equivalent low-pass received signal at the centralized receiver is

$r(t) = \sum_{i=1}^{K} b_i s_i(t) + n(t)$. In the conventional receiver, $r(t)$ is fed to the filters matched to the K users' signature waveforms. The resulting output is $y_i = \int_0^T r(t)s_i(t)\mathrm{d}t$, $i = 1, 2, \ldots, K$. If we define the correlation between two signature sequences as $R_{i,j} = \int_0^T s_i(t)s_j(t)\mathrm{d}t$, $\forall\, i, j = 1, 2, \ldots, K$, and the $K \times K$ correlation matrix $\mathbf{R} = \{R_{i,j}\}$, the matched filter (MF) output vector $\mathbf{y} = [y_1, y_2, \ldots, y_K]^T$ satisfies

$$\mathbf{y} = \mathbf{Rb} + \mathbf{n}. \tag{3.1}$$

In equation (3.1), $\mathbf{n} = [n_1, n_2, \ldots, n_K]^T$ is a zero-mean Gaussian noise vector with the elements $n_i = \int_0^T n(t)s_i(t)\mathrm{d}t$, $i = 1, 2, \ldots, K$, and the autocorrelation matrix $N_0\mathbf{R}$. Note that we retain the terminology of CDMA systems for the CC model. Although its primary applications are in multicarrier, space-time and other systems, the mathematical models for these applications are equivalent to those used in CDMA systems.

3.1.2 Single-path Decentralized Channels (DC)

As shown in Fig. 3.2, the DC model corresponds to the downlink of CDMA systems. In this channel model, the transmitter is centralized; the receivers of different users are separate, resource-constrained and do not have the knowledge of spreading codes of other users. Therefore, the processing burden is placed in the transmitter.
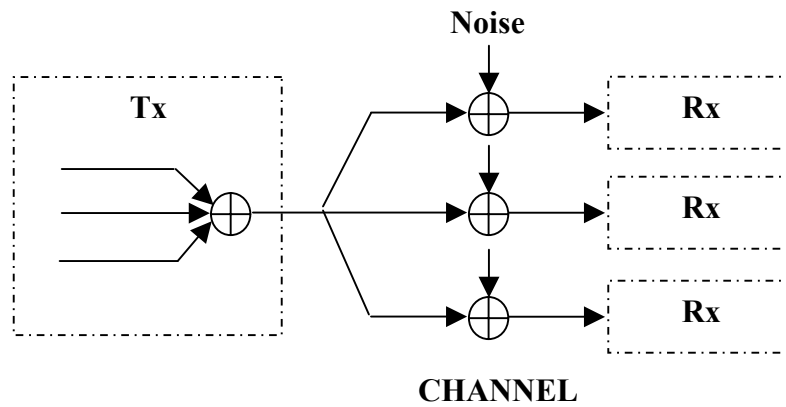
Figure 3.2 Decentralized Channel Model

For the DC model, e.g., the downlink of a CDMA system, the equivalent low-pass received signal at the ith receiver is $r_i(t) = \sum_{i=1}^{K} b_i s_i(t) + n_i(t)$, where $n_i(t)$ represents white Gaussian noise with zero mean and power spectrum density N_0. In the ith user's receiver, $r_i(t)$ is fed to the filter matched to $s_i(t)$. The resulting output is $y_i = \int_0^T r_i(t) s_i(t) \mathrm{d}t, \ \forall i = 1, 2, \ldots, K.$The

MF output has the same form as equation (3.1), but for DC model the autocorrelation matrix

of $\mathbf{n}$ is $N_0\mathbf{I}$. ($\mathbf{I}$ is the $K \times K$ identity matrix.) In practice, these channels are not degraded by

MAI due to the orthogonal signature sequences and synchronous transmission, and thus, do

not require Tx precoding. However, as in [VJ98, TC94], we employ this simple model with

non-orthogonal users' codes to illustrate the general principle of multiuser THP precoding.

3.1.3   THP for Centralized Channel (THP-CC)

From equation (3.1), we observe that MAI is caused by the non-diagonal elements of

matrix $\mathbf{R}$. For CC systems, as well as for the uplink of DS–CDMA, the interference can be

conveniently canceled by the linear decorrelating MUD [Ver98] The output is $\mathbf{R}^{-1}\mathbf{y} = \mathbf{b}+\mathbf{z}$.

Since the linear MUD enhances noise, the nonlinear DF-MUD was proposed in [Due93]. The

positive definite symmetric matrix $\mathbf{R}$ is decomposed by Cholesky factorization [GVL96],

$$\mathbf{R} = \mathbf{F}^T\mathbf{F}, \tag{3.2}$$

where $\mathbf{F}$ is a lower triangular matrix. For DF-MUD, a nonlinear feedback loop and a feed-

forward filter are used to cancel the partial MAI expressed by $\mathbf{F}$ and $\mathbf{F}^T$ respectively. This

approach avoids noise enhancement and outperforms linear decorrelating method; however,

because the feedback is based on past decisions, the performance is degraded by error

propagation.

Fig. 3.3 shows the system diagram of THP-CC. The feedback filter in the transmitter

is defined as

$$\mathbf{B}_{CC} = \{B_{ij}\}_{K \times K} = diag(\mathbf{F})^{-1} \times \mathbf{F} - \mathbf{I}, \tag{3.3}$$

where $\mathbf{F}$ is as in equation (3.2), and $diag(\mathbf{F})^{-1} = diag(\mathbf{F}^{-1})$ is the diagonal matrix that contains

the diagonal elements of $\mathbf{F}^{-1}$. Thus, $\mathbf{B}_{CC}$ is a lower triangular matrix with zeros along the

diagonal. A bank of mod-2M operators are used to limit the transmit power. For user i, given

an arbitrary real input β, the output of the mod-2M operator $\tilde{\beta}$ satisfies $\tilde{\beta}/A_i = \beta/A_i + 2Md_i$,

(a) Transmitter   (b) Receiver
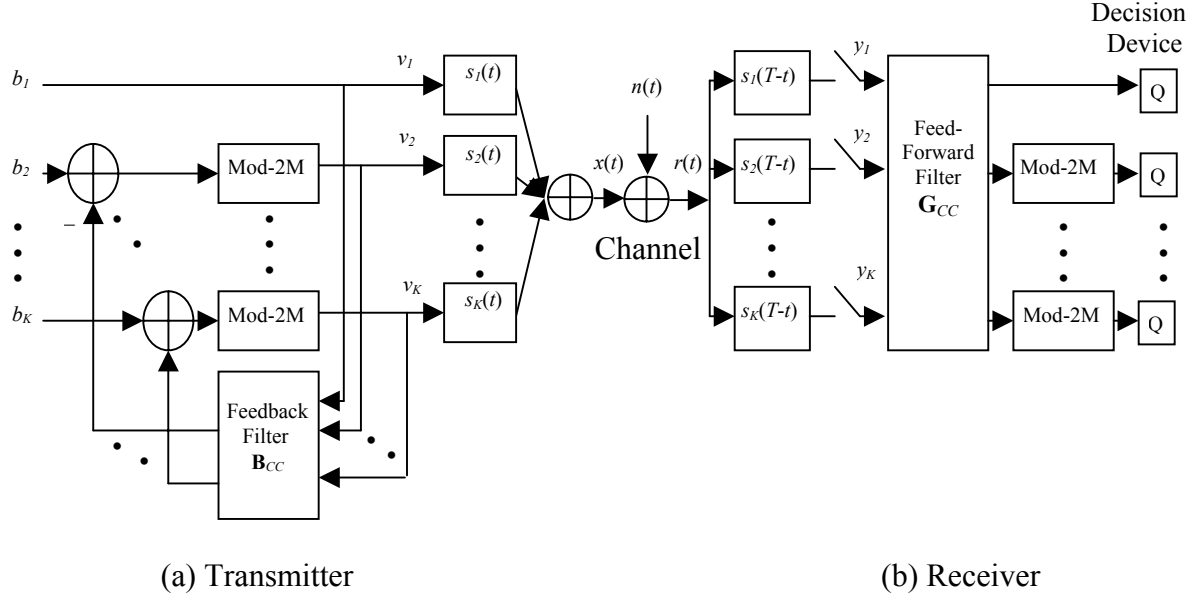
Figure 3.3 Diagram of THP for a Centralized-Channel (CC) System

where d_i is the integer to render $\tilde{\beta}/A_i$ within $(-M, M]$. In Fig. 3.3(a), the output vector of the

mod-2M operator bank $\mathbf{v} = [v_1, v_2, \ldots, v_K]^T$ satisfies

$$\mathbf{v} = \mathbf{b} - \mathbf{B}_{CC}\mathbf{v} + 2M\mathbf{A}\mathbf{d} = (\mathbf{B}_{CC} + \mathbf{I})^{-1}(\mathbf{b} + 2M\mathbf{A}\mathbf{d}), \tag{3.4}$$

where $\mathbf{A} = diag\{A_i\}_{K \times K}$ and $\mathbf{d} = [d_1, d_2, \ldots, d_K]^T$ is an integer vector. For the ith user,

$i = 1, 2, \ldots, K$, d_i is chosen to guarantee v_i in the range $(-A_iM, A_iM]$. Equation (3.4) is

equivalent to $(\mathbf{B}_{CC} + \mathbf{I})\mathbf{v} = \mathbf{b} + 2M\mathbf{A}\mathbf{d}$. Note that $(\mathbf{B}_{CC} + \mathbf{I})$ is a lower triangular matrix with

28

ones along the diagonal. Thus, $v_1=b_1$ and $d_1=0$, i.e., mod-2M is not required for user 1; for the ith user, $i = 2, 3, \ldots, K$, we can successively determine d_i and v_i based on the values of v_1, $v_2,\ldots, v_{i\text{-}1}$,

$$v_i = (b_i - \sum_{j=1}^{i-1} B_{ij}v_j) + 2MA_i d_i. \tag{3.5}$$

The feedback structure is similar to that of DF-MUD. However, because the feedback in the transmitter is based on the actual values of user data instead of past decisions, error propagation is avoided.

The received signal is $r(t) = \mathbf{s}^T(t)\mathbf{v}+n(t)$. In Fig. 3.3(b), the output vector of the MF bank, $\mathbf{y} = [y_1, y_2, \ldots, y_K]^T$, is

$$\mathbf{y} = \mathbf{Rv} + \mathbf{n}. \tag{3.6}$$

Given (3.3) and (3.4), equation (3.6) is equivalent to

$$\mathbf{y} = \mathbf{F}^T diag(\mathbf{F})(\mathbf{b}+2M A \mathbf{d}) + \mathbf{n}. \tag{3.7}$$

To recover the original data $\mathbf{b}$, the feed-forward filter should be defined as

$$\mathbf{G}_{CC} = diag(\mathbf{F})^{-1}\mathbf{F}^{-T}, \tag{3.8}$$

Where $\mathbf{F}^{-T} = (\mathbf{F}^{-1})^T = (\mathbf{F}^T)^{-1}$, thus the output of $\mathbf{G}_{CC}$ is

$$\mathbf{G}_{CC}\mathbf{y} = \mathbf{b} + 2M A \mathbf{d} + \mathbf{z}_{CC}, \tag{3.9}$$

where $\mathbf{z}_{CC} = \mathbf{G}_{CC}\mathbf{n}$. Equation (3.9) shows that MAI has been completely eliminated at the output of the feed-forward filter. Finally, the mod-2M operations are performed for users 2 through K (mod-2M is not required for user 1 because $d_1 = 0$). The input vector to the detector is $\mathbf{b}+\mathbf{z}_{CC}$. The autocorrelation matrix of $\mathbf{z}_{CC}$ is $N_0 diag(\mathbf{F})^{-2}$, that is, the noise is

whitened. The average transmit signal to noise ratio (SNR) per bit for the ith user, γ_{bi}, equals [Pro01]

$$\gamma_{bi} \equiv \frac{E_{bi}}{N_0} = \frac{(M^2-1)A_i{}^2}{6N_0\log_2 M}, \quad i = 1, 2, \ldots, K. \tag{3.10}$$

Then the theoretical symbol error rate (SER) is

$$Pe_i = \frac{2(M\text{-}1)}{M}Q\left(\sqrt{\frac{6\log_2 M}{M^2\text{-}1}f_{ii}{}^2 \gamma_{bi}}\right), \quad i = 1, 2, \ldots, K, \tag{3.11}$$

where f_{ii} is the ith diagonal element of **F.** The SER given by (3.11) is identical to that of DF-MUD assuming no error propagation. It is observed that the order of users affects performance. For the first user, the ideal performance of THP equals that of the linear decorrelating MUD; for the last user, the ideal SER achieves the single user bound (SUB) since $f_{KK} = 1$.

Note that in the transmitter the mod-2M operator output v_i is in the range $(-A_iM, A_iM]$, which is larger than the range of original signal b_i, $[-A_i(M-1), A_i(M-1)]$, i.e., the signal power reduced by modulo operation is still larger than the original signal power. This power penalty diminishes as M increases and can be ignored for large M ($M \geq 8$) [LM94]. It also should be noted the actual performance is slightly worse than the ideal performance because of the "end effect" of modulo operations in the receiver. The property that the detection errors for outer signals are less likely than for other signals is lost due to the mod-2M operations in the receiver, because any outer symbol will be re-assigned a bounded magnitude. However, as observed in the simulation examples, the end effect also diminishes as M increases [LM94].

3.1.4 THP for Decentralized Channel (THP-DC)

The scheme proposed in the previous section can be applied in DC systems by using adaptive linear processing in the receivers. However, it is often desirable to make the receivers of DC systems (e.g. the mobile stations in downlink CDMA) as simple as possible. Therefore, in this section we propose a different THP design in which the receivers are as simple as in a single-user system. The diagram of this design is shown in Fig. 3.4. The relocation of the feed-forward filter from the receiver to the transmitter causes the changes in the structures of the feedback and the feed-forward filters denoted by $\mathbf{B}_{DC}$ and $\mathbf{G}_{DC}$, respectively. The signal received at the ith user's receiver site can be expressed as $r_i(t) = \mathbf{s}^T(t)\mathbf{G}_{DC}\mathbf{v}+n_i(t)$. With transmitter precoding, the output vector of the scaled MF bank is

$$\mathbf{y} = diag(\mathbf{F})^{-1}(\mathbf{RG}_{DC}\mathbf{v} + \mathbf{n}) = diag(\mathbf{F})^{-1}[\mathbf{F}^T\mathbf{FG}_{DC}(\mathbf{B}_{DC}+\mathbf{I})^{-1}(\mathbf{b}+2M\mathbf{Ad}) + \mathbf{n}]. \quad (3.12)$$

Although the scaled MF in the ith user receiver needs the knowledge of f_{ii}, this requirement does not significantly increase receiver complexity. To cancel MAI, we define $\mathbf{B}_{DC}$ and $\mathbf{G}_{DC}$ as

$$\mathbf{B}_{DC} = diag(\mathbf{F})^{-1}\mathbf{F}^T-\mathbf{I}, \quad (3.13)$$

$$\mathbf{G}_{DC} = \mathbf{F}^{-1}. \quad (3.14)$$

From (3.13), the feedback filter $\mathbf{B}_{DC}$ is now upper triangular with zeros along the diagonal. Thus the computation of the elements of $\mathbf{v}$ is in the reverse order relative to CC systems, i.e., $v_K = b_K$ and $d_K = 0$ (the mod-2M operation is not required for the last user). For $i = K\text{-}1, K\text{-}2,\ldots, 1$, $v_i=(b_i - \sum\limits_{j=i+1}^{K}B_{ij}v_j)+2MA_id_i$. It can be shown that the feed-forward filter given by equation (3.14) does not increase the average transmit power and the power scaling factor is not required.

Substituting (3.13) and (3.14) into (3.12), we obtain $\mathbf{y} = \mathbf{b}+2M\mathbf{A}\mathbf{d}+\mathbf{z}_{DC}$. Mod-2M operations are then applied to eliminate the term $2M\mathbf{A}\mathbf{d}$. The noise component $\mathbf{z}_{DC} = diag(\mathbf{F})^{-1}\mathbf{n}$ is whitened since its autocorrelation matrix is $N_0 diag(\mathbf{F})^{-2}$. The ideal SER of THP-DC is also given by (3.11).

In summary, THP-CC, THP-DC and DF-MUD have the same ideal performance provided that the effect of mod-2M operation in the THP schemes and the error propagation in DF-MUD are ignored. Since DF-MUD improves upon the linear decorrelating MUD for all but the first user [Due93], the proposed THP methods also have better performance than the linear decorrelating MUD. While this conclusion is valuable for CC systems, it is more meaningful to compare THP-DC with the linear transmitter precoding methods. For example, if equal transmit powers are employed for all users and all the transmit signals have the same cross-correlation, the linear decorrelating precoding has the same performance as the linear decorrelating MUD, and is outperformed by THP. The advantage of THP over linear schemes will be further demonstrated in numerical experiments.

(a) Transmitter   (b) Receiver
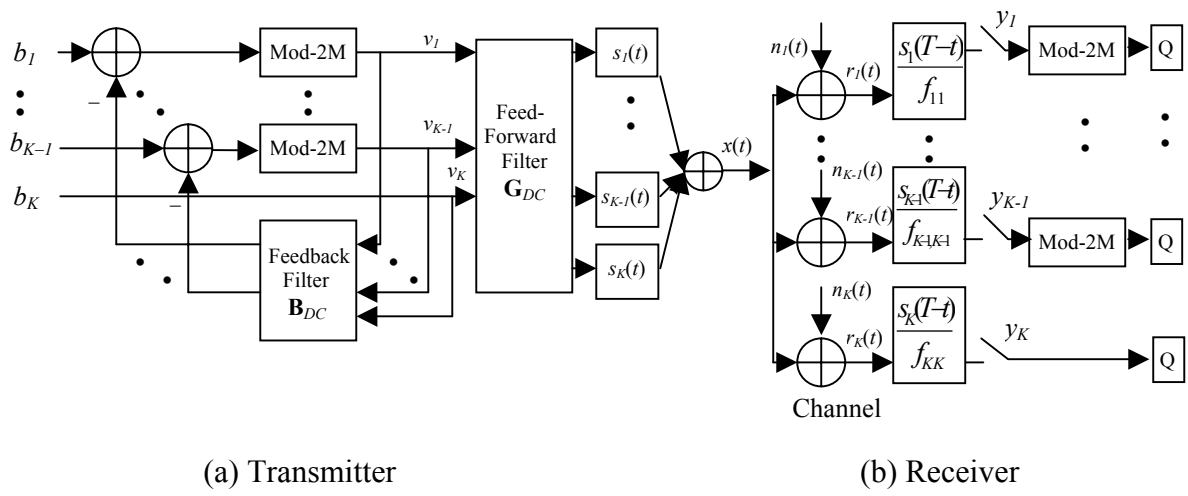
Figure 3.4 Diagram of THP for a Decentralized-Channel (DC) System

3.2 THP for Flat Rayleigh Fading Channels

In this section, we extend the THP approach to flat Rayleigh fading channels. In the symbol interval of interest, the channel gain for the ith user is denoted as $c_i = \alpha_i e^{j\phi_i}$, where the envelope α_i has Rayleigh distribution and the phase ϕ_i is uniformly distributed over $(-\pi, \pi]$, $i = 1, 2, \ldots, K$. Define the channel gain matrix for K users as $\mathbf{C} = diag\{c_i\}_{K \times K}$.

For the DC system, the signal received at the ith user receiver is $r_i(t) = c_i \mathbf{s}^T(t)\mathbf{v} + n_i(t)$. With the THP-DC, the output vector of the MF bank equals

$$\mathbf{y} = \mathbf{CRv} + \mathbf{n} = \mathbf{C}diag(\mathbf{F})(\mathbf{b} + 2M\mathbf{Ad}) + \mathbf{n}. \tag{3.15}$$

The received signals are detected coherently, scaled and passed through the mod-2M operators. The input of the detection device in the ith user receiver is $\alpha_i f_{ii} b_i + n_i$. The average SNR per bit at the input of the detection device γ_{bi} has the mean

$$\bar{\gamma}_{bi} = \frac{(M^2 - 1)f_{ii}^2 A_i^2}{6N_0 \log_2 M} E\{\alpha_i^2\}, \quad i = 1, 2, \ldots, K. \tag{3.16}$$

For the ith user, the average SER is given by [Pro01]

$$Pe_i = \frac{M-1}{M}\left(1 - \sqrt{\frac{3(\log_2 M)\bar{\gamma}_{bi}}{M^2 - 1 + 3(\log_2 M)\bar{\gamma}_{bi}}}\right). \tag{3.17}$$

For the CC model over the Rayleigh fading channel, the received signal is $r(t) = \sum_{i=1}^{K} c_i v_i s_i(t) + n(t)$. The MF bank in the receiver is followed by the diagonal matrix $\mathbf{C}^H$, resulting in the output $\mathbf{y} = \mathbf{C}^H\mathbf{RCv} + \mathbf{C}^H\mathbf{n}$. Define $\hat{\mathbf{F}} = \mathbf{FC}$, which is also a lower triangular matrix, then the feedback and feed-forward filters are the same as (3.3) and (3.8) except that $\hat{\mathbf{F}}$ replaces $\mathbf{F}$. The output of the feed-forward filter is $\mathbf{b} + 2M\mathbf{Ad} + \mathbf{z}_{CC}$, where $\mathbf{z}_{CC} = \mathbf{G}_{CC}\mathbf{C}^H\mathbf{n}$ is

white noise vector with auto-correlation matrix $N_0 diag(\mathbf{F})^{-2}\mathbf{C}^{-2}$. Thus, the mean of average SNR per bit at the detector input and the average SER are still given by (3.16) and (3.17), respectively.

For the THP-CC above, we assumed perfect knowledge of the channel coefficients at the transmitter. More generally, the channel coefficients are required for Tx precoding in multipath channels and asynchronous channels. In practice, these coefficients need to be fed back and/or estimated. For rapidly varying fading channels, accurate long range fading prediction is also required [DHH00]. The effect of quantized feedback, estimation and prediction errors need to be addressed in future performance investigation of various precoding methods.

3.3 Numerical Results and Analysis

In this section, we provide the numerical evaluations of the performance of THP designs for single-path channels. In the first numerical experiment, consider the downlink of a 2-user M-PAM CDMA system over an AWGN channel. Suppose the transmit powers of the two users are equal and the two signature sequences have cross-correlation $R_{12} = 0.5$. For user 1, the theoretical SERs of THP (both THP-DC and THP-CC), linear decorrelating MUD and linear decorrelating precoding are equal in this case. In Fig. 3.5, we demonstrate the difference between the simulation result for THP-DC and the theoretical SER. The gap between the theoretical and the simulated SER is caused by the "end effect" of mod-2M operation in receiver and the transmit power increase due to mod-2M operation in transmitter. The "end effect" diminishes as M or the transmit SNR increases. The transmit power penalty is reduced as M increases and is not related to the original transmit SNR. In this example, as $M = 2, 4, 8, 16$, the corresponding power penalty for user 1 are 0.67dB, 0.08dB, 0.03dB and 0.006dB, respectively. In this case, the performance degradation due to mod-2M operation is negligible for 8-PAM systems with transmit SNR larger than 20dB, and for 16-PAM systems.

Then we consider another example of a heavily loaded 3-user 8-PAM system over an AWGN channel. The cross-correlation between any two users is 0.8. All users have equal powers. Fig. 3.6 shows the performance of four methods: THP-DC, linear decorrelating transmitter precoding (Dp.), DF-MUD, and linear decorrelating MUD Receiver (Dr.). The performance of THP-CC (not shown) is very close to that for THP-DC. The only difference is that the performance degradation due to the mod-2M operation affects users 1 through $K-1$

in the THP-DC system and users 2 through K in the THP-CC system. The SUB and the conventional system performance are also plotted for comparison purposes. We notice that the linear decorrelating methods have the same performance for all users because of equal transmit powers and equal signal correlations. For THP-DC, the simulation results are very close to the theoretical performance since the end effect of mod-2M is slight for 8-PAM system. User 3 benefits the most from using THP. The THP achieves the SUB and has much lower error rate than DF-MUD and the linear methods. The worst performance is for user 1 and is theoretically the same as that of DF-MUD for user 1 and the linear methods for all users. For user 2, THP-DC outperforms the linear methods and DF-MUD. Clearly, the THP schemes improve on the linear schemes for most users. Although THP methods and DF-MUD achieve the same performance theoretically, the actual performance of THP is better than that of DF-MUD in this case since the latter technique suffers from error propagation when user powers are similar.

We now investigate a 4-user, 16-PAM system in a flat fading channel. Assume the channel gains are i.i.d. Rayleigh fading, and the power of channel fading is normalized. Let the signal cross-correlation between any two users be 0.8, and $A_1{}^2$: $A_2{}^2$: $A_3{}^2$: $A_4{}^2$ = 8:4:2:1. Thus the first user is the strongest, and the last user is the weakest. The two linear decorrelating approaches have the same performance under these given conditions. Since THP designs for CC and DC systems have similar performance, we only compare THP-DC with the linear decorrelating methods. As shown in Fig. 3.7, user 1 achieves the best performance since its signal is the strongest. The three approaches result in similar SER for user 1 and user 2 as expected; while for the weakest users (user 3 and user 4) it is shown that THP-DC significantly outperforms the linear decorrelating schemes. The order of users

presented here aids the weakest user. However, on the downlink, it might be desirable to order the users in the opposite order, so that a further user which needs larger transmit power is aided by the THP most. Thus, the overall average and peak transmit power can be reduced.
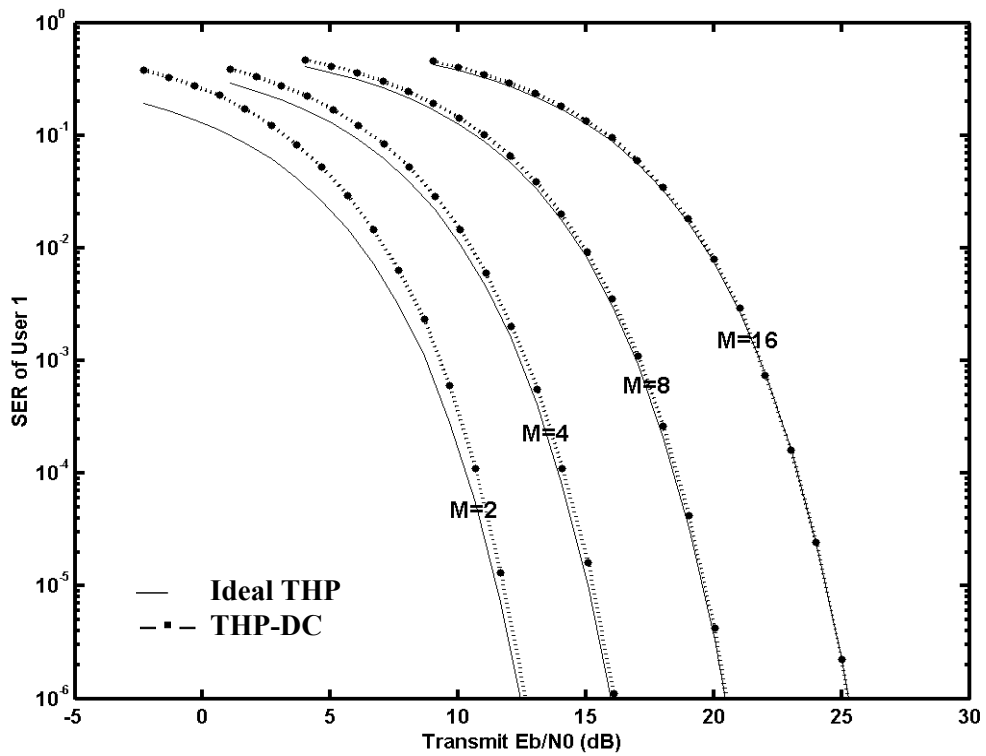
Figure 3.5 Symbol error rate for user 1 of a 2-user system in AWGN channel, *M*-PAM, $A_1=A_2$, $R_{12} = 0.5$.
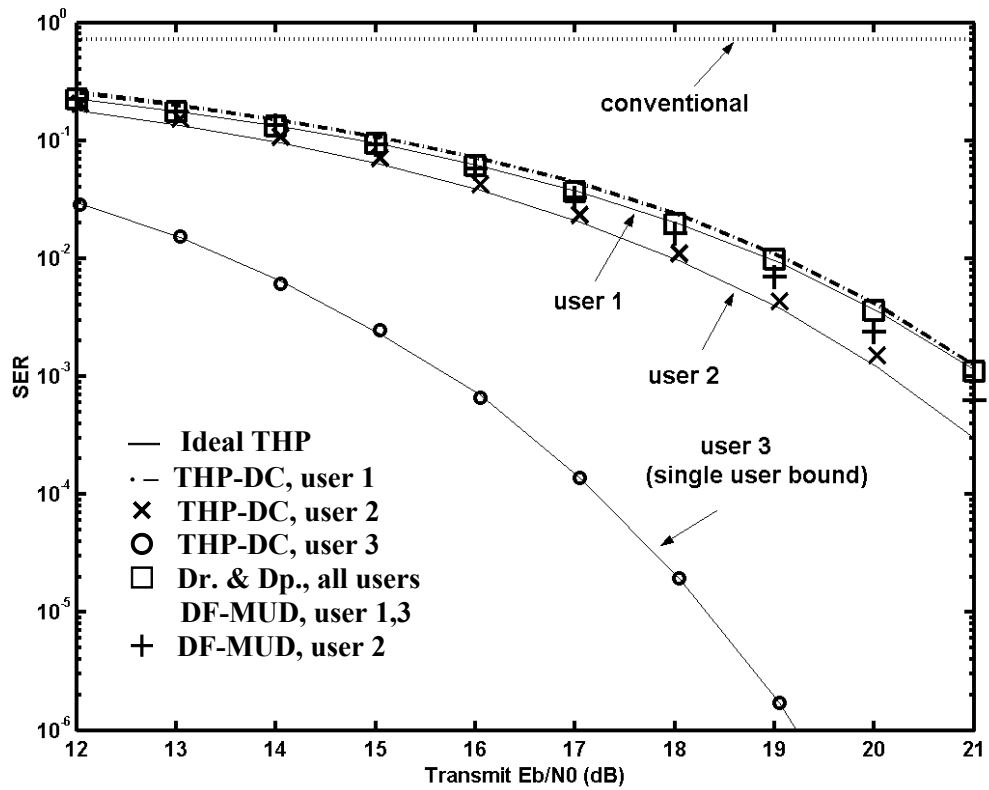
Figure 3.6 THP-DC, DF-MUD, decorrelating precoding and decorrelating MUD in AWGN channels, 3 users, 8-PAM, $A_1=A_2=A_3$, $R_{12} = R_{13} = R_{23} = 0.8$.
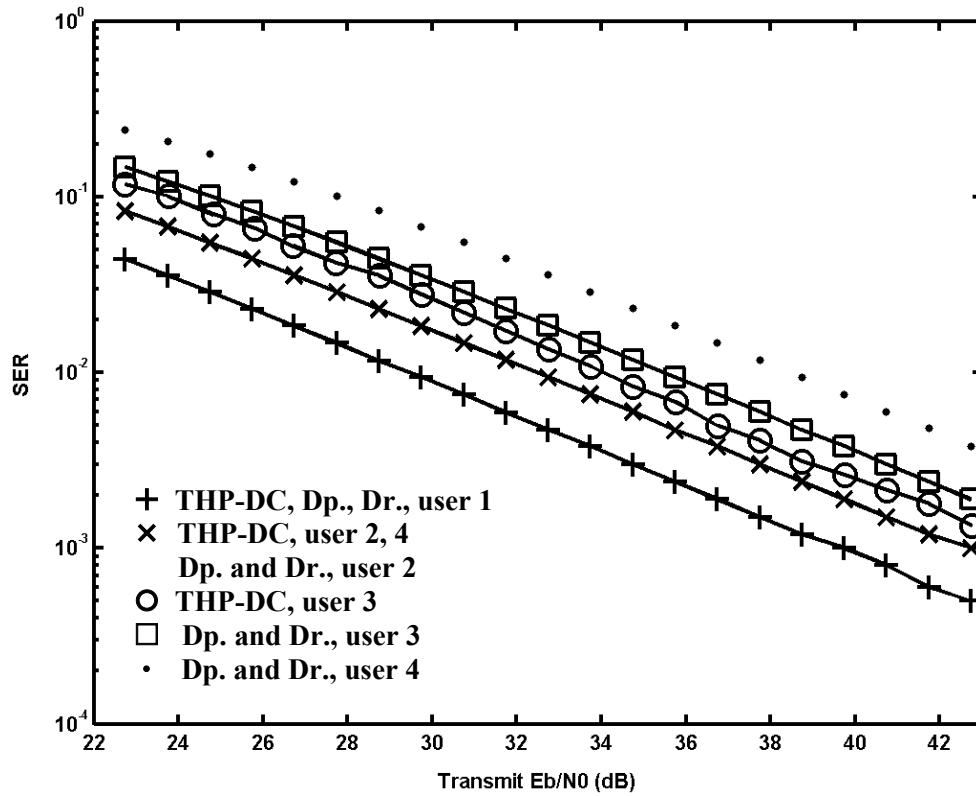
Figure 3.7 THP, decorrelating precoding and decorrelating MUD in Rayleigh fading channel, 4 users, 16-PAM, A_1^2: A_2^2: A_3^2: A_4^2 = 8:4:2:1, signal cross-correlation 0.8.

Chapter 4

TOMLINSON-HARASHIMA MULTIUSER PRECODING (THP) FOR

MULTIPATH FADING CHANNELS

4.1 Frequency-selective Fading Downlink CDMA Channel Model

Consider the downlink channel of a K-user DS-CDMA system. Suppose the transmitted

signals are subject to frequency selective slow fading with N resolvable multipath

components for every user. By assuming that the multipath spread is small relative to the

symbol duration, the inter-symbol interference (ISI) is minor and ignored in the following

discussions. For user i, $c_{i,n} = \alpha_{i,n}e^{j\varphi_{i,n}}$ represents the gain of the nth path component,

$\forall i = 1,2,\ldots,K$ and $n = 0,1,\ldots, N-1$. The received equivalent baseband signal at the ith mobile

user receiver site can be expressed by

$$r_i(t) = \sum_{k=1}^{K} \sum_{n=0}^{N-1} c_{i,n}b_k s_k(t-nT_c) + n_i(t),\tag{4.1}$$

where b_k is the data symbol for the kth user in the symbol interval $[0,T)$, $s_k(t)$ is the signature

sequence for the kth user, T_c is the chip duration, and $n_i(t)$ is complex white Gaussian noise

with zero mean and variance N_0. Define the channel gain vector for the ith user

$\mathbf{c}_i=[c_{i,0},c_{i,1},\ldots,c_{i,N-1}]$, the column vector of datasymbols for all K users $\mathbf{b}=[b_1,b_2,\ldots,b_K]^T$, and

the diagonal matrix $\mathbf{A}=diag\{A_1,A_2,\ldots,A_K\}$.

To avoid the transmit power increase due to multipath Pre-RAKE combining, we use

the normalized fading channel coefficients in the transmitter. For the ith user, define the

normalization factor $S_i \equiv \left(\sum_{n=0}^{N-1} |c_{i,n}|^2 \right)^{-1/2}$, then the normalized fading coefficient is obtained by

$\hat{c}_{i,n} \equiv S_i\, c_{i,n}$, and the normalized vector corresponding to $\mathbf{c}_i$ is $\hat{\mathbf{c}}_i = \left[\hat{c}_{i,0},\, \hat{c}_{i,1}, \ldots,\, \hat{c}_{i,N-1} \right]$. For the convenience of derivations, for all K users define a K-row, $(K \times N)$-column channel gain matrix $\mathbf{C} = diag\{\mathbf{c}_1, \mathbf{c}_2, \ldots, \mathbf{c}_K\}$ and the corresponding normalized matrix $\hat{\mathbf{C}} = diag\{\hat{\mathbf{c}}_1,\, \hat{\mathbf{c}}_2, \ldots, \hat{\mathbf{c}}_K\}$. Let $\mathbf{S} = diag\{S_1, S_2, \ldots, S_K\}$, then $\hat{\mathbf{C}} = \mathbf{S}\mathbf{C}$.

4.2 PreRAKE Multipath Diversity Combining
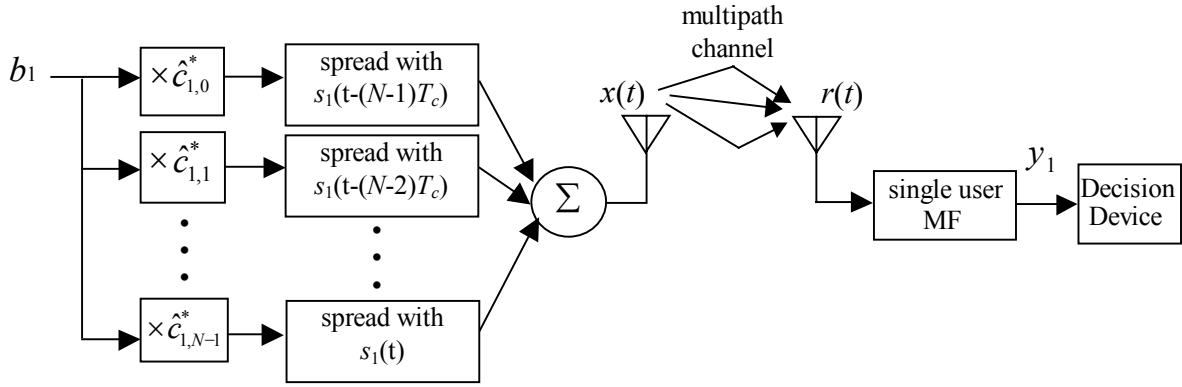
Figure 4.1 Diagram of PreRAKE System, single user, *N* resolvable channel paths

For direct-sequence spread spectrum (DS-SS) communications (single-user systems), RAKE receiver is known as the optimum maximum ratio combining detector, where signals of the individual paths are added in a way to accentuate more credible signals and suppress less credible ones. Compared to a single-path receiver, the RAKE combiner is more complicated and needs the instantaneous channel information for setting weighing factors. For the downlink channels, in order to minimize the mobile unit cost and power consumption, PreRAKE combiner was proposed in [EN93]. It concentrates all the processing required for the RAKE combination at the BS and keeps the mobile user receiver as simple as a non-combining single path receiver.

In PreRAKE method, the RAKE combining process is performed before transmission. In order to determine the combiner parameters, the future channel gain

coefficients have to be known by transmitter. This information could be obtained by feeding it back from the receivers. However, the inaccuracy due to the delay of feedback has to be considered, especially when the channel fading changes fast. For rapidly varying fading channels, the channel information can be accurately predicted by the long-range channel prediction algorithm, which is illustrated in section 4.4.

The system diagram of a PreRAKE transmitter and receiver is shown in Fig. 4.1. In the transmitter, the spread signal is delayed and weighed for a number of times. The estimated channel path profile for future transmission is used to set the weighing factors. To illustrate the principle of PreRAKE combining, we only consider the single-user system in this section, i.e., suppose only user 1 is active. With PreRAKE combining, the transmitted signal is given by

$$x(t) = \sum_{n=0}^{N-1} \hat{c}_{1,n}{}^* b_1 s_1(t-N-1+nT_c).$$
(4.2)

After traveling through the N-path fading channel, the signal received at the receiver is

$$r_1(t) = \sum_{l=0}^{N-1} \sum_{n=0}^{N-1} c_{1,l} \hat{c}_{1,n}{}^* b_1 s_1(t-(N-1-n+l)T_c) + n_1(t)$$
(4.3)

At the receiver end, the desired output of the PreRAKE combining system occurs at moment $t = (N-1)T_c$. The receiver is a simple single path receiver which decodes only the $(N-1)$th peak of the matched filter output for each transmitted symbol,

$$y_1 = \int_{(N-1)Tc}^{T+(N-1)Tc} r(t)s_1(t-(N-1)T_c)dt = b_1 \sum_{l=0}^{N-1} \sum_{n=0}^{N-1} c_{1,l} \hat{c}_{1,n}{}^* \int_0^T s_1(t)s_1(t-(n-l)T_c)dt + n_1,$$
(4.4)

45

where n_1 is the Gaussian noise component with zero mean and variance $E\{n_1 n_1{}^*\}=N_0$. It can be observed from equation (4.4) that there is self-interference in the MF output caused by the multipath. The effect of self-interference on the PreRAKE performance is analyzed in [ESN99]. If the selected spreading sequence has very small auto-correlation, the self-interference can be ignored. With this assumption, the received SNR is given by

$$\mathbf{SNR}_{\text{Rx}} = \frac{E_b}{N_0}\left(\sum_{n=0}^{N-1} c_{1,i}\hat{c}_{1,n}{}^*\right) = S_1^{-1}\mathbf{SNR}_{\text{Tx}}, \tag{4.5}$$

It can be observed that the Tx-based PreRAKE combiner is equivalent to the Rx-based RAKE combiner. By moving all multipath diversity combining operations to transmitter, the PreRAKE efficiently reduces the complexity of MS.

4.3 THP for Frequency-selective Fading Channels

4.3.1 PreRAKETHP
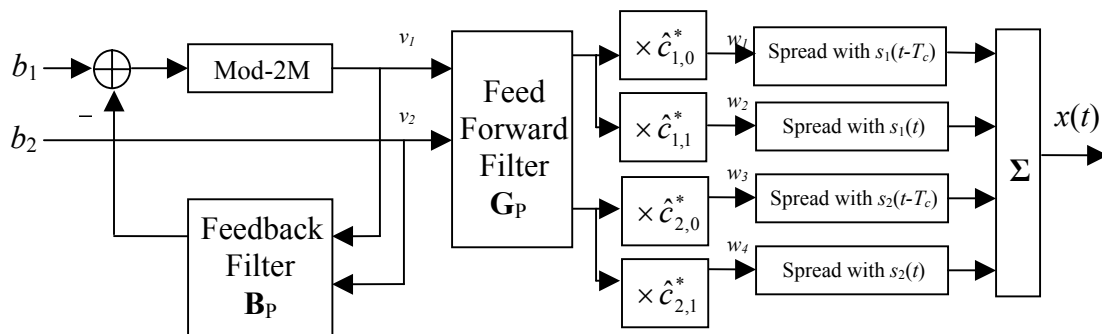
Figure 4.2 Transmitter of PreRAKETHP for a 2-user 2-channel path/user system

The transmitter structure of PreRAKETHP for a 2-user 2-channel path/user system is shown in Fig. 4.2. The basic THP decorrelating structure is similar to that for the single-path case, and is followed by a pre-RAKE combiner. The FB and FF filters for PreRAKETHP are denoted by $\mathbf{B_P}$ and $\mathbf{G_P}$, respectively. With the same derivation as for single-path channels, the output vector of the mod-2M operator bank satisfies $\mathbf{v} = (\mathbf{B_P}+\mathbf{I})^{-1}(\mathbf{b}+2M\mathbf{Ad})$. As we will see later, $\mathbf{B_P}$ is a complex matrix related to the channel fading; as a result, the inputs of the mod-2M operators are complex numbers. The mod-2M operations are performed to constrain the magnitudes of the real part and imaginary part of the input number respectively. Thus for the ith user, d_i is a complex number with integral real and imaginary parts. As in Fig. 4.2, the outputs of the FF filter $\mathbf{G_P}$ are multiplied with the conjugates of normalized fading

coefficients. The output vector of the pre-RAKE combiner, $\mathbf{w} = \hat{\mathbf{C}}^H \mathbf{G}_P \mathbf{v}$, has $K \times N$ elements.

Following the signature sequence spreading, the ultimate transmitted signal is given by

$$x(t) = \sum_{k=1}^{K} \sum_{l=0}^{N-1} w_{kN-l} s_k (t - lT_c).$$ (4.6)

The equivalent baseband received signal at the ith user receiver site is given by

$$r_i(t) = \sum_{k=1}^{K} \sum_{n=0}^{N-1} \sum_{l=0}^{N-1} c_{i,n} w_{kN-l} s_k (t - lT_c - nT_c) + n_i(t).$$ (4.7)

The output of the MF is sampled at $t = (N-1)T_c$, and for the ith user is given by

$$y_i = \int_{(N-1)T_c}^{T+(N-1)T_c} r_i(t) s_i (t - (N-1)T_c) dt.$$ (4.8)

The cross-correlations between delayed signature sequences can be represented as

$$M_{i,k}^m = \int_0^T s_i(t) s_k (t + mT_c) dt, \ m \in \{-(N-1), \ldots, (N-1)\}.$$ (4.9)

From (4.7), (4.8) and (4.9), we have

$$y_i = \sum_{k=1}^{K} \sum_{n=0}^{N-1} \sum_{m=-(N-1)}^{N-1} c_{i,n} M_{i,k}^m w_{(k-1)N+m+n+1} + n_i,$$ (4.10)

where n_i is the filtered noise component with power N_0. $\forall \ i, k \in \{1, 2, \ldots, K\}$, define the $N \times N$ correlation matrix $\mathbf{M}_{i,k}$ with the jth row equal $[M_{i,k}^{1-j}, M_{i,k}^{2-j}, \ldots, M_{i,k}^{N-j}]$, $j=1, 2, \ldots, N$. Construct the $(K \times N)$-row and $(K \times N)$-column matrix $\mathbf{M}$ by superimposing the $K \times K$ non-overlapping submatrices $\mathbf{M}_{i,k}$, $i, k \in \{1, 2, \ldots, K\}$. Then (4.10) reduces to

$$\mathbf{y} = \mathbf{CMw} + \mathbf{n} = \mathbf{S}^{-1}\hat{\mathbf{C}}\mathbf{M}\hat{\mathbf{C}}^H \mathbf{G}_P (\mathbf{B}_P + \mathbf{I})^{-1}(\mathbf{b} + 2M\mathbf{Ad}) + \mathbf{n},$$ (4.11)

where $\mathbf{y} = [y_1, y_2, \ldots, y_K]^T$ and $\mathbf{n} = [n_1, n_2, \ldots, n_K]^T$. Define $\mathbf{R}_P \equiv \mathbf{CMC}^H$ and

$\hat{\mathbf{R}}_P \equiv \mathbf{S}^2 \mathbf{R}_P = \hat{\mathbf{C}} \mathbf{M} \hat{\mathbf{C}}^H$. The matrix $\mathbf{R}_P$ is obviously positive definite. Consequently, it can be

factorized as $\mathbf{F}_P{}^H \mathbf{F}_P$ using the Cholesky factorization, where $\mathbf{F}_P = \{f_{Pij}\}_{K \times K}$ is complex lower

triangular matrix with real diagonal elements. The normalized matrix corresponding to $\mathbf{F}_P$ is

$\hat{\mathbf{F}} = \{\hat{f}_{ij}\}_{K \times K} = \mathbf{S} \mathbf{F}_P$. To cancel the MAI, the FB and FF filters are defined as

$$\mathbf{B}_P \equiv diag(\hat{\mathbf{F}})^{-1} \hat{\mathbf{F}}^H - \mathbf{I}, \tag{4.12}$$

$$\mathbf{G}_P \equiv \hat{\mathbf{F}}^{-1}. \tag{4.13}$$

Then equation (4.11) can be simplified as

$$\mathbf{y} = diag(\mathbf{F}_P)(\mathbf{b} + 2M\mathbf{A}\mathbf{d}) + \mathbf{n}. \tag{4.14}$$

We assume the channel gains and, therefore, f_{Pii} are estimated in the receivers. Then for the

ith user, we have $f_{Pii}{}^{-1} y_i = b_i + 2MA_i d_i + f_{Pii}{}^{-1} n_i$. The term $2MA_i d_i$ will then be cancelled by

mod-2M operation. The instantaneous ideal SER of the ith user is given by

$$Pe_i = \frac{2(M-1)}{M} \left(\sqrt{\frac{6(\log_2 M) f_{Pii}{}^2}{M^2 - 1} \gamma_{bi}} \right) \tag{4.15}$$

The PreRAKETHP described above is related to several precoders and MUDs for

frequency-selective CDMA channels. It represents the transmitter precoding version of the

nonlinear multiuser detector that consists of the RAKE receiver followed by the DF MUD.

This detector can be viewed as a nonlinear (DF) version of the RAKE Decorrelating Detector

(RDD) [HS94], the optimum linear MUD for multipath channels (or, equivalently, of the pre-

RDD precoder in [Gun03]). In this detector, the decorrelating DF processing is applied at the

output of the filter bank matched to the signature sequences convolved with the channel

responses for all users (the RAKE receiver), while in the RDD, the matched filter bank is followed by the linear decorrelating detection. Therefore, this DF detector is the optimal decorrelating DF MUD for the frequency selective CDMA channel. Since PreRAKETHP is the equivalent Tx-based implementation of this DF detector, it is the optimal THP method according to the decorrelating (ZF) and MMSE criteria.

To compare the nonlinear PreRAKETHP with the linear RDD, first we note that the correlation matrix $\mathbf{R}$ in [HS94] corresponds to $\mathbf{R}_\mathrm{P}^T$ above. Since $\mathbf{R}_\mathrm{P}^{-T} = (\mathbf{F}_\mathrm{P}^{-T})^H \mathbf{F}_\mathrm{P}^{-T}$, $(\mathbf{R}^{-1})_{ii}$ in equation (7) in [HS94] is equal to or larger than $f_{\mathrm{P}ii}^{-2}$ (equality is satisfied for $i=1$). Comparing the error rate formulas for PreRAKETHP (equation (4.15)) and RDD (equation (7) in [HS94]), we observe that PreRAKETHP outperforms the RDD for all users $i>1$. For the first user, these methods have the same SER. For the last user, since $f_{\mathrm{P}KK}^2 = [\mathbf{R}_\mathrm{P}]_{KK} = \mathbf{c}_K [\mathbf{M}]_{KK} \mathbf{c}_K^H$, the performance of PreRAKETHP given by equation (4.15) achieves that of the RAKE receiver in the absence of MAI. Similarly, it can be demonstrated that the PreRAKETHP has better performance than the pre-RDD in [Gun03]. Since it has been proved in [HS94] that the RDD outperforms the Multipath Decorrelating Detector (MDD) [ZB96], the PreRAKETHP also outperforms the MDD.

4.3.2 Multipath Decorrelating THP (MDTHP)
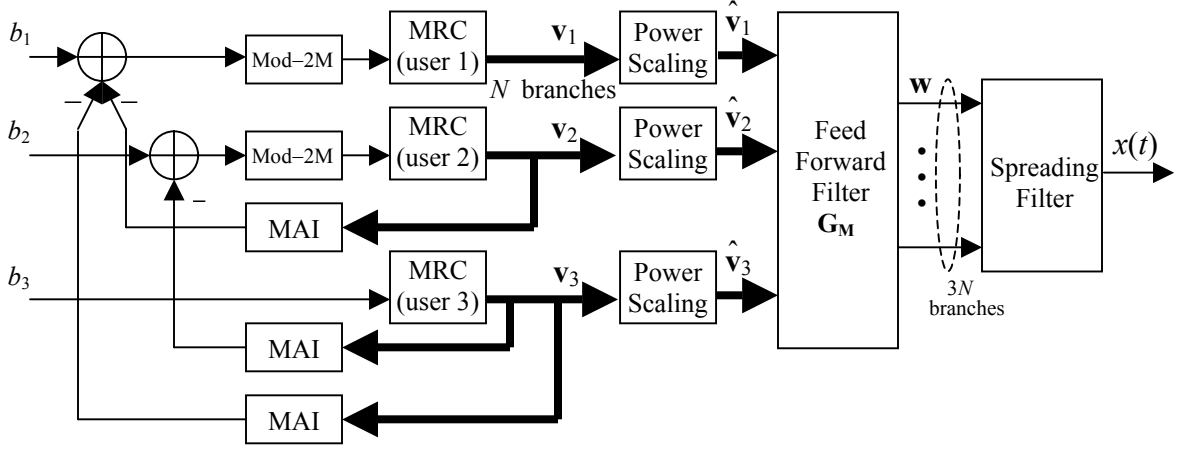
Figure 4.3 Transmitter of MDTHP for a 3-user N-channel paths/user system

One drawback of the PreRAKETHP is that the coefficients of the FB and FF filters depend on the channel gains. Consequently, the matrix factorization and inversion required for the computation of these coefficients have to be performed frequently, especially for rapidly varying fading channels. In this section, we present an alternative THP design, MDTHP, to alleviate this problem.

The transmitter diagram for the MDTHP is shown in Fig. 4.3. Because $\mathbf{M}$ is symmetric and positive definite in practice, we can decompose $\mathbf{M} = \mathbf{F_M}^T\mathbf{F_M}$ by Cholesky factorization, where $\mathbf{F_M}$ is a lower triangular matrix. Divide $\mathbf{F_M}$ into $K \times K$ blocks, where each block is an $N \times N$ submatrix; and represent the block on the ith row and jth column as $[\mathbf{F_M}]_{ij}$, $\forall\ i, k \in \{1, 2, \ldots, K\}$. The FB loop in the transmitter works in the following way. First, the N-

dimension vector $\mathbf{v}_K$ is computed by applying N weights to the input symbol of the last user, $\mathbf{v}_K = b_K \cdot ([\mathbf{F}_M]_{KK}\hat{\mathbf{c}}_K{}^H)$. The interference caused by user K is calculated from $\mathbf{v}_K$, and fed back to be canceled from the signals of other users. This procedure is repeated consecutively for $k = K{-}1, K{-}2, \ldots, 2$, thus forming vectors $\mathbf{v}_k$. For user i, $\forall i = 1, 2, \ldots, K{-}1$, the feedback from user j, $j = i{+}1, i{+}2, \ldots, K$, is given by $\dfrac{\hat{\mathbf{c}}_i[\mathbf{F}_M]_{ji}{}^T \mathbf{v}_j}{\sqrt{\beta_i \beta_j}}$, where $\beta_i \equiv \hat{\mathbf{c}}_i[\mathbf{F}_M]_{ii}{}^T [\mathbf{F}_M]_{ii}\hat{\mathbf{c}}_i{}^H$. Thus, for users 1 through $K{-}1$, the output of the FB loop is

$$\mathbf{v}_i = \left(b_i - \sum_{j=i+1}^{K} \frac{\hat{\mathbf{c}}_i[\mathbf{F}_M]_{ji}{}^T \mathbf{v}_j}{\sqrt{\beta_i \beta_j}} + 2MA_i d_i \right) \cdot [\mathbf{F}_M]_{ii}\hat{\mathbf{c}}_i{}^H , \tag{4.16}$$

The output power is normalized by multiplying $\mathbf{v}_i$ by the scaling factor

$$S_{vi} = (\hat{\mathbf{c}}_i[\mathbf{F}_M]_{ii}{}^T [\mathbf{F}_M]_{ii}\hat{\mathbf{c}}_i{}^H)^{-1/2} = \beta_i^{-1/2}, \tag{4.17}$$

Let $\hat{\mathbf{v}}_i = S_{vi} \cdot \mathbf{v}_i$, $i = 1, 2, \ldots, K$. Represent the input of the FF filter by the vector $\hat{\mathbf{v}} = [\hat{\mathbf{v}}_1{}^T, \hat{\mathbf{v}}_2{}^T, \ldots, \hat{\mathbf{v}}_K{}^T]^T$. Then its output is $\mathbf{w} = \mathbf{G}_M\hat{\mathbf{v}}$, where the FF filter is defined as $\mathbf{G}_M = \mathbf{F}_M{}^{-1}$. Following the derivation similar to that for the PreRAKETHP above, we obtain the matched filter bank output in the receivers as $\mathbf{y} = \mathbf{CMw} + \mathbf{n}$. For user i, this output is

$$y_i = \sqrt{\beta_i}/S_i (b_i + 2MA_i d_i) + n_i, \quad i = 1, 2, \ldots, K, \tag{4.18}$$

where $S_i = \left(\displaystyle\sum_{n=0}^{N-1} |c_{i,n}|^2 \right)^{-1/2}$. Consequently, the ideal instantaneous SER for the ith user is

$$Pe_i(\gamma_{bi}) = \frac{2(M{-}1)}{M} Q\left(\sqrt{\frac{6(\log_2 M)\mathbf{c}_i[\mathbf{F}_M]_{ii}{}^T [\mathbf{F}_M]_{ii}\mathbf{c}_i{}^H}{M^2 - 1}} \, \gamma_{bi} \right) \tag{4.19}$$

52

The MDTHP method significantly simplifies transmitter precoding compared to the PreRAKETHP, since it employs the factorization of the channel gain-independent matrix $\mathbf{M}$. Thus even for rapidly varying mobile radio channels the matrix factorization and inversion operations do not have to be performed frequently. These filters depend only on the signature sequences and the order of the users. The MDTHP is related to several other simplified MUD and transmitter precoding methods that also employ the matrix $\mathbf{M}$. First, equation (4.19) is identical to the theoretical performance of the Multipath Decorrelating Decision Feedback Receiver (MDDFR) (equation (16) in [SK97]). However, since DF MUD is degraded by error propagation, the MDTHP has better actual performance than the MDDFR.

For the purpose of comparing the MDTHP with linear decorrelating precoders, in [LDj04, Appendix] we described a linear multipath decorrelating precoder closely related to the MDTHP. This linear precoder can be regarded as the Tx-based counterpart of the Multipath Decorrelating Detector (MDD) [ZB96]. Therefore we call it Pre-MDD. Compare the decision statistic of the MDTHP, $\mathbf{c}_i[\mathbf{F}_\mathbf{M}]_{ii}^T[\mathbf{F}_\mathbf{M}]_{ii}\mathbf{c}_i^H$, with that of the Pre-MDD (c.f. equation (A.1) in [LDj04]), $\mathbf{c}_i([\mathbf{M}^{-1}]_{ii})^{-1}\mathbf{c}_i^H$. Based on the theorem for the inverse of a partitioned symmetric matrix [HJ85, p.18], it is easy to prove that $\mathbf{c}_i[\mathbf{F}_\mathbf{M}]_{ii}^T[\mathbf{F}_\mathbf{M}]_{ii}\mathbf{c}_i^H \geq \mathbf{c}_i([\mathbf{M}^{-1}]_{ii})^{-1}\mathbf{c}_i^H$ (the equality is satisfied for $i = 1$). Therefore, for user 1, the MDTHP, Pre-MDD as well as MDD have the same performance; and for other users the MDTHP outperforms the Pre-MDD and MDD.

Since $f_{PKK}^2 = \mathbf{c}_K[\mathbf{M}]_{KK}\mathbf{c}_K^H = \mathbf{c}_K[\mathbf{F}_\mathbf{M}]_{KK}^T[\mathbf{F}_\mathbf{M}]_{KK}\mathbf{c}_K^H$, by equations (4.15) and (4.19), the PreRAKETHP and MDTHP have the same performance for the last user. Their SER is the same as for an isolated single user with RAKE receiver. We can obtain some insight into the

performance comparison of the two THP schemes for other users by considering their decision statistics averaged over the channel fading. Considering that the channel fading along the paths towards different user receivers are independent random processes, it can be derived from $\mathbf{CMC}^H = \mathbf{F_P}^H\mathbf{F_P}$ that $E\{|f_{Pij}|^2\} << E\{|f_{Pii}|^2\}$, $\forall\ i\neq j$ ($E\{\cdot\}$ is the expectation over the channel gains). which is also observed in simulation examples. Therefore, we have $E\{f_{Pii}^2\} \approx E\{\mathbf{c}_i[\mathbf{M}]_{ii}\mathbf{c}_i^H\}$, $\forall\ i = 1, 2, \ldots, K$.   On   the   other   hand, $\forall\ i\neq K$,

$$\mathbf{c}_i[\mathbf{M}]_{ii}\mathbf{c}_i^H = \mathbf{c}_i\sum_{j=i}^{K} [\mathbf{F_M}]_{ji}^T[\mathbf{F_M}]_{ji}\mathbf{c}_i^H > \mathbf{c}_i[\mathbf{F_M}]_{ii}^T[\mathbf{F_M}]_{ii}\mathbf{c}_i^H.$$ These arguments indicate that on average

the decision statistics for PreRAKETHP, f_{Pii}^2, is larger than that for MDTHP, $\mathbf{c}_i[\mathbf{F_M}]_{ii}^T[\mathbf{F_M}]_{ii}\mathbf{c}_i^H$. This observation provides the theoretical explanation for the better performance of the PreRAKETHP. This conclusion is further verified by simulation results. On the other hand, the MDTHP is easier to implement as discussed above. In summary, there is a performance-complexity tradeoff between the PreRAKETHP and MDTHP.

For M-PAM/QAM systems, the practical performance of THP methods is degraded when M is small due to the power penalty and end effect of mod-2M operation [LM94]. Usually the first user suffers the worst degradation and the last user is not influenced at all. Therefore, to achieve more balanced performance, we sort users in the order of decreasing received powers in simulation examples. For larger values of M, since THP methods are not affected by error propagation, different user ordering might be desirable in practice [LD03].

4.4 Long-Range Channel Prediction

To implement transmitter-based MAI cancellation and diversity techniques, the CSI must be available at the transmitter. CSI can be estimated at the receiver and sent to the transmitter via a feedback channel. Thus the feedback delay, overhead and processing delay have to be taken into account in the performance analysis of the transmitter-based techniques. For very slowly fading channels, outdated CSI is sufficient for reliable adaptive system design. For faster fading which corresponds to realistic mobile speeds, however, even a small delay will cause significant performance degradation, because the channel variation due to large Doppler shifts usually results in a different channel at the time of transmission than at the time of channel estimation. To realize the potential of transmitter precoding techniques, these channel variations have to be reliably predicted at least several milliseconds ahead.

The LRP algorithm characterizes the fading channel using an autoregressive (AR) model and computes the minimum mean squared error (MMSE) estimate of a future coefficient sample based on a number of past observations. In contrast to conventional channel estimation, LRP uses considerably lower sampling rate to forecast future values of the fading coefficient far ahead. Assume the complex Rayleigh fading process $c(t)$ is sampled at the rate $f_s=1/T_s$, which is at least twice the maximum Doppler shift f_{dm}. The sample of channel state information (CSI) is represented by $c_n=c(nT_s)$. The linear MMSE prediction of the future CSI sample $\hat{c}_n$ based on p previously observed CSI samples $c_{n-1}, c_{n-2}, \ldots, c_{n-p}$ is

$$\hat{c}_n = \sum_{j=1}^{p} d_j c_{n-j} \,, \tag{4.20}$$

where d_j are the coefficients of LP filter and p is the AR model order. The one-step prediction in equation (4.20) can be generalized to predict any time τ ahead, that is, we hope

to find the MMSE estimate of a future sample c(τ) by observing p previous samples collected

at and prior to the moment zero.

$$\hat{c}(\tau) = \hat{c}_\upsilon = \sum_{j=0}^{p-1} d_j c_{-j}, \qquad\qquad (4.21)$$

where $\tau = \upsilon T_s$ is the prediction range. υ can be any positive real number; specifically, when υ

is an integer, the prediction is called υ-step prediction. The optimal coefficients d_j are

determined by the orthogonal principle as

$$\mathbf{d} = \mathbf{R}^{-1}\mathbf{r}, \qquad\qquad (4.22)$$

where $\mathbf{d}=[d_0, \ d_1, \ \ldots, \ d_{p-1}]^T$, $\mathbf{R}$ is the $p \times p$ autocorrelation matrix with elements

$R_{ij}=E\{c(t+\tau+iT_s)c(t+\tau+jT_s)^*\}$ and $\mathbf{r}$ is the $p \times 1$ autocorrelation vector with elements

$r_j=E\{c(t)c(t+\tau+jT_s)^*\}$. For Rayleigh fading, $r_j=r(\tau+jT_s)=J_0(2\pi f_{dm}(\tau+jT_s))$ is shown in Fig. 4.4.

By the solution of (4.22), the MSE, $E\{|e(\tau)|^2\} \equiv E\{|c(\tau) - \hat{c}(\tau)|^2\}$, is minimized. The resulting

MMSE is given by

$$E\{|e(\tau)|^2\} = 1 - \sum_{j=0}^{p-1} d_j r_j. \qquad\qquad (4.23)$$

Since the CSI samples are predicted at the frequency f_s, it is necessary to use

interpolation to obtain the intermediate coefficients of the channels. The predicted CSI values

are filtered by a lowpass interpolating filter, so that the CSI at the transmit data rate is

obtained.
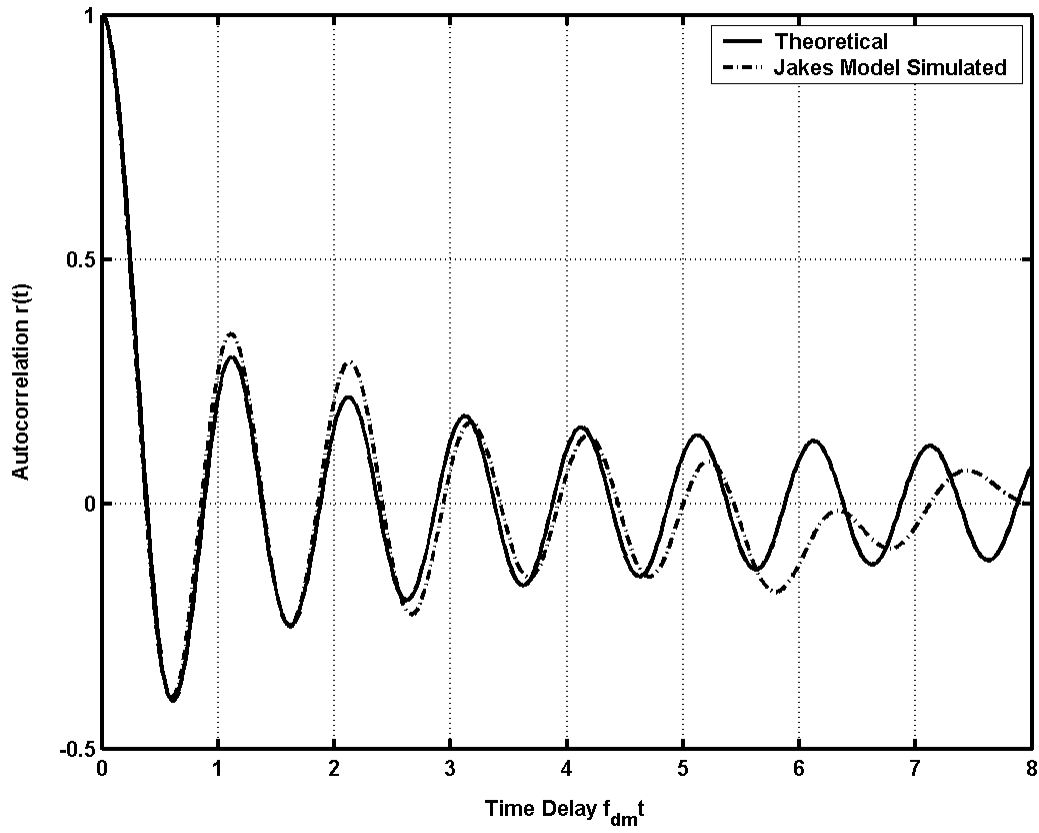
Figure 4.4 Autocorrelation of Rayleigh fading signal, maximum Doppler shift 200Hz, 9 offset oscillators in Jakes model.

4.5 Numerical Results and Analysis

In this section, we address the multipath fading channels that result in different received powers. Power control is often needed in these channels. Since the order of users influences the SER in THP systems, we propose to select the order that saves the total transmit power. As mentioned in section II, the practical performance of THP schemes for M-PAM/QAM systems is degraded when M is small due to the power penalty and end effect of mod-2M operation. Usually the first user suffers the worst degradation and the last user is not influenced at all. Moreover, similarly to DF-MUD, as the users' order increases, the benefit of the THP becomes more pronounced. Therefore, to achieve more balanced performance and to minimize transmit power, we sort users in the order of decreasing received powers in the following simulation experiments. In practice, it might be desirable to maintain constant user order for an extended period of time to minimize complexity. (Note that unlike DF-MUD, THP is not affected by error propagation, so ordering users according to their powers is not required for maintaining reliable performance.)

In Fig. 4.5-4.9 we investigate the performance of transmitter precoding in multipath fading environments. In these examples, we employ orthogonal 32-chip Hadamard codes as the signature sequences. All channel paths experience i.i.d. Rayleigh fading and the total average channel power is normalized to one for each user. First, consider an 8-user, 4-channel paths/user system. Fig. 4.5 and Fig. 4.6 show the SER averaged over all users for BPSK and 16-QAM, respectively. (We do not employ power control in this paper, although in practice it is required to maintain the target SER.) The transmit powers of all users are equal. In both figures, the THP methods significantly outperform the conventional RAKE receiver and linear decorrelating precoding with RAKE receiver in [VJ98] (labeled as "Lin.

Prec. RAKE"). When the bit error rate (BER) is lower than 10^{-3}, PreRAKETHP is the best among all the Tx-based and Rx-based, linear and nonlinear decorrelating methods, and MDTHP is better than the MDDFR, Pre-MDD and MDD, as expected from theoretical analysis. For higher SNR values, both THP methods outperform other techniques. This confirms that the inherent advantage of nonlinear THP methods overcomes the adverse influence of modulo operation even if M is very small. The linear precoding in [VJ98] is seriously degraded by transmit power scaling. The SUB is also shown for reference. It is given by the performance of isolated single user with RAKE receiver.

In Fig. 4.7, the best and poorest user performances of the three precoding methods and the optimum linear decorrelating detector RDD are further compared with 8-PAM modulation. We observe that the SER of linear precoding is higher than those of other methods, and the lowest SER is achieved by the PreRakeTHP. As we have analyzed, the PreRakeTHP and MDTHP result in the same SER for the last user. Due to the bit-by-bit user ordering, the last user experiences the worst instantaneous fading, and thus its average SER is the highest among all users in this example.

Next, consider a 4-user 3-channel paths/user BPSK system, where the transmit powers for all users are equal. In addition to short-term multipath Rayleigh fading, the transmitted signal is also subject to long-term shadow fading modeled by log-normal distribution with variance 6dB [Stu01]. Suppose the average received signal powers for the four users satisfy the ratio of 8:4:2:1. The instantaneous received power order is corresponding to the order of average power, so bit-by-bit reordering is not performed. Fig. 4.8 demonstrates the BER of the weakest user. The proposed two nonlinear techniques and the linear techniques of Pre-RDD, Pre-MDD and linear precoder with RAKE receiver in

[VJ98] (labeled as "Lin. Prec. RAKE") are compared. As expected, for the last user PreRAKETHP and MDTHP result in the same performance as for the isolated single user with RAKE receiver (SUB), while other methods have poorer performance. Equivalently, the users that experience greater propagation loss will require lower power to satisfy the target BER. Thus, in practice the overall transmit power can be reduced when THP methods are employed.

A critical assumption for the above simulation experiments is that the channel state information (CSI) is perfectly known at the transmitter. Next we observe the performance of the THP techniques under the condition that the CSI is estimated at the Rx and fed back to the Tx. Consider a BPSK modulated 4-user 3-channel paths/user wideband-CDMA (W-CDMA) system with the following parameters; the carrier frequency is 2GHz, the maximum Doppler frequency is 200 Hz and the transmit data rate is 128kbps [ICM98]. The frequency selective Rayleigh fading is simulated by the Jakes model [Jak93]. In Fig. 4.9, the average BER of the proposed precoding methods is shown for three different cases: CSI is perfectly known at the transmitter; CSI is predicted; CSI is fed back to the transmitter (no prediction is used). For CSI prediction, the 3-step LRP algorithm for W-CDMA [DHH00] is utilized with the channel sampling frequency of 1600Hz and the prediction range of 0.625ms (the slot interval). Since the channel sampling and prediction frequency is less than the data rate, it is necessary to interpolate the intermediate channel gain coefficients. In the case of delayed fed back CSI (FBCSI), the channel gains are fed back without prediction with the feedback delays of 0.3125ms and 0.625ms. Note that transmitter precoding aided by channel prediction achieves almost the same performance as for the case when the channel is perfectly known at the Tx, while feeding back delayed CSI without prediction results in

60

significant performance degradation. Thus, accurate LRP is required for reliable multiuser precoders in practical mobile radio channels.
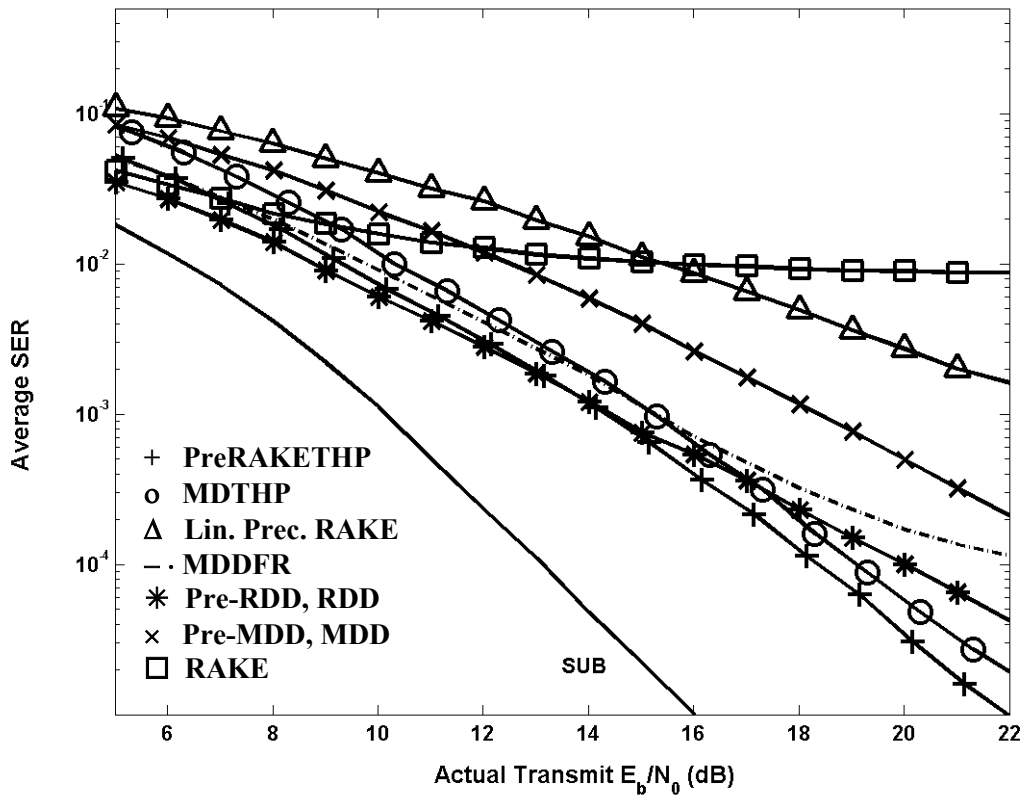
Figure 4.5 Performance comparison of various techniques in multipath fading channels, 8 users with equal transmit powers, 4 channel-paths/user, BPSK.
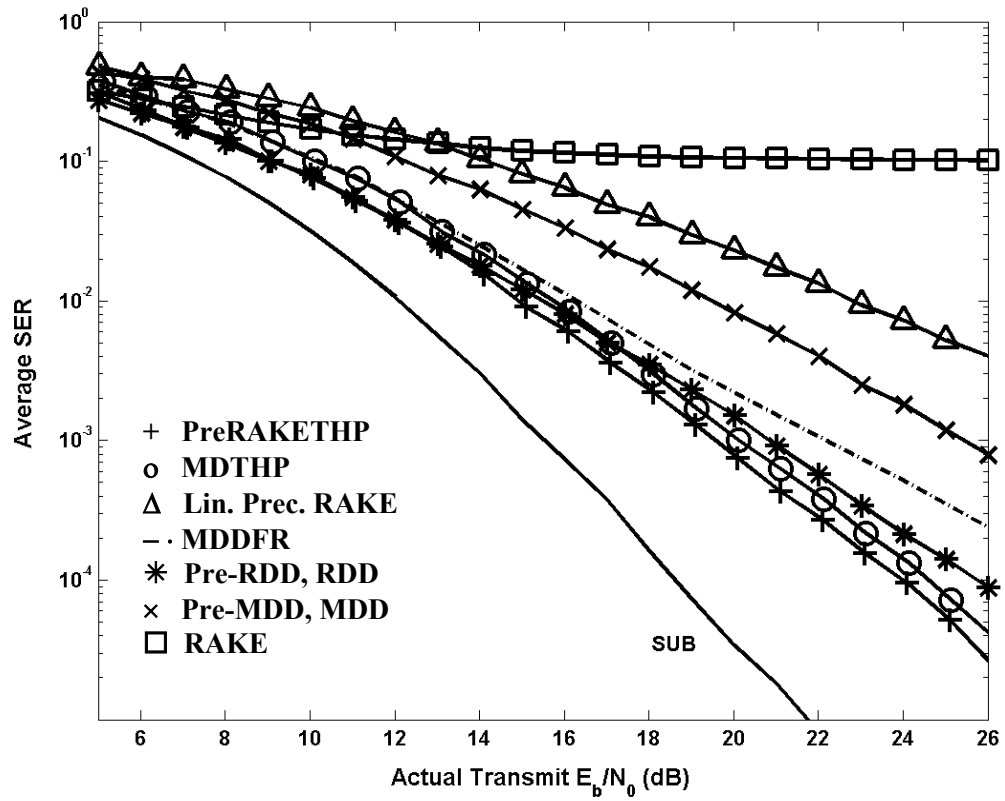
Figure 4.6 Performance comparison of various techniques, 8 users with equal transmit powers, 4 channel-paths/user, 16-QAM.
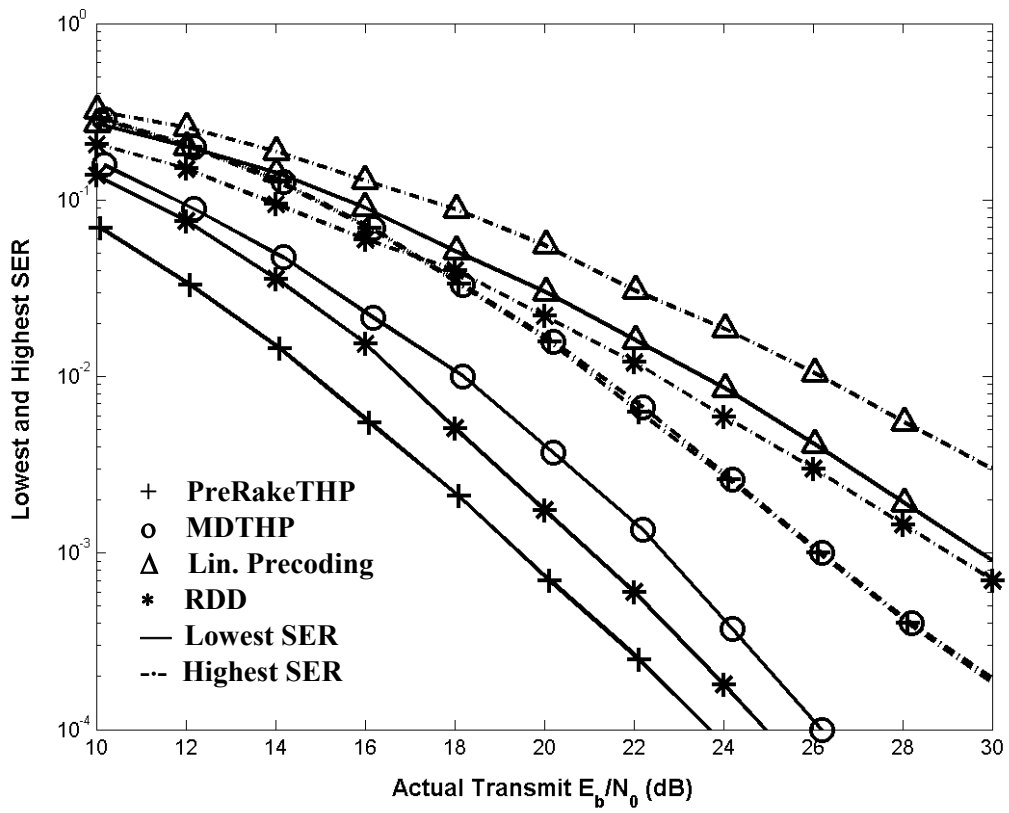
Figure 4.7 Best and poorest user SER for 8 users, 4 channel-paths/user, 8-PAM.
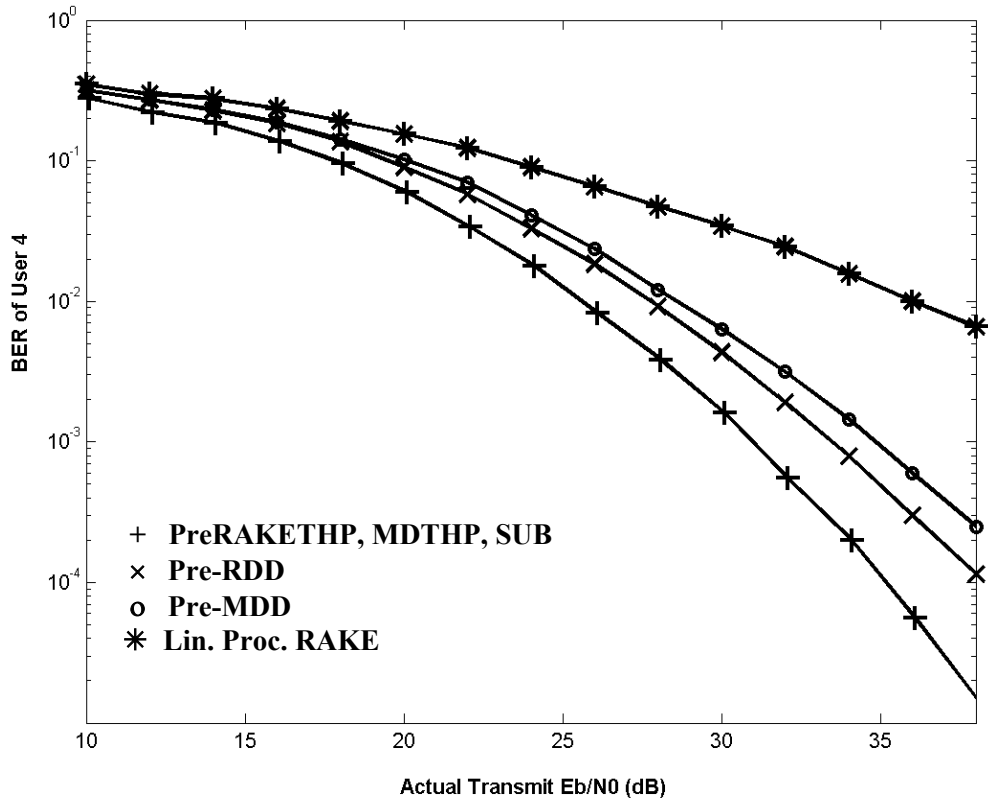
Figure 4.8 BER of the weakest user in large scale lognormal multipath fading channels, 4 users with equal transmit power, 3 channel paths/user, ratio of the received signal powers 8:4:2:1, BPSK.
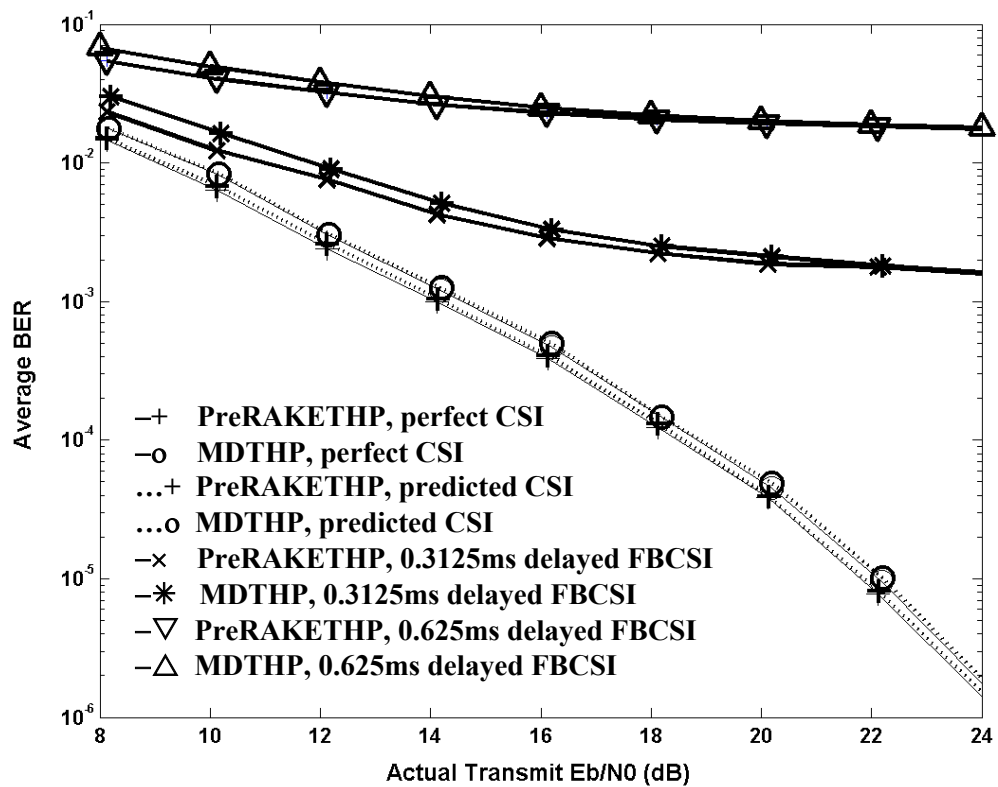
Figure 4.9 Performance comparison of precoding aided by CSI prediction and by CSI feedback.

Chapter 5

LINEAR DECORRELATING MULTIUSER PRECODING

In last two chapters, we have investigated the nonlinear THP technique for MAI cancellation. We find that although THP can efficiently reduce MAI, its performance advantage over linear methods is not obvious for small-M systems, such as BPSK and QPSK, due to the power penalty and end effect of mod-2M operation. In addition, the nonlinear THP designs have higher complexity than the existing linear decorrelating precoders. In this chapter, we first describe the previously proposed linear decorrelating precoding methods, and then develop a few novel linear precoding schemes. The combination of precoding and diversity techniques is discussed in detail. Without loss of generality, only BPSK modulated systems are considered in the following derivations.

5.1 Linear Decorrelating Precoding with RAKE Receiver

In this method [VJ98], the traditional RAKE receiver is employed, which acts as the matched filter (MF). The notation for the frequency-selective channel model remains the same as in section 4.1. For the ith user, the output of the RAKE receiver is

$$y_i = \sum_{l=0}^{N-1} \int_{lTc}^{T+lTc} c_{i,l}^* r_i(t) s_i(t-lT_c) dt = \sum_{l=0}^{N-1} \sum_{n=0}^{N-1} \sum_{k=1}^{K} c_{i,n} c_{i,l}^* b_k \int_{0}^{T} s_i(t) s_k(t-nT_c+lT_c) dt + z_i, \qquad (5.1)$$

where z_i is given by

$$z_i = \sum_{l=0}^{N-1} \int_{0}^{T} c_{i,l}^* n_i(t) s_i(t-lT_c) dt. \qquad (5.2)$$

Define $m = (n-l)$, therefore $m \in [-(N-1), -(N-2),\ldots, N-2, N-1]$. Denote the integral in equation (5.1) as

67

$$R_{i,k}^m \equiv \int_0^T s_i(t)s_k(t-mT_c)dt, \tag{5.3}$$

which is the cross-correlation between signature waveforms. Then the correlation matrices are given by

$$\mathbf{R}_{i,k} \equiv \{R_{i,k}^m\}_{N \times N}$$
$$= \begin{bmatrix} R_{i,k}^0 & R_{i,k}^{-1} & R_{i,k}^{-2} & \cdots & R_{i,k}^{-(N-1)} \\ R_{i,k}^1 & R_{i,k}^0 & R_{i,k}^{-1} & \cdots & R_{i,k}^{-(N-2)} \\ R_{i,k}^2 & R_{i,k}^1 & R_{i,k}^0 & \cdots & R_{i,k}^{-(N-3)} \\ \cdots & \cdots & \cdots & \cdots & \cdots \\ R_{i,k}^{N-1} & R_{i,k}^{N-2} & R_{i,k}^{N-3} & \cdots & R_{i,k}^0 \end{bmatrix}, \quad i,k \in \{1, 2,\ldots, K\}, \tag{5.4}$$

and

$$\mathbf{R} = \{\mathbf{R}_{i,k}\}_{(N \times K) \times (N \times K)} = \begin{bmatrix} \mathbf{R}_{1,1} & \mathbf{R}_{1,2} & \cdots & \cdots & \mathbf{R}_{1,K} \\ \mathbf{R}_{2,1} & \mathbf{R}_{2,2} & \cdots & \cdots & \mathbf{R}_{2,K} \\ \cdots & \cdots & \cdots & \cdots & \cdots \\ \cdots & \cdots & \cdots & \cdots & \cdots \\ \mathbf{R}_{K,1} & \mathbf{R}_{K,2} & \cdots & \cdots & \mathbf{R}_{K,K} \end{bmatrix}. \tag{5.5}$$

In order to express equation (5.1) in a compact form for all the K users, we also define the matrices of channel gains. For the ith user, the row vector of channel gains is $\mathbf{c}_i = [c_{i,0}, c_{i,1}, \ldots, c_{i,N-1}]$; then the K-row ($N \times K$)-column matrix $\mathbf{C}_i$ is defined as

$$\mathbf{C}_i = diag\{\mathbf{c}_i\} = \begin{bmatrix} \mathbf{c}_i & \mathbf{0} & \cdots & \cdots & \mathbf{0} \\ \mathbf{0} & \mathbf{c}_i & \mathbf{0} & \cdots & \mathbf{0} \\ \cdots & \cdots & \cdots & \cdots & \cdots \\ \mathbf{0} & \cdots & \cdots & \mathbf{0} & \mathbf{c}_i \end{bmatrix}, \quad i = 1, 2,\ldots, K, \tag{5.6}$$

in which $\mathbf{0} = \{0\}_{1 \times N}$. For the ith user, define $\mathbf{R}(i) \equiv \mathbf{C}_i \mathbf{R} \mathbf{C}_i^H$; and the kth row vector of $\mathbf{R}(i)$ is denoted by $\mathbf{R}(i)_k, \forall k = 1, 2,\ldots, K$. Based on these definitions, the matrix that combines the

channel gains and cross-correlations of signature sequences is given by $\mathbf{R}_c \equiv [\mathbf{R}(1)_1{}^H, \mathbf{R}(2)_2{}^H, ..., \mathbf{R}(K)_K{}^H]^H$, which is a $K \times K$ matrix. Represent the RAKE combiner outputs of all the K users by the vector $\mathbf{y} = [y_1, y_2, ..., y_K]^T$, and the noise components by $\mathbf{z} = [z_1, z_2, ..., z_K]^T$. Then for K users, equation (5.1) can be transformed into the compact form

$$\mathbf{y} = \mathbf{R}_c\mathbf{b} + \mathbf{z}, \tag{5.7}$$

Equation (5.7) is in the similar form as the output of the matched filter bank for case of AWGN channels, therefore the matrix $\mathbf{R}_c$ can be interpreted as matrix of the cross-correlations between the received user signal waveforms in multipath case. It is practically reasonable to assume $\mathbf{R}_c$ always invertible. Based on the assumption that the transmitter can correctly predict all the channels, we insert the linear filter $\mathbf{T} = \mathbf{R}_c{}^{-1}$ into the transmitter. The corresponding RAKE combiner output is $\mathbf{y} = \mathbf{b} + \mathbf{z}$, thus the interference among the user signals is eliminated. Although from the above derivations $\mathbf{T} = \mathbf{R}_c{}^{-1}$ is obtained as the zero forcing filter, it also satisfies the MMSE criterion [VJ98, Appendix A]. Similarly to the linear decorrelating precoding in AWGN channels, the total transmit power is increased as a consequence of the linear transmitter precoding. Without precoding, the total average transmit energy per symbol interval for a BPSK system is $E_{\text{av}} = \sum_{i=1}^{K} A_i^2$. With the assumption that the spreading sequences for all users are orthogonal to one another, the total average transmit energy per symbol interval equals to $E_{\text{av}} = \sum_{i=1}^{K} A_i^2 (\mathbf{R}_c{}^{-T}\mathbf{R}_c{}^{-1})_{i,i}$. Therefore, the power-scaling factor Sf is given by the ratio

69

$$\frac{1}{Sf^2} = \frac{\sum_{i=1}^{K} A_i^2 (\mathbf{R}_c^{-H} \mathbf{R}_c^{-1})_{i,i}}{\sum_{i=1}^{K} A_i^2}. \tag{5.8}$$

The actual transmit signal should be $x(t) = Sf\mathbf{s}^T(t)\mathbf{R}_c^{-1}\mathbf{b}$. At the receivers, the symbol detector input is $Sf\mathbf{b} + \mathbf{z}$. From equation (5.2), the noise component for the ith user has zero mean and variance

$$\text{var}\{z_i^2\} = N_0 \sum_{l=0}^{N-1} \sum_{n=0}^{N-1} R_{i,i}^{l-n} c_{i,l} c_{i,n}^*. \tag{5.9}$$

Hence, the BER for the ith user, $i = 1, 2,\ldots, K$, is given by

$$Pe_i = Q\left(\sqrt{\frac{2Sf^2 \gamma_{bi}}{\sum_{l=0}^{N-1} \sum_{n=0}^{N-1} R_{i,i}^{l-n} c_{i,l} c_{i,n}^*}}\right), \tag{5.10}$$

Although this precoding method completely eliminates the MAI, it is shown by equation (5.10) that the BER is increased by the power scaling factor Sf. Also, this method does not completely simplify the mobile user receiver, since it uses the Rx-based RAKE combiner.

5.2 Linear Decorrelating Prefilters

In the method of linear decorrelating transmitter precoding with RAKE receiver, the linear filtering is applied directly to the data symbols and followed by spreading; while another way to apply a linear filter in the transmitter is to filter the transmit signal which has already been spread, this approach was named as decorrelating prefilters [BD00].

For a K-user system, the data symbols of every user is first spread with its signature sequence, and then passed through a L_p-tap linear filter. For the ith user, represent the

70

prefilter coefficients by a column vector $\mathbf{p}_i = [p_{i,0}, \ p_{i,1}, \ \ldots, \ p_{i,Lp-1}]^T$, $i=1,2,\ldots,K$. The final transmit signal is given by

$$x(t) = \sum_{k=1}^{K} \sum_{j=0}^{Lp-1} b_k p_{k,j} s_k(t - jT_c). \tag{5.11}$$

In the ith user receiver, the received signal is

$$r_i(t) = \sum_{l=0}^{N-1} \sum_{k=1}^{K} \sum_{j=0}^{Lp-1} c_{i,l} p_{k,j} b_k s_k(t - (j+l)T_c) + n_i(t). \tag{5.12}$$

The received signal is fed into the filter simply matched to $s_i(t)$ instead of the RAKE combiner, since in this approach the multipath interference is aimed to be rejected in the transmitter, and the mobile user receivers remain as simple as those in single-path channels.

With the notation $a_{i,j}^{k} \equiv \sum_{l=0}^{N-1} c_{i,l} \int_{0}^{T} s_k(t-(j+l)T_c)s_i(t)dt$, the output of the matched filter in the ith user receiver equals

$$y_i = \sum_{k=1}^{K} \left(b_k \sum_{j=0}^{Lp-1} p_{k,j} a_{i,j}^{k} \right) + n_i, \tag{5.13}$$

where $n_i = \int_{0}^{T} n_i(t)s_i(t)dt$. Thus to recover b_i from y_i, the prefilter optimization problem can be expressed mathematically as

$$\max_{p_{i,j}} \left(\sum_{j=0}^{Lp-1} p_{i,j} a_{i,j}^{i} \right), \tag{5.14}$$

subject to the constraints

$$\sum_{j=0}^{Lp-1} p_{k,j} a_{i,j}^{k} = 0, \ \forall \ k \neq i,$$

71

and

$$\left\| \sum_{j=0}^{Lp-1} p_{k,j} s_k(t - jT_c) \right\| = 1, \quad \forall \, k = 1, 2, \ldots, K.$$

The latter constraint is to avoid transmit power increase due to the prefilter. ($\| \cdot \|$ is the standard 2-norm.) Define matrices

$$\mathbf{A}_i \equiv \begin{bmatrix} a_{1,0}^i & a_{1,1}^i & \ldots & a_{1,Lp-1}^i \\ a_{2,0}^i & a_{2,1}^i & \ldots & a_{2,Lp-1}^i \\ \ldots & \ldots & \ldots & \ldots \\ a_{K,0}^i & a_{K,1}^i & \ldots & a_{K,Lp-1}^i \end{bmatrix}, \qquad i = 1, 2, \ldots, K. \tag{5.15}$$

For user i, the solution for vector $\mathbf{p}_i$ which satisfies (5.14) as well as the constraints can be found by solving the equation about an L_p-tuple vector $\hat{\mathbf{p}}_i = [\hat{p}_{i,0}, \hat{p}_{i,1}, \ldots, \hat{p}_{i,Lp-1}]^T$

$$\mathbf{A}_i \times \hat{\mathbf{p}}_i = \mathbf{e}_i, \tag{5.16}$$

where vector $\mathbf{e}_i$ is an all-zero vector except for a unity entry at position i. If $\mathbf{A}_i$ is a consistent matrix, an exact zero-forcing solution can be obtained; otherwise, a lease square solution can be obtained by minimizing $\| \mathbf{e}_i - \mathbf{A}_i \times \hat{\mathbf{p}}_i \|$. The prefilter coefficients $\mathbf{p}_i$ are obtained by normalizing $\hat{\mathbf{p}}_i$, $\mathbf{p}_i = Sf_i \hat{\mathbf{p}}_i$, in which the power scaling factor Sf_i is given by

$$Sf_i = \frac{1}{\left\| \sum_{j=0}^{Lp-1} \hat{p}_{i,j} s_i(t - jT_c) \right\|}, \qquad i = 1, 2, \ldots, K. \tag{5.17}$$

It is noted that each user prefilter is normalized individually, which allows each user to achieve a specified received symbol energy-to-noise ratio, instead of using a global transmit signal normalization as in the linear decorrelating precoding scheme.

By the prefilter optimization, the symbol detector input in the ith user receiver is $Sf_i b_i + \mathrm{Re}[n_i]$, $i = 1, 2, \ldots, K$, therefore, the BER for user i is given by

$$Pe_i = Q\left(\sqrt{2Sf_i^2 \gamma_{bi}}\right).$$
(5.18)

An important advantage of the linear decorrelating prefilter is that it effectively applies the preprocessing matrix to the output of the spread spectrum encoder, so it can be applied externally to an existing design. However, as shown by the simulation results in [BD00] and our simulation in section 5.5, this method does not have performance benefit compared to the linear precoder in [VJ98].

5.3 PreRAKE Multiuser Precoding (Pre-RDD)

The Pre-RDD [Gun03] was inspired from the Rx-based RDD described in section 2.2.1. In the transmitter of Pre-RDD, a linear decorrelating filter is followed by a Pre-RAKE combiner. Suppose the linear filter is represented by a $K \times K$ matrix $\mathbf{G}$. The output vector of the filter is thus given by $\mathbf{w} = [w_1, w_2, ..., w_K]^T = \mathbf{Gb}$. The result of Pre-RAKE combining is normalized by a global power scaling factor S_f. Therefore, the ultimate transmit signal from BS is given by

$$x(t) = S_f \sum_{k=1}^{K} \sum_{n=0}^{N-1} w_k \hat{c}_{k,n}{}^* s_k (t - (N-1-n)T_c) \tag{5.19}$$

At the mobile user receivers, simple matched filters are used. For all K users, the MF output vector $\mathbf{y} = [y_1, y_2, ..., y_K]^T$ can be expressed in a compact form $\mathbf{y} = S_f \mathbf{CR}\hat{\mathbf{C}}^H \mathbf{Gb} + \mathbf{n}$. Define the correlation matrix $\tilde{\mathbf{R}} = \mathbf{CRC}^H$ and the precoding filter $\mathbf{G} = \mathbf{S}^{-2} \tilde{\mathbf{R}}^{-1} = (\hat{\mathbf{C}}\mathbf{R}\hat{\mathbf{C}}^H)^{-1}$. Then the MF output is simplified into $\mathbf{y} = S_f \mathbf{S}^{-1} \mathbf{b} + \mathbf{n}$, where the diagonal matrix of channel gain normalization factors $\mathbf{S}$ follows the definition in section 4.1. Equivalently, the MF output for the ith user is

$$y_i = \frac{S_f}{S_i} b_i + n_i \tag{5.20}$$

To normalize the total transmit power, the average transmitted signal energy per symbol $E_\mathbf{b} \left\{ \int_0^T |x(t)|^2 dt \right\}$ should be equal to the original average transmit energy $E_\mathbf{b} \{\mathbf{b}^T \mathbf{b}\}$. That is, we need to satisfy

$$S_f^2 \sum_{i=1}^{K} A_i^2 \left[\mathbf{G}^H \hat{\mathbf{C}} \mathbf{R} \hat{\mathbf{C}}^H \mathbf{G} \right]_{ii} = \sum_{i=1}^{K} A_i^2 . \tag{5.21}$$

Therefore, the global power scaling factor is given by

$$S_f^2 = \frac{\displaystyle\sum_{i=1}^{K} A_i^2}{\displaystyle\sum_{i=1}^{K} A_i^2 S_i^{-2} \left[\tilde{\mathbf{R}}^{-1} \right]_{ii}} \tag{5.22}$$

By equation (5.20), the BER of the kth user in BPSK systems is

$$Pe_k = Q\left(\sqrt{\frac{2\displaystyle\sum_{i=1}^{K} A_i^2 \displaystyle\sum_{n=0}^{N-1} |c_{k,n}|^2}{\displaystyle\sum_{i=1}^{K} A_i^2 \left[\tilde{\mathbf{R}}^{-1} \right]_{ii} \displaystyle\sum_{n=0}^{N-1} |c_{i,n}|^2}} \cdot \gamma_{bi} \right) \tag{5.23}$$

Although the Pre-RDD has the same decorrelating filter and RAKE combining structure as the Rx-based RDD, their theoretical BER are different. From equation (5.23), we observe that if the transmit power for all users are equal, for Pre-RDD all users have identical error rate. This is because all users share the same power scaling factor. As derived in section 2.2.1, for RDD, different users can have different error rates.

5.4 Linear Decorrelating Multiuser Precoding Combined with Transmit Antenna Diversity

5.4.1 Transmitter-Based Antenna Diversity and Multi-Input-Single-Output (MISO) Channel model

For the downlink of mobile radio systems, transmitter-based diversity techniques enable to shift signal processing from MS to BS, where power and computational complexity are more abundant, thus the mobile user receiver units are simplified. Transmit antenna diversity at the BS has been identified as an efficient way of improving the downlink data rate without expanding the bandwidth, especially in low-mobility environments, where there is insufficient time or frequency diversity [Ala98, Lo99, BZP04]. Indeed, transmit diversity has already been adopted by the 3GPP standards [TSG01].

Closed-loop transmit antenna diversity techniques achieve better performance than open-loop methods, but they require feedback of the channel state information from the MS, as shown in Fig. 5.1. However, in practical rapidly varying fading channels, the fed back CSI is not up-to-date which results in performance degradation. The LRP algorithm has superior performance relative to conventional channel prediction methods, because of its much longer memory span obtained by using lower sampling rate [DH00]. The performance of transmit antenna diversity techniques aided by LRP are analyzed in [GD05].

The hybrid designs which combines transmitter-based MAI cancellation with transmit antenna diversity are described in this chapter. We only elaborate the combination of linear precoding with multiple transmit antennas; however, these space-time designs can be easily extended to nonlinear precoding.
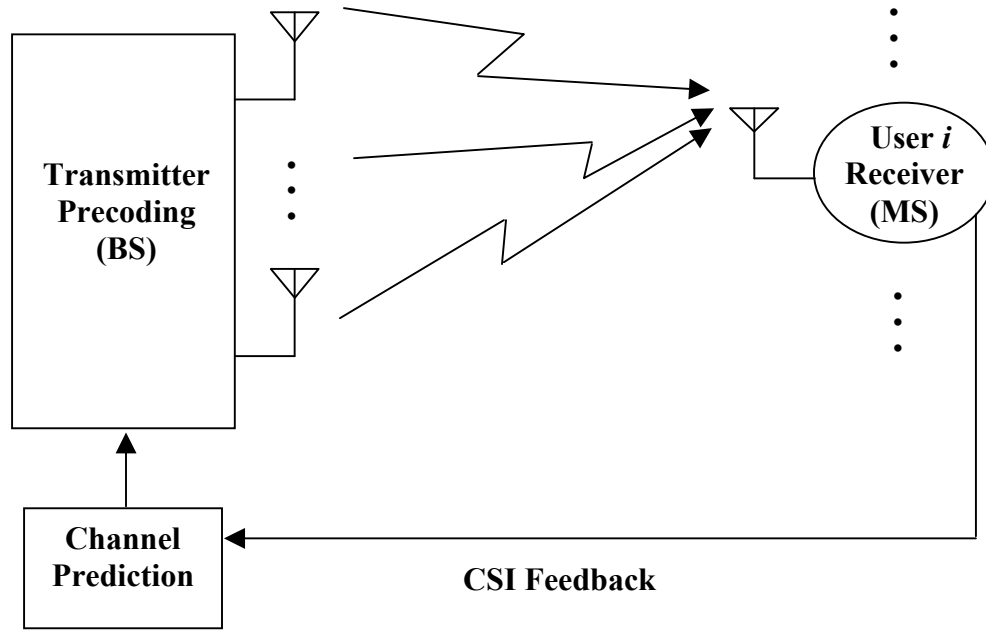
Figure 5.1 System Diagram of Closed-loop Transmit Antenna Diverisy

Fig. 5.1 shows the MISO channel diagram. Consider a downlink DS/CDMA system with K active mobile users in a cell. The BS employs L transmit antennas, and the MS for each user employs single receive antenna. The channels from the antennas at the BS to the MSs are each subject to frequency-selective Rayleigh fading with N resolvable paths. If the baseband-equivalent signal transmitted from the lth antenna in the data interval of interest is denoted by $x^{(l)}(t)$, $l = 1, 2, \ldots, L$, then the signal received by the ith user can be expressed as

$r_i(t) = \sum_{n=0}^{N-1} \sum_{l=1}^{L} c_{i,n}^{(l)} x^{(l)}(t - nT_c) + n_i(t)$, where T_c is the chip duration, $c_{i,n}^{(l)}$ is the channel gain

coefficient of the nth path from the lth transmit antenna to the ith user's receiver and $n_i(t)$ is

the complex AWGN with power spectral density N_0, for $\forall$ $i = 1, 2, \ldots, K$ and $n = 0, 1, \ldots, N-1$. The channel coefficients $c_{i,n}^{(l)}$ are modeled as independent and identically distributed (i.i.d) Rayleigh fading random variables with $E\{\sum_{n=0}^{N-1} | c_{i,n}^{(l)} |^2\} = 1$. ($E\{\cdot\}$ is the expectation.) With the previously defined notations for user data and spreading codes, when no Tx-based processing is applied, the signal received by the ith user is given by

$$r_i(t) = \sum_{n=0}^{N-1} \sum_{l=1}^{L} \sum_{k=1}^{K} c_{i,n}^{(l)} b_k s_k (t - nT_c) + n_i(t). \qquad (5.24)$$

For the convenience of derivation, define the channel gain row vector for the ith user corresponding to the lth transmit antenna as $\mathbf{c}_i^{(l)} = [c_{i,0}^{(l)}, c_{i,1}^{(l)}, \ldots, c_{i,N-1}^{(l)}]$; and for all K users, define the K-row ($N{\times}K$)-column channel gain matrix $\mathbf{C}^{(l)} = diag\{\mathbf{c}_1^{(l)}, \mathbf{c}_2^{(l)}, \ldots, \mathbf{c}_K^{(l)}\}$, $\forall l = 1, 2, \ldots, L$. To avoid the transmit power increase incurred by channel gain coefficients, we use the normalized values of channel gain coefficients in precoding. For the ith user, the channel gain normalization factor is defined as

$$S_{ci} = \left(\sum_{l=1}^{L} \sum_{n=0}^{N-1} \left| c_{i,n}^{(l)} \right|^2 \right)^{-1/2}. \qquad (5.25)$$

Then the normalized channel gain coefficient is $\hat{c}_{i,n}^{(l)} = S_{ci} c_{i,n}^{(l)}$. Define the normalized vector $\hat{\mathbf{c}}_i^{(l)} = S_{ci} \cdot \mathbf{c}_i^{(l)}$ and matrix $\hat{\mathbf{C}}^{(l)} = diag\{\hat{\mathbf{c}}_1^{(l)}, \hat{\mathbf{c}}_2^{(l)}, \ldots, \hat{\mathbf{c}}_K^{(l)}\}$, respectively. By representing the normalization factors with a diagonal $K{\times}K$ matrix $\mathbf{S_c} = diag\{S_{c1}, S_{c2}, \ldots, S_{cK}\}$, we obtain the relation $\hat{\mathbf{C}}^{(l)} = \mathbf{S_c} \mathbf{C}^{(l)}$.

5.4.2 Zero Forcing (ZF)-based PreRAKE Linear Decorrelating Precoding (PreRAKELDP)
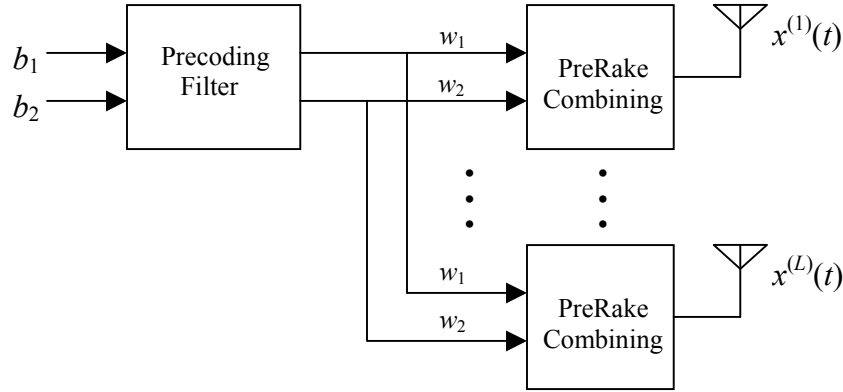
Figure 5.2 Transmitter diagram of PreRAKELDP for a 2-user, *L*-antenna System

The transmitter diagram of the PreRAKELDP with multiple Tx antennas is shown in Fig. 5.2. The linear MAI pre-cancellation process actually increases the required transmit power. To offset the power increase, we scale the amplitude of the transmit signal b_i by a factor S_{fi}, $\forall i = 1, 2, \ldots, K$. For all users, define the diagonal scaling factor matrix $\mathbf{S_f} = diag\{S_{f1}, S_{f2}, \ldots, S_{fK}\}$. Suppose the decorrelating (ZF) filter is a $K \times K$ matrix $\mathbf{G}$, and the result of power scaling and decorrelating is denoted by vector $\mathbf{w}$. Then $\mathbf{w} = [w_1, w_2, \ldots, w_K]^T = \mathbf{GS_f b}$. The transmitted signal from the *l*th antenna, $x^{(l)}(t)$, is generated by passing the decorrelating filter output through the *l*th branch of the preRAKE combiner

$$x^{(l)}(t) = \sum_{k=1}^{K}\sum_{n=0}^{N-1} w_k \hat{c}_{k,n}^{(l)\,*} s_k(t-(N-1-n)T_c). \tag{5.26}$$

At the ith user receiver, the equivalent baseband received signal is given by

$$r_i(t) = \sum_{p=0}^{N-1}\sum_{l=1}^{L} c_{i,p}^{(l)} x^{(l)}(t-pT_c) + n_i(t). \tag{5.27}$$

A channel-gain-independent matched filter (MF) is used at the front end of each user's receiver. To obtain the largest received signal energy, the output of the matched filters should be sampled at the moment $t = (N-1)T_c$ [ESN99]. The output of the ith user's MF is given by

$$y_i = \int_{(N-1)T_c}^{T+(N-1)T_c} r_i(t) s_i(t-(N-1)T_c)\,dt. \tag{5.28}$$

Substituting (5.26) and (5.27) into (5.28), we obtain

$$y_i = \sum_{k=1}^{K}\sum_{n=0}^{N-1}\sum_{m=-n}^{N-1-n}\sum_{l=1}^{L} c_{i,m+n}^{(l)} \hat{c}_{k,n}^{(l)\,*} w_k R_{i,k}^m + n_i, \tag{5.29}$$

where n_i is the filtered noise component with power $E\{n_i n_i^*\} = N_0$. Define vectors $\mathbf{y} = [y_1, y_2, \ldots, y_K]^T$ and $\mathbf{n} = [n_1, n_2, \ldots, n_K]^T$. Then the vector of MF outputs of all K users

$$\mathbf{y} = \mathbf{S_c}^{-1}\left(\sum_{l=1}^{L}\hat{\mathbf{C}}^{(l)}\mathbf{R}\hat{\mathbf{C}}^{(l)\,H}\right)\mathbf{G}\mathbf{S_f}\mathbf{b} + \mathbf{n}. \tag{5.30}$$

Let

$$\hat{\mathbf{R}} = \sum_{l=1}^{L}\hat{\mathbf{C}}^{(l)}\mathbf{R}\hat{\mathbf{C}}^{(l)\,H}. \tag{5.31}$$

To recover the desired user signal, define the decorrelating precoding filter

$$\mathbf{G} = \hat{\mathbf{R}}^{-1}. \tag{5.32}$$

Then equation (5.30) can be simplified as

$$\mathbf{y} = \mathbf{S_c}^{-1}\mathbf{S_f}\mathbf{b} + \mathbf{n}. \tag{5.33}$$

It is obvious that the MF output for each user, $y_i = \left(S_{fi}/S_{ci}\right)b_i + n_i$, does not contain MAI.

Now we determine the values of the transmit power scaling factors. The total average energy of the transmit signal during one symbol interval should satisfy $E_{\mathbf{b}}\left\{\sum_{l=1}^{L}\int_0^T \left|x^{(l)}(t)\right|^2 dt\right\} = E_{\mathbf{b}}\{\mathbf{b}^T\mathbf{b}\}$, where $E_{\mathbf{b}}\{\cdot\}$ is the expected value with respect to the data symbols. From equation (5.26), $E_{\mathbf{b}}\left\{\sum_{l=1}^{L}\int_0^T \left|x^{(l)}(t)\right|^2 dt\right\} = E_{\mathbf{b}}\{\mathbf{b}^T\mathbf{G}^H\mathbf{S_f}^2\mathbf{b}\}$; hence, it is sufficient to require user i to satisfy $G_{ii}S_{fi}^2 = 1$, $i = 1, 2, \ldots, K$. From (5.31) and (5.32), we find that the diagonal elements of $\mathbf{G}$ are real. Therefore, the power scaling factor for user i is

$$S_{fi}^2 = \frac{1}{G_{ii}} = \frac{1}{[\hat{\mathbf{R}}^{-1}]_{ii}}. \tag{5.34}$$

Consequently, for user i, the BER of the PreRAKELDP with individual power scaling in terms of the average transmit signal-to-noise ratio (SNR) γ_{bi} is

$$Pe_i(\gamma_{bi}) = Q\left(\sqrt{\frac{2\sum_{n=0}^{N-1}\sum_{l=1}^{L}\left|c_{i,n}^{(l)}\right|^2}{[\hat{\mathbf{R}}^{-1}]_{ii}}\gamma_{bi}}\right), \tag{5.35}$$

where $\gamma_{bi} = E_{bi}/N_0 = A_i^2/(2N_0)$. Comparing equation (5.35) with the BER formula of RDD [HS94], we find that in the absence of antenna diversity, i.e., when $L=1$, the performance of the PreRAKELDP with power scaling is identical to that of RDD. The Pre-RDD [Gun03] is equivalent to the precoder derived in this section for a single antenna, but a global power scaling factor instead of individual power scaling factors is utilized. As a result, all users have the same BER given by the average of all users' BERs of the PreRAKELDP method. In

practice, the PreRAKELDP is more flexible because it allows different users to satisfy their individual reliability criteria.

Comparing the Pre-RDD, ZF-based PreRAKELDP and the linear decorrelating precoding with RAKE receiver in [VJ98], we can find that all the three methods utilize RAKE multipath diversity technique; the only difference is that the method in [VJ98] uses RAKE combining in receiver, while the other two methods use it in transmitter. However, this different in structure results in the performance difference between the method in [VJ98] and the two PreRAKE precoding methods. The detailed performance analysis for a 2-user system is provided in the Appendix. More comparison results are obtained by simulation examples in section 5.5.

5.4.3 Minimum Mean Square Error (MMSE)-based PreRAKELDP

From (5.35), we observe that the power scaling factors degrade precoding performance. With the same transmitter structure as in Fig.1, in this section our goal is to design the optimum linear precoding filter $\mathbf{G}$ in the sense of MMSE criterion under the total average transmit power constraint. Similarly to equation (5.30), with linear precoding, the sampled MF output vector at the receiver is given by

$$\mathbf{y} = \sum_{l=1}^{L} \mathbf{C}^{(l)} \mathbf{R} \hat{\mathbf{C}}^{(l)H} \mathbf{G} \mathbf{b} + \mathbf{n}. \tag{5.36}$$

The filter $\mathbf{G}$ should be the solution of

$$\min_{\mathbf{G} \in C^{K \times K}} \quad E_{\mathbf{b}}\{\|\mathbf{b} - \mathbf{S_c}\mathbf{y}\|^2\}$$

subject to

82

$$E_{\mathbf{b}}\left\{\sum_{l=1}^{L}\int_{0}^{T}\left|x^{(l)}(t)\right|^{2}dt\right\} = E_{\mathbf{b}}\{\mathbf{b}^{T}\mathbf{b}\} \ . \tag{5.37}$$

For the convenience of following derivations, define the amplitude matrix for all users as

$\mathbf{A_m} = diag\{\sqrt{E_{b1}}, \sqrt{E_{b2}}, \ldots, \sqrt{E_{bK}}\}$. It is easily known that $E_{\mathbf{b}}\left\{\int_{0}^{T}x^{2}(t)dt\right\} = \mathrm{tr}\{\mathbf{G}^{H}\hat{\mathbf{R}}\mathbf{G}\mathbf{A_m}^{2}\}$. By

means of Lagrange multiplier method, it is desired to find $\mathbf{G}$ which minimizes

$$\varepsilon \equiv E_{\mathbf{b}}\{\|\mathbf{b}\text{-}\mathbf{S_c}\mathbf{y}\|^{2}\}+\lambda \ tr\{\mathbf{G}^{H}\hat{\mathbf{R}}\mathbf{G}\mathbf{A_m}^{2}\}. \tag{5.38}$$

The derivative of the first term with respect to each element of $\mathbf{G}$ is

$$\frac{\partial}{\partial G_{i,j}}E_{\mathbf{b}}\{\|\mathbf{b}\text{-}\mathbf{S_c}\mathbf{y}\|^{2}\} = \frac{\partial}{\partial G_{i,j}}E_{\mathbf{b}}\{(\mathbf{b}^{T}\mathbf{G}^{T}\hat{\mathbf{R}}+\mathbf{n}^{T}\mathbf{S_c})(\hat{\mathbf{R}}\mathbf{G}\mathbf{b}+\mathbf{S_c}\mathbf{n})$$

$$= 2[\hat{\mathbf{R}}^{2}\mathbf{G}\mathbf{A_m}^{2}]_{i,j}-2[\hat{\mathbf{R}}\mathbf{A_m}^{2}]_{i,j} \tag{5.39}$$

The derivative of second term w.r.t. each element of $\mathbf{G}$ is

$$\frac{\partial(\lambda \cdot tr\{\mathbf{G}^{H}\hat{\mathbf{R}}\mathbf{G}\mathbf{A_m}^{2}\})}{\partial G_{i,j}} = \lambda E_{bj}\frac{\partial}{\partial G_{i,j}}\sum_{m=1}^{K}G_{m,j}\sum_{n=1}^{K}\hat{R}_{m,n}G_{n,j}$$

$$= 2\lambda E_{bj}\sum_{n=1}^{K}\hat{R}_{i,n}G_{n,j} = 2\lambda[\hat{\mathbf{R}}\mathbf{G}\mathbf{A_m}^{2}]_{i,j} \ . \tag{5.40}$$

Since $\dfrac{\partial \varepsilon}{\partial G_{i,j}} = 0$, we get

$$[\hat{\mathbf{R}}^{2}\mathbf{G}\mathbf{A_m}^{2}]_{i,j}-[\hat{\mathbf{R}}\mathbf{A_m}^{2}]_{i,j} = \lambda[\hat{\mathbf{R}}\mathbf{G}\mathbf{A_m}^{2}]_{i,j} \ . \tag{5.41}$$

In terms of matrices, (5.41) is equivalent to

$$\hat{\mathbf{R}}^{2}\mathbf{G}\mathbf{A_m}^{2}-\hat{\mathbf{R}}\mathbf{A_m}^{2} = \lambda\hat{\mathbf{R}}\mathbf{G}\mathbf{A_m}^{2}$$

$$\mathbf{G} = (\hat{\mathbf{R}}+\lambda\mathbf{I})^{-1} \tag{5.42}$$

where the value of λ can be determined from the constraint (5.37), which is equivalent to

$\mathrm{tr}\{\mathbf{G}^H\hat{\mathbf{R}}\mathbf{G}\mathbf{A_m}^2\} = \mathrm{tr}\{\mathbf{A_m}^2\}$. Note that $\hat{\mathbf{R}}$ is positive definite. Suppose its eigenvalues are a_1,

$a_2,\ldots, a_K$. Define the unitary matrix $\mathbf{F}=\{F_{ij}\}_{K\times K}$ with jth column given by the eigenvector of

$\hat{\mathbf{R}}$ corresponding to a_j, $j = 1, 2, \ldots, K$. Therefore, $\hat{\mathbf{R}} = \mathbf{F}diag\{a_j\}\mathbf{F}^H$ and

$\mathbf{G} = \mathbf{F}diag\{(a_j+\lambda)^{-1}\}\mathbf{F}^H$, where $diag\{a_j\}$ represents the $K\times K$ diagonal matrix with a_j at the jth

diagonal position. The total power constraint can be expressed as

$$\sum_{i=1}^{K}\left(A_i^2\sum_{j=1}^{K}\frac{|F_{ij}|^2 a_j}{(\lambda+a_j)^2}\right) = \sum_{i=1}^{K}A_i^2. \tag{5.43}$$

By solving this equation we can obtain the value of λ.

The total power constraint optimization for single-path AWGN channel was studied in [VJ98] and [HKT02]. It was shown that for the single-path channel with highly-correlated signature sequences, the total power constraint optimization does not have the BER performance advantage over the transmit power scaling method, due to the severe residual MAI in the received signals. However, we consider a different channel model in this paper corresponding to the orthogonal downlink CDMA over multipath fading channels. For this model, the residual MAI is very small for the total power constraint approach. Therefore, the total power constraint optimization results in better performance than the individual power scaling for the PreRAKELDP. This conclusion will be verified by simulation results. On the other hand, optimization under the total power constraint has much higher complexity than the transmit power scaling.

It should be noted that to achieve a simple and practical transmitter design for a system with large number of users, the allocation of individual user transmit powers is not

taken into account in the PreRAKELDP designs. Since the pre-RAKE combiner is equivalent to a matched filter which is matched to the multipath fading channels, the PreRAKELDP with individual user power scaling and that with total transmit power constraint are the optimum linear ZF and MMSE precoders, respectively.

5.4.4 Multipath Decorrelating Precoding (MDP)

In the PreRAKELDP, the calculation of precoding filter coefficients requires the operation of matrix inversion of a CSI-dependent matrix, which results in high computational complexity. To simplify the transmitter, we present an alternative precoding algorithm, MDP. As in the PreRAKELDP, in the MDP design each MS only needs to use a simple and CSI-independent matched filter for data detection.

As shown in Fig. 5.3, for a system with L transmit antennas, the precoding process consists of L parallel and independent branches. Fig. 5.4 demonstrates the detailed structure of each branch. In the lth branch, the data symbols for the K users are first weighed by the normalized channel gains, with the output given by the ($K \times N$)-element vector $\hat{\mathbf{C}}^{(l)^H}\mathbf{b}$. As shown in Fig. 5.4, the channel gain weighed signals are filtered by the power control filter and decorrelating filter. The decorrelating filter is defined as $\mathbf{G} = \mathbf{R}^{-1}$. The power control filter for the ith user is defined as $\mathbf{T}_i = \widetilde{S}_i ([\mathbf{G}]_{ii})^{-1}$ ($[\mathbf{G}]_{ij}$ represents the (I, j)th $N \times N$ block of $\mathbf{G}$); for all K users, define the compact form as $\mathbf{T} \equiv diag\{\mathbf{T}_1, \mathbf{T}_2, \ldots, \mathbf{T}_K\}$, which is a ($K \times N$)-row ($K \times N$)-column matrix with $\mathbf{T}_i$ as the ith diagonal $N \times N$ block, $i = 1, 2, \ldots, K$. Note that the notation for the power control filters and decorrelating filter are not identified with an antenna index, which means these filters have exactly the same definitions for all the L branches. The output of the decorrelating filter for the lth branch is given by

$\mathbf{w}^{(l)} = [w_1^{(l)}, w_2^{(l)}, ..., w_{K \times N}^{(l)}]^T = \mathbf{GT\hat{C}}^{(l)H}\mathbf{b}$. Following the signature sequence spreading, the transmitted signal from the lth antenna is

$$x^{(l)}(t) = \sum_{k=1}^{K}\sum_{n=0}^{N-1} w_{k \times N - n}^{(l)} s_k(t - nT_c).$$ (5.44)

It is sufficient to require the individual users to satisfy $\sum_{l=1}^{L}\hat{\mathbf{c}}_i^{(l)}\mathbf{T}_i^T[\mathbf{G}]_{ii}^T\mathbf{T}_i\hat{\mathbf{c}}_i^{(l)H} = 1$, $i = 1, 2, ..., K$. It can be calculated that $\widetilde{S}_i$ is

$$\widetilde{S}_i = \left(\sum_{l=1}^{L}\hat{\mathbf{c}}_i^{(l)}([\mathbf{G}]_{ii})^{-1}\hat{\mathbf{c}}_i^{(l)H}\right)^{-1/2}.$$ (5.45)

At the ith user's receiver, the baseband-equivalent received signal is given by

$$r_i(t) = \sum_{p=0}^{N-1}\sum_{l=1}^{L} c_{i,p}^{(l)} x^{(l)}(t - pT_c) + n_i(t).$$ (5.46)

With the same MF as in the PreRAKELDP, the MF result for the ith user is

$$y_i = \sum_{k=1}^{K}\sum_{n=0}^{N-1}\sum_{p=0}^{N-1}\sum_{l=1}^{L} c_{i,p}^{(l)} w_{k \times N - n}^{(l)} R_{i,k}^{N-1-(n+p)} + n_i,$$ (5.47)

where n_i is the filtered noise component with power $E\{n_i n_i^*\} = N_0$. For all K users, the compact form of the MF output is given by

$$\mathbf{y} = \mathbf{S_c}^{-1}\left(\sum_{l=1}^{L}\hat{\mathbf{C}}^{(l)}\mathbf{T}\hat{\mathbf{C}}^{(l)H}\right)\mathbf{b} + \mathbf{n}.$$ (5.48)

Therefore, the simplified result of y_i is

$$y_i = \left(\sum_{l=1}^{L}\mathbf{c}_i^{(l)}([\mathbf{R}^{-1}]_{ii})^{-1}\mathbf{c}_i^{(l)H}\right)b_i + n_i.$$ (5.49)

86

Note that the MAI is completely cancelled by transmitter precoding. The BER in terms of γ_{bi} is given by

$$Pe_i(\gamma_{bi}) = Q\left(\sqrt{2\sum_{l=1}^{L}\mathbf{c}_i^{(l)}([\mathbf{R}^{-1}]_{ii})^{-1}\mathbf{c}_i^{(l)H}\gamma_{bi}}\right). \tag{5.50}$$

The BER of single-antenna MDP is identical to that of the Rx-based MDD [ZB96, Zvo96]. The MDD is a suboptimal linear decorrelating MUD. It is shown in [HS94] that the RDD outperforms the MDD. Since the PreRAKELDP with individual power scaling has identical performance to the RDD, it has better performance than the MDD and MDP. However, as the precoding process in MDP does not involve the inverse operation of CSI-related matrix, the MDP is computationally simpler than the PreRAKELDP and the RDD.

The STPR MUP in [GDv03] employs the same decorrelating filter $\mathbf{R}^{-1}$ as the MDP does; thus it has similar complexity to the MDP. For the simple case of equal transmit power for all users (i.e., $A_1 = A_2 = \ldots = A_K$), the following derivation shows that the MDP has lower BER than the STPR MUP. Without losses of generality, we only illustrate the case of single transmit antenna. Using the notations defined above, the BER for the STPR MUP is given by

$$Pe_i(\gamma_{bi}) = Q\left(\sqrt{\frac{2K}{S_{ci}^2\sum_{k=1}^{K}\hat{\mathbf{c}}_k[\mathbf{R}^{-1}]_{kk}\hat{\mathbf{c}}_k^{H}}\gamma_{bi}}\right). \tag{5.51}$$

Considering $\mathbf{c}_i = S_{ci}^{-1}\hat{\mathbf{c}}_i$ and from equations (5.50) and (5.51), it is known that comparing the performance of these two methods is equivalent to comparing the decision statistics for the MDP, $X_i \equiv \hat{\mathbf{c}}_i([\mathbf{R}^{-1}]_{ii})^{-1}\hat{\mathbf{c}}_i^{H}$, and that for STPR MUP, $Y \equiv K\left(\sum_{k=1}^{K}\hat{\mathbf{c}}_k[\mathbf{R}^{-1}]_{kk}\hat{\mathbf{c}}_k^{H}\right)^{-1}$. Although

direct comparison between X_i and Y does not lead to definite conclusion due to the fact that the comparison result is influenced by the instantaneous channel gain coefficients and signature sequences assignment among users, it is still inspiring to analyze the BER averaged over all users for these two methods by means of comparing X_i and $Y_i \equiv \left(\hat{\mathbf{c}}_i [\mathbf{R}^{-1}]_{ii} \hat{\mathbf{c}}_i^H\right)^{-1}$, $\forall\ i = 1, 2, \ldots, K$.

From the definition of matrix $\mathbf{R}$, we know it is positive definite; thus $\mathbf{R}^{-1}$, its $N \times N$ principle submatrix $[\mathbf{R}^{-1}]_{ii}$ and $([\mathbf{R}^{-1}]_{ii})^{-1}$ are also positive definite [HJ85], $i = 1, 2, \ldots, K$. Matrix $[\mathbf{R}^{-1}]_{ii}$ can be factored into $\mathbf{U}\mathbf{\Lambda}\mathbf{U}^H$, where $\mathbf{U}$ is an $N \times N$ unitary matrix and $\mathbf{\Lambda}$ is a diagonal matrix with the eigenvalues of $[\mathbf{R}^{-1}]_{ii}$, $\beta_1, \beta_2, \ldots, \beta_N$, on its diagonal. Notice that X_i, Y_i and all eigenvalues of $[\mathbf{R}^{-1}]_{ii}$ are positive real numbers, $\forall\ i = 1, 2, \ldots, K$. The ratio of X_i to Y_i is given by

$$X_i / Y_i = \hat{\mathbf{c}}_i ([\mathbf{R}^{-1}]_{ii})^{-1} \hat{\mathbf{c}}_i^H \hat{\mathbf{c}}_i [\mathbf{R}^{-1}]_{ii} \hat{\mathbf{c}}_i^H = \hat{\mathbf{c}}_i \mathbf{U}\mathbf{\Lambda}^{-1}\mathbf{U}^H \hat{\mathbf{c}}_i^H \hat{\mathbf{c}}_i \mathbf{U}\mathbf{\Lambda}\mathbf{U}^H \hat{\mathbf{c}}_i^H. \tag{5.52}$$

Denote the product of $\hat{\mathbf{c}}_i \mathbf{U}$ as $\mathbf{u} = [u_1, u_2, \ldots, u_N]$. Therefore,

$$X_i / Y_i = \mathbf{u}\mathbf{\Lambda}^{-1}\mathbf{u}^H \mathbf{u}\mathbf{\Lambda}\mathbf{u}^H = \left(\sum_{i=1}^{N} |u_i|^2 \beta_i\right)\left(\sum_{j=1}^{N} \frac{|u_j|^2}{\beta_j}\right)$$

$$= \left(\sum_{i=1}^{N} |u_i|^2\right)^2 + \sum_{m=1}^{N}\sum_{\substack{n=1 \\ n \neq m}}^{N} |u_n u_m|^2 \left(\frac{\beta_m}{\beta_n} + \frac{\beta_n}{\beta_m} - 2\right). \tag{5.53}$$

In this result, the first term is equal to $\mathbf{u}\mathbf{u}^H = \hat{\mathbf{c}}_i \mathbf{U}\mathbf{U}^H \hat{\mathbf{c}}_i^H = 1$ and the second term is non-negative; thus $X_i / Y_i \geq 1$. Therefore, it is proved that $X_i \geq Y_i$. This analysis indicates that the average performance of MDP is better than that of the STPR MUP. More accurate comparison among linear precoders is given by simulation experiments.
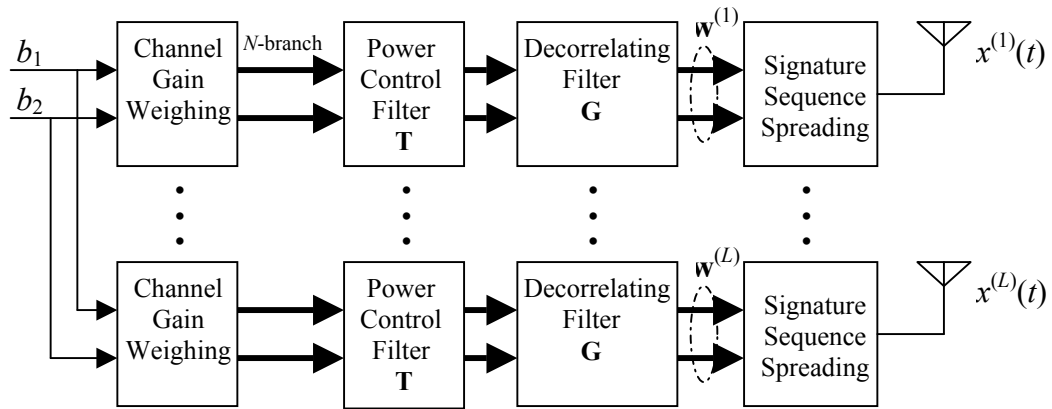
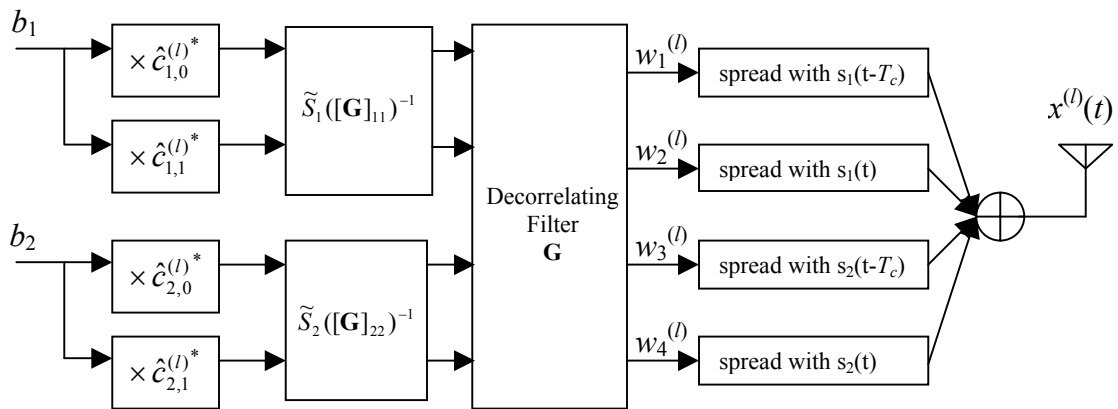**Figure 5.3 Transmitter Diagram of MDP for a 2-user, *L*-antenna, *N*-channel paths/user system**

Figure 5.4 The Structure of the *l*th branch in the MDP transmitter for a 2-user, 2-path/user system

5.5 Numerical Results and Analysis

In this section, we observe the performance of linear precoding techniques by a few numerical experiments. For all simulation examples, BPSK modulation, orthogonal signature sequence spreading and equal transmit power for all users are assumed. There are three resolvable channel paths from each Tx antenna at BS to each user's Rx antenna. In the first example, consider a 4-user uncoded system with single transmit antenna. Fig. 5.5 shows the BER averaged over all users for the ZF-based approaches: PreRAKELDP with individual power scaling (labeled as"PreRAKELDP_ps"), MDP, linear precoding with RAKE receiver (labeled as "Prec. With RAKE") [VJ98], linear decorrelating prefilters (labeled as "Prefilters") [BD00], STPR MUP [GDv03], Rx-based RDD [HS94] and MDD [ZB96]. As analyzed before, the proposed PreRAKELDP_ps and MDP have identical BER to RDD and MDD, respectively. Observe that the two new precoders significantly outperform other methods. The MDP has modestly higher BER than the PreRAKELDP_ps.

Next, we compare the performance of the three ZF precoders, PreRAKELDP_ps, MDP and STPR MUP, with multiple Tx antennas. An 8-user uncoded system is considered. Fig. 5.6 shows the average BER of these methods with one and three transmit antennas, respectively. Obviously, the antenna diversity results in significant performance improvement. Fig. 5.7 shows the BER averaged over all users versus the number of users. The transmit SNR is fixed at 0dB. Observe that the BER saturates as the number of users becomes greater than eight. This observation is consistent with the result in [Ver98, p255] that for decorrelating (ZF) MAI cancellation methods, the BER converges as the number of users $K \rightarrow \infty$.

In Fig. 5.8, we compare the performance of the PreRAKELDP with individual power scaling (PreRAKELDP_ps) and with total power constraint (PreRAKELDP_pc). An 8-user single-transmit antenna system is considered. Both coded and uncoded cases are simulated. For the coded system, we employ the rate ½ convolutional code with generator vectors 753 and 561, based on WCDMA standard [ICM98]. At the receiver end, the soft decision decoding is implemented by the standard Viterbi decoder at the MF output. It is shown that for both coded and uncoded cases, the PreRAKELDP_pc has lower BER than PreRAKELDP_ps.
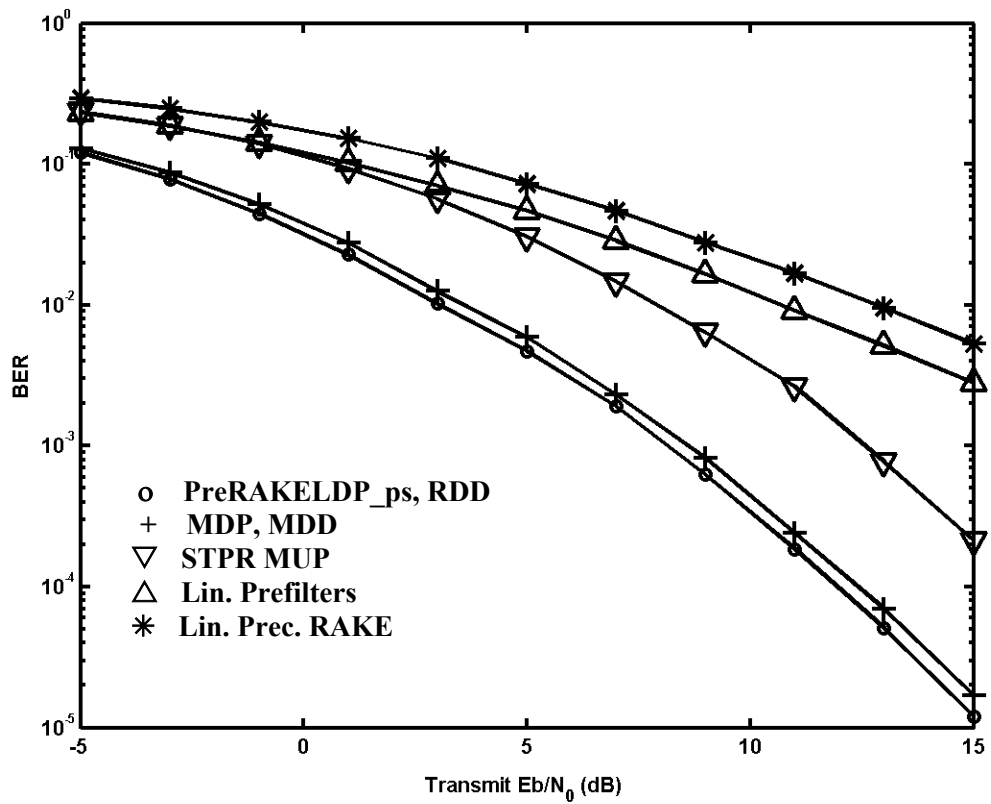
Figure 5.5 Performance comparison of linear precoding techniques in multipath fading channels, 4 users with equal transmit powers, 3 channel-paths/user, single transmit antenna.

Figure 5.6 Performance comparison of three space-time precoding methods, 8 users with equal transmit powers, 3 channel-paths/user.

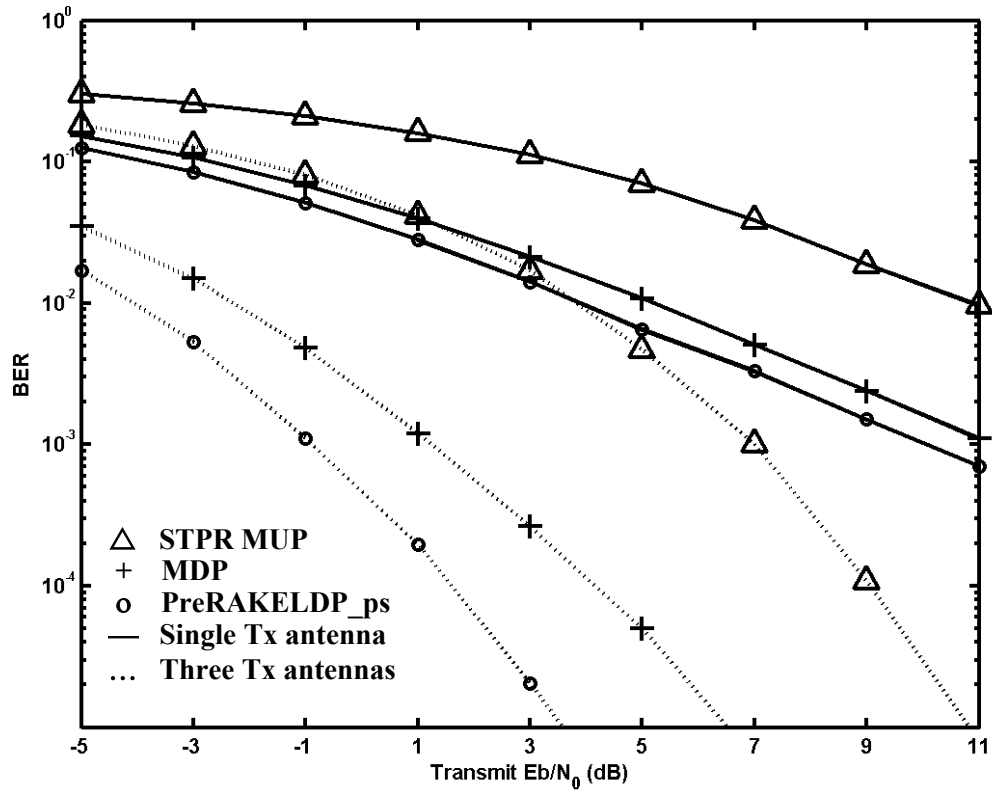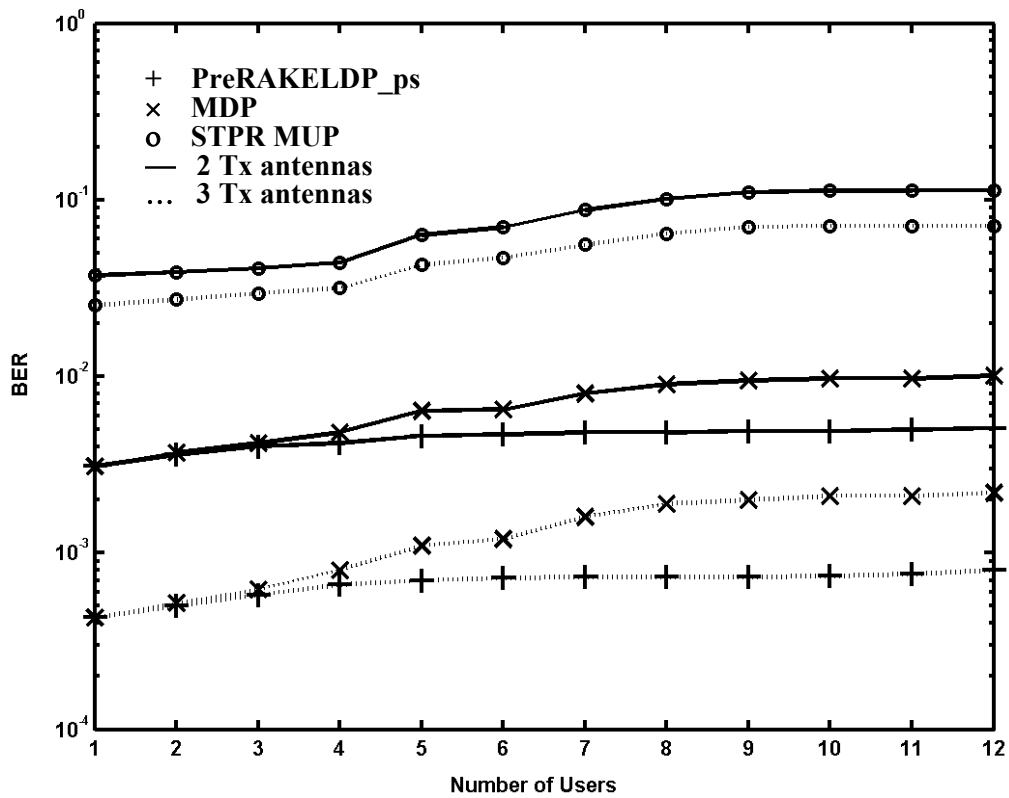**Figure 5.7 Performance comparison of three space-time precoding methods, 1 to 12 users with equal transmit powers, 3 channel-paths/user, transmit E_b/N_0=0dB.**
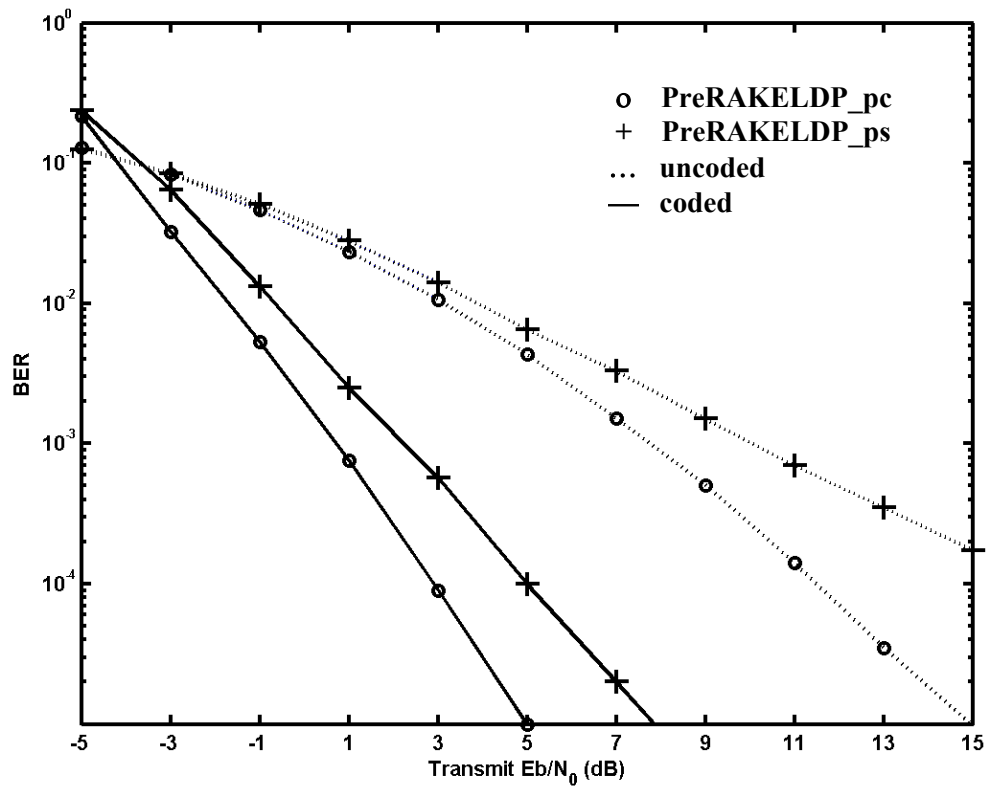
94

Figure 5.8 Performance comparison of individual power scaling and total power constraint for the PreRAKELDP, 8 users with equal transmit powers, 3 channel-paths/user, single antenna.

Chapter 6

CONCLUSIONS

This thesis has concentrated on multiuser precoding and transmitter diversity for the downlink of DS-CDMA systems. We mainly focused on the nonlinear THP and linear decorrelating precoding algorithms, transmitter-based multipath diversity and antenna diversity. These techniques significantly increase the downlink capacity while keeping low complexity of mobile user receivers.

For the purpose of analyzing the duality between the Tx-based and Rx-based MAI cancellation methods, we first introduced the Rx-based linear and nonlinear decorrelating multiuser detection techniques. The proposed Tx-based THP algorithm uses the same MAI cancellation principle as the Rx-based DF multiuser detector. In particular, for frequency-selective fading channels, the PreRAKETHP and MDTHP have the same theoretical performance as the RDDFR and MDDFR, respectively. However, the Tx-based methods avoid the error propagation problem; therefore, the actual performance of THP designs is better than that of the DF multiuser detectors. In addition to the Tx-based THP design applied to downlink CDMA channels, we also presented the Tx-Rx joint THP optimization algorithm for MIMO channels. In this derivative design, the feed-forward filter is shifted to the receiver; as a result, the transmitter and receiver have more balanced complexity.

By theoretical analysis and simulation experiments, it is shown that the THP significantly outperforms the linear decorrelating precoding schemes for M-ary PAM and QAM modulated systems when M is large. However, for small M, due to the end effect and power penalty of modulo operation, the performance advantage of THP over the linear

methods diminishes. Therefore, the linear precoding techniques are more suitable for small-constellation modulated systems, such as BPSK and QPSK. For multipath fading channels, we proposed the linear precoding techniques, PreRAKELDP and MDP. From the view of structure and performance, The Tx-based PreRAKELDP and MDP for the downlink are equivalent to the Rx-based RDD and MDD for the uplink, respectively. The analytical and numerical results show that the PreRAKELDP and MDP have better performance than the previously proposed linear precoding methods with similar complexity, including the linear decorrelating precoding with RAKE receiver, the linear decorrelating prefilter and the space-time Pre-RAKE multiuser precoding.

To obtain the benefit of multipath diversity, all the proposed linear and nonlinear precoding schemes utilize the Tx-based multipath combining. The Pre-RAKE multipath combiner, which is used in the PreRAKETHP and PreRAKELDP, is perfectly matched to the multipath fading channels. Thus it can collect the signal energy to the maximum extent. The PreRAKETHP and PreRAKELDP are the optimal THP and linear precoders, respectively, by the ZF and MMSE criteria. However, the performance gain for these two methods is achieved at the expense of high computational complexity, since the precoding filters are CSI-dependent and therefore have to be updated frequently. Both the nonlinear MDTHP and linear MDP use suboptimal multipath combining method. Although their performance is worse than the PreRAKETHP and PreRAKELDP, respectively, they have lower computational complexity than the PreRAKE-based precoders, because their precoding filters are independent of CSI and only determined by the users' spreading codes. In summary, there is a performance-complexity tradeoff between the nonlinear PreRAKETHP and MDTHP, and between the linear PreRAKELDP and MDP. We also investigated the

97

combination of multiuser precoding and multiple transmit antennas. It is shown that the employment of multiple transmit antennas significantly improves the system performance, especially when the transmit power is large.

A critical requirement for implementation of the proposed transmitter-based techniques is the knowledge of CSI at the transmitter, which can be satisfied by the long range channel prediction (LRP). It is shown that for rapidly time varying fading channels, the multiuser precoding aided by LRP achieves similar performance to the case that the CSI is perfectly known at the transmitter.

BIBLIOGRAPHY

[Ala98] S. M. Alamouti, "A Simple Transmit Diversity Techniques for Wireless Communications", *IEEE J. Select. Areas in Commun.*, vol. 16, pp. 1451-1458, Oct. 1998.

[ANC01] N. Al-Dhahir, A. Naguib and A. Calderbank, "Finite-length MIMO decision feedback equalization for space-time block-coded signals over multipath-fading channels**,** *IEEE Trans. Vehicular Tech*., vol.50, pp.1176 -1182, Jul 2001.

[BBG00] P. Bender, P. Black, M. Grob, R. Padovani, N. Sindhushayana and A. Viterbi, "CDMA/HDR: A Bandwidth-Efficient High-Speed Wireless Data Service for Nomadic Users", *IEEE Commun. Mag.*, vol. 38, pp. 70-77, July 2000.

[BD00] M. Brandt-Pearce and A. Dharap, "Transmitter-based Multiuser Interference Rejection for the Down-link of a Wireless CDMA System in a Multipath Environment", *IEEE J. Select. Areas Commun.*, vol. 18, pp. 407-417, March 2000.

[BZP04] B. A. Bjerke, Z. Zvonar and J. G. Proakis, "Antenna Diversity Combining Schemes for WCDMA Systems in Fading Multipath Channels", *IEEE Trans. Wireless Commun.*, vol. 3, pp. 97-106, Jan. 2004.

[DHH00] A. Duel-Hallen, S. Hu and H. Hallen, "Long-range Prediction of Fading Signals", *IEEE Signal Processing Mag., Special Issue on Advances in Wireless and Mobil Commun.*, vol. 17, pp. 62-75, May 2000.

[Due92] A. Duel-Hallen, "Equalizers for multiple input/ multiple output channels and PAM aystems with cyclostationary input sequences", *IEEE J. on Sel. Areas in Commun.*, vol. 10, pp. 630-639, April 1992.

[Due93] A. Duel-Hallen, "Decorrelating decision-feedback multiuser detector for synchronous code-division multiple-access channel", *IEEE Trans. Commun.*, vol. 41, pp. 285-290, Feb. 1993.

[Due95] A. Duel-Hallen, "A Family of Multiuser Decision-Feedback Detectors for Asynchronous Code-Division Multiple-Access Channels", *IEEE Trans. Commun.*, vol. 43, pp. 421-434, Feb. 1995.

[EDH98] T. Eyceoz, A. Duel-Hallen and H. Hallen, "Deterministic Channel Modeling and Long Range Prediction of Fast Fading Mobile Radio Channels", *IEEE Commun. Letters*, vol. 2, pp. 254-256, Sept. 1998.

[EN93] R. Esmailzadeh and M. Nakagawa, "Pre-RAKE Diversity Combining for Direct Sequence Spread Spectrum Communications Systems", *ICC '93*, vol.1, pp. 463-467, May 1993.

[ESN99] R. Esmailzadeh, E. Sourour, M. Nakagawa, "PreRAKE diversity combining in time-division duplex CDMA mobile communications", *IEEE Trans. Vehiclular. Tech.*, vol. 48, pp. 795-801, May 1999.

[GDc03] S. Guncavdi and A. Duel-Hallen, "Pre-RAKE Multiuser Transmitter Precoding for DS/CDMA Systems", *Proc. CISS'03*, March 2003.

[GDv03] S. Guncavdi and A. Duel-Hallen, "Space-Time Pre-RAKE Multiuser Transmitter Precoding for DS/CDMA Systems", *Proc. IEEE VTC'03*, Oct. 2003.

[GD05] S. Guncavdi and A. Duel-Hallen, "Performance analysis of space-time transmitter diversity techniques for WCDMA using long range prediction", *IEEE Trans. Wireless Commun.*, vol.4, pp.40-45, Jan. 2005.

[GJP91] K. Gilhousen, I. Jacobs, R. Padovani, A. Viterbi, L. Weaver and C. Wheatley III, "On the Capacity of a Cellular CDMA System", *IEEE Trans. Vehicular Tech.*, vol.40, pp. 303-312, May 1991.

[Gun03] S. Guncavdi, "Transmitter Diversity and Multiuser Precoding for Rayleigh Fading Code Division Multiple Access Channels", *Ph.D. Thesis*, North Carolina State Univ., May 2003.

[GVL96] G. Golub and C. Van Loan, *Matrix Computations*. Baltimore, MD: Johns Hopkins Univ. Press, 1996.

[HJ85] R. A. Horn and C. R. Johnson, *Matrix Analysis*, New York: Cambridge Univ. Press, 1985.

[HKT02] E. S. Hons., A. K. Khandani and W. Tong, "An optimized transmitter precoding scheme for synchronous DS-CDMA", *Proc. IEEE ICC'02*, vol. 3, pp. 1818-1822, 2002.

[HM89] R. Haeb and H. Mayr, "A Systematic Approach to Carrier Recovery and Detection of Digitally Phase Modulated Signals and Fading Channels*", IEEE Trans. on Commun.*, vol. 37, pp. 748-754, July 1989.

[HS94] H.Huang and S.Schwartz, "A Comparative Analysis of Linear Multiuser Detectors for Fading Multipath Channels", *Proc. IEEE GLOBECOM'94*, vol.1, pp.11-15, Nov. 1994.

[ICM98] *IEEE Commun. Mag.*, Wideband CDMA issue, pp. 46-95, Sept. 1998.

[Jak93] W. C. Jakes, *Microwave Mobile Communications*, IEEE Press, 1993.

[KS93] C.Kchao and G.Stuber, "Performance analysis of a single cell direct sequence mobile radio system," *IEEE Trans. Comm.*, vol.41, pp 1507-1516, Oct. 1993.

[LD03] J. Liu and A. Duel-Hallen, "Tomlinson-Harashima Transmitter Precoding for Synchronous Multiuser Communications", *Proc. CISS'03*, March 2003.

[LD04] J. Liu and A. Duel-Hallen, "Nonlinear Multiuser Precoding for Downlink DS-CDMA Systems over Multipath Fading Channels", *Proc. IEEE GLOBECOM'04*, Nov. 2004.

[LDj04] J. Liu and A. Duel-Hallen, "Transmitter-based Joint Nonlinear Multiuser Interference Cancellation and Multipath Diversity Combining for DS/CDMA Systems", submitted to *IEEE Tran. Commun.*, Dec. 2004.

[LDg05] J. Liu and A. Duel-Hallen, "Performance Analysis of Tomlinson-Harashima Multiuser Precoding in Multipath CDMA Channels", *the 4G Mobile Forum 2005 Annual Conf.*, July 2005.

[LDm05] J. Liu and A. Duel-Hallen, "Linear Multiuser Precoding with Transmit Antenna Diversity for DS/CDMA Systems", submitted to *IEEE MILCOM'05*, Oct. 2005.

[LM94] E. A. Lee and D. G. Messerschmitt, *Digital Communication*. Norwell, MA: Kluwer Academic Publishers, 1994.

[Lo99] T. K. Y. Lo, "Maximum Ratio Transmission", *IEEE Trans. Commun.*, vol. 47, pp. 1458-1461.

[LP02] A. Lozano and C. Papadias, "Layered space-time receivers for frequency-selective wireless channels", *IEEE Trans. Comm.*, vol. 50, pp. 65 -73, Jan 2002.

[LPL95] J. Lin, J. G. Proakis, F. Ling and H. Lev-Ari, "Optimal Tracking of Time-Varying Channels: A Frequency Domain Approach for Known and New Algorithms", *IEEE Trans. on Sel. Areas in Commun.*, vol. 13, pp. 141-154, Jan. 1995.

[LV89] R. Lupas and S. Verdu, "Linear Multiuser Detectors for Synchronous CDMA Channels", *IEEE Trans. Information Theory*, vol. 35, pp. 123-136, Jan. 1989.

[Pro01] J. G. Proakis, *Digital Communications*, New York: Mcgraw-Hill, 2001.

[SK97] S.H.Shin and K.S.Kwak, "Multiuser Receiver with Multipath Diversity for DS/CDMA Systems", *Proc. 6th IEEE ICUPC*, vol.1, pp. 15-19, Oct. 1997.

[Stu01] G. L. Stuber, *Principles of Mobile Communication*, Boston: Kluwer Academic Press, 2001.

[TC94] Z. Tang and S. Cheng, "Interference cancellation for DS-CDMA systems over flat fading channels through pre-decorrelating", *Proc. IEEE PIMRC'94*, pp. 435-438, 1994.

[TSG01] Technical Specifications Group Radio Access Network, *3GPP TR 25.848 Physical layer aspects of UTRA High Speed Downlink Packet Access*, 3rd Generation Partnership Project, v4.0.0 ed., March 2001.

[VCLM98] L. Vandendorpe, L. Cuvelier, J. Louveaux and B. Maison, "Asymptotic performance of MMSE MIMO decision-feedback equalization for uncoded single carrier and multicarrier modulations", *IEEE ICC 1998*, vol.1, pp. 6 -10, 1998.

[Ver98] S. Verdu, *Multiuser Detection*, Cambridge University Press, 1998.

[VJ98] B. R. Vojcic and W. Jang, "Transmitter Precoding in Synchronous Multiuser Communica-tions", *IEEE Trans*. *Commun*., vol. 46, pp. 1346-1355, Oct. 1998.

[WD95] H. Y. Wu and A. Duel-Hallen, "Performance Comparison of Multiuser Detectors with Channel Estimation for Flat Rayleigh Fading Channels", *Special Issue of Interference in Mobile Wireless Systems, Wireless Personal Commun. Journal*, Kluwer, Dec. 1995.

[WFVH04] C. Windpassinger, R. F. H. Fischer, T. Vencel and J. B. Huber, "Precoding in Multiantenna and Multiuser Communications", *IEEE Trans. Wireless Commun.*, vol. 3, pp. 1305-1316, July 2004.

[ZB95] Z. Zvonar and D. Brady, "Suboptimal multiuser detector for frequency-selective Rayleigh fading synchronous CDMA channels", *IEEE Trans. Commun.*, vol. 43, pp. 154 − 157, Feb. 1995.

[ZB96] Z. Zvonar and D. Brady, "Linear Multipath-Decorrelating Receivers for CDMA Frequency-Selective Fading Channels", *IEEE Trans. Commun.*, vol. 44, pp. 650-653, June 1996.

[ZS96] Z. Zvonar and M. Stanjovic, "Performance of Antenna Diversity Multiuser Receivers in CDMA Channels with Imperfect Channel Estimation", *Wireless Personal Commun. Journal*, Kluwer, pp. 91-110, July 1996.

[Zvo96] Z. Zvonar, "Combined multiuser detection and diversity reception for wireless CDMA systems", *IEEE Trans. VTC*, vol. 45, pp. 205-211, Feb. 1996.

APPENDIX

Performance Comparison between Linear Precoding with RAKE Receiver and Linear

PreRAKE Precoding

Consider a 2-user, 2-channel paths/user system ($K=2$, $N=1$). Suppose the transmit power for the two users are equal, i.e., $A_1 = A_2$, and the channel gain coefficients along different paths are i.i.d random processes, and for every user the total average power of channel gains are normalized to one. From equation (5.10), the BER for the method of linear decorrelating precoding with RAKE receiver [VJ98] (named "Lin. RAKE" for short) can be written as $Pe_i = Q\left(\sqrt{2\gamma_{bi} X_i}\right)$, where the decision statistic $X_i = \dfrac{Sf^2}{\sum\limits_{l=0}^{N-1}\sum\limits_{n=0}^{N-1} R_{i,i}^{l-n} c_{i,l} c_{i,n}^*}$. Since the signature sequences are normalized, $R_{i,i}^0 = 1, \quad \forall i = 1,2...,K$. By the definition of power scaling factor Sf in equation (5.8), X_i in the considered 2-user system is given by

$$X_i = \frac{2}{tr\{\mathbf{R}_c^{-H}\mathbf{R}_c^{-1}\}\left(\left|c_{i,0}\right|^2 + \left|c_{i,1}\right|^2 + R_{i,i}^{-1} c_{i,0} c_{i,1}^* + R_{i,i}^1 c_{i,0}^* c_{i,1}\right)}. \tag{A.1}$$

Given the definition of correlating matrix $\mathbf{R}_c$ as in section 5.1, and $R_{i,j}^0 = 0, \forall i \neq j$, due to the orthogonality of signature sequences, the correlation matrix for the Lin. RAKE method is simplified as

$$\mathbf{R}_c = \begin{bmatrix} \left(\left|c_{1,0}\right|^2 + \left|c_{1,1}\right|^2\right) + c_{10}c_{11}^* R_{11}^{-1} + c_{10}^* c_{11} R_{11}^1 & c_{10}c_{11}^* R_{12}^{-1} + c_{10}^* c_{11} R_{12}^1 \\ c_{20}c_{21}^* R_{21}^{-1} + c_{20}^* c_{21} R_{21}^1 & \left(\left|c_{2,0}\right|^2 + \left|c_{2,1}\right|^2\right) + c_{20}c_{21}^* R_{22}^{-1} + c_{20}^* c_{21} R_{22}^1 \end{bmatrix}. \tag{A.2}$$

Denote $\mathbf{R}_c^{-1} = \begin{bmatrix} a_{11} & a_{12} \\ a_{21} & a_{22} \end{bmatrix}$, thus $tr\{\mathbf{R}_c^{-H}\mathbf{R}_c^{-1}\} = a_{11}^2 + a_{22}^2 + a_{12}^2 + a_{21}^2$. Equation (A.1) can

be re-written as

$$X_i = \frac{2}{(a_{11}^2 + a_{22}^2 + a_{12}^2 + a_{21}^2)(|c_{i,0}|^2 + |c_{i,1}|^2 + R_{i,i}^{-1}c_{i,0}c_{i,1}^* + R_{i,i}^1 c_{i,0}^* c_{i,1})} \quad (A.3)$$

Represent the BER formula for the Pre-RDD as $Pe_i = Q\left(\sqrt{2\gamma_{bi}Y_i}\right)$. The decision

statistics for the Pre-RDD is given by

$$Y_i = \frac{2(|c_{i,0}|^2 + |c_{i,1}|^2)}{(|c_{1,0}|^2 + |c_{1,1}|^2)[\tilde{\mathbf{R}}^{-1}]_{11} + (|c_{2,0}|^2 + |c_{2,1}|^2)[\tilde{\mathbf{R}}^{-1}]_{22}} \quad (A.4)$$

The correlation matrix for Pre-RDD, $\tilde{\mathbf{R}}$, is defined in section 5.3. In the discussed system, it

is equal to

$$\tilde{\mathbf{R}} = \begin{bmatrix} (|c_{1,0}|^2 + |c_{1,1}|^2) + c_{10}c_{11}^* R_{11}^{-1} + c_{10}^* c_{11} R_{11}^1 & c_{20}c_{11}^* R_{12}^{-1} + c_{21}c_{10}^* R_{12}^1 \\ c_{10}c_{21}^* R_{21}^{-1} + c_{11}c_{20}^* R_{21}^1 & (|c_{2,0}|^2 + |c_{2,1}|^2) + c_{20}c_{21}^* R_{22}^{-1} + c_{20}^* c_{21} R_{22}^1 \end{bmatrix}. \quad (A.5)$$

Denote $\tilde{\mathbf{R}}^{-1} = \begin{bmatrix} b_{11} & b_{12} \\ b_{21} & b_{22} \end{bmatrix}$. Therefore, (A.4) is equivalent to

$$Y_i = \frac{2(|c_{i,0}|^2 + |c_{i,1}|^2)}{(|c_{1,0}|^2 + |c_{1,1}|^2)b_{11} + (|c_{2,0}|^2 + |c_{2,1}|^2)b_{22}} \quad (A.6)$$

The BER formula for PreRAKELDP is given by equation (5.35). For the convenience

for comparison with other methods, here we only consider the case of single transmit

antenna. If represent the BER in the form of $Pe_i = Q\left(\sqrt{2\gamma_{bi}Z_i}\right)$, then the decision statistics for

PreRAKELDP is

$$Z_i = \frac{S_i^{-2}}{[\hat{\mathbf{R}}^{-1}]_{ii}} = \frac{1}{[\widetilde{\mathbf{R}}^{-1}]_{ii}} = \frac{1}{b_{ii}} .$$ (A.7)

Compare matrices $\mathbf{R}_c$ and $\widetilde{\mathbf{R}}$, we find that they have identical and real diagonal elements. Based on the previously mentioned practical constraints on the channel gain coefficients, an approximate analysis can be given as follows: the diagonal elements of these two matrices are close to one, while their non-diagonal elements have the absolute values much smaller than one; as a result, a_{ii} and b_{ii} have close values that are larger than one. Therefore, a_{ii}^{2} is usually larger than b_{ii} in practical fading channels.

Comparing the BER of the three linear precoders of interest is equivalent to compare their decision statistics X_i, Y_i and Z_i, for $i = 1, 2$. In the special case that the instantaneous power of the channel gains equals unity, i.e., $|c_{10}|^{2} + |c_{11}|^{2} = |c_{20}|^{2} + |c_{21}|^{2} = 1$, obviously the value of X_i averaged over the channel gain coefficients of user i is smaller than that of Y_i. More accurate comparison of X_i, Y_i and Z_i is given by the statistical simulation results. Without loss of generality, we observe the values of X_1, Y_1 and Z_1 in the following simulation example. Taking 10^{4} samples of multipath Raleigh fading coefficient for each channel path, we calculated X_1, Y_1 and Z_1 according to (A.3), (A.6) and (A.7). Fig. A.1 shows the histograms for X_1, Y_1 and Z_1 in a 3-user 3-channel paths/user system. It is observed that in most cases, X_1 is smaller than Y_1 and Z_1.

The above analysis indicates the better performance of the Pre-RDD and PreRAKELDP than the Lin. RAKE precoder.
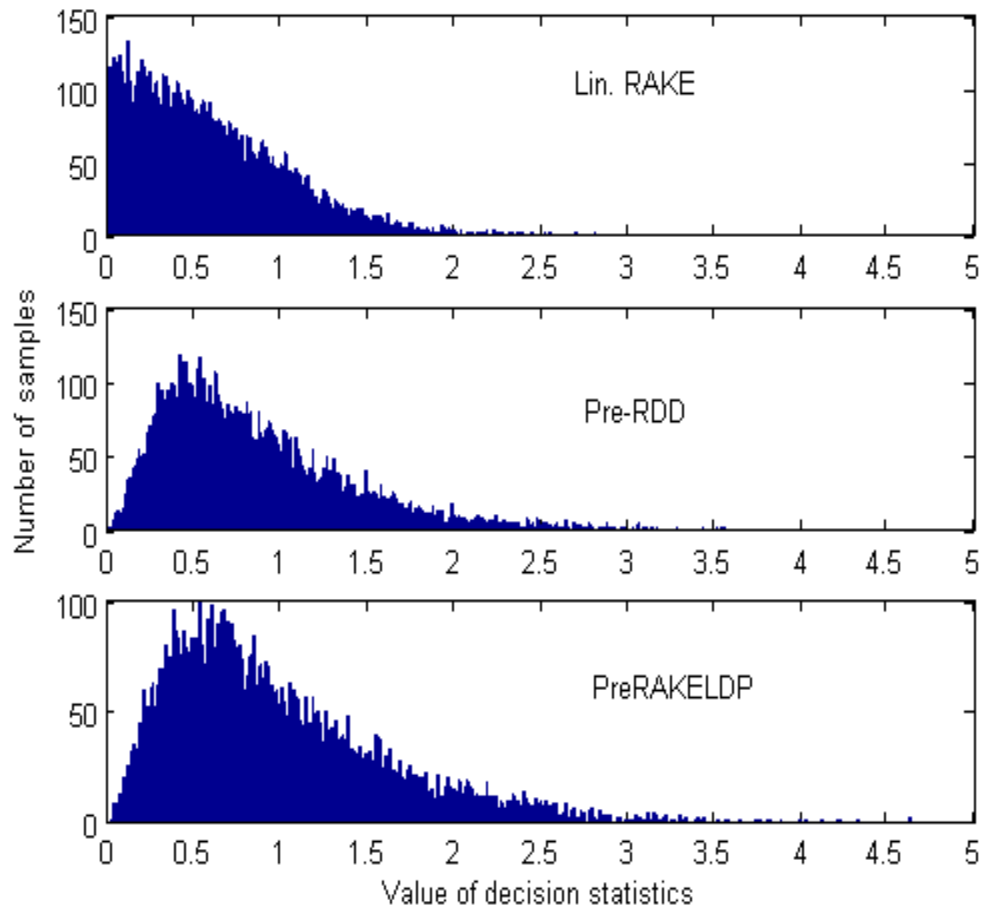
Figure A.1 Histograms for the decision statistics of the linear decorrelating precoding with RAKE receiver (Lin. RAKE), Pre-RDD and PreRAKELDP.